STUDY OF THE REGULATION OF GENES ASSOCIATED WITH FLOWER and LEAF ABSCISSION IN TOMATO (*Lycopersicon esculentum* Mill.)

Thesis submitted
for the degree of MASTER OF SCIENCE in AGRICULTURE
The Robert H. Smith Faculty of Agriculture, Food & Environment
The Hebrew University of Jerusalem

By
Srivignesh Sundaresan

April 2010 **Rehovot, Israel**

Declaration

This study was conducted under the supervision of:

Dr. Shimon Meir

Department of Postharvest Science of Fresh Produce,

Agricultural Research Organization (ARO)

The Volcani Center

Prof. Joseph Riov (Emeritus)

The Robert H. Smith Institute of Plant Sciences and Genetics in Agriculture

The Robert H. Smith Faculty of Agriculture, Food & Environment

The Hebrew University of Jerusalem.

…….

Dr. Shimon Meir

(Supervisor)

…….

Prof. Joseph Riov

(Supervisor)

…….

Srivignesh Sundaresan

(Student)

DEDICATED TO MY LOVABLE PARENTS and

MURUGAN UNCLE

ACKNOWLEDGEMENTS

At the outset I am reminded of the saying, "A person who is not grateful to his fellow cannot be grateful to god". I therefore take this opportunity to express my heartfelt thanks and gratitude to all those people who have helped immensely in the successful completion of my research work.

I deem it as a great pleasure and privilege to place on record my profound sense of gratitude, indebtness and heartfelt thanks to my beloved supervisor, **Dr. Shimon Meir***, Department of Postharvest Science of Fresh Produce, ARO, The Volcani Center, for rendering incessant guidance, cooperation, efficacious advice, and giving valuable suggestions throughout the course of the investigation and the preparation of the thesis.*

I owe a great debt to my honorable supervisor, **Prof. Joseph Riov** *(EMERITUS), The Robert H. Smith Institute of Plant Sciences and Genetics in Agriculture, and to* **Dr. Sonia Philosoph-Hadas***, Department of Postharvest Science of Fresh Produce, for their laudable counseling, illuminating suggestions and constructive criticisms.*
I wish to register my indebtness to **Dr. Amnon Lers** *and* **Dr. Shaul Burd***, Department of Postharvest Science of Fresh Produce, for their unreserved help, incessant motivation and encouragement during the tenure of my research work.*

I feel hard to find a word to express my special thanks to **Mr. Alon Glick, Dr. Jabatsingh, Dr. Sinilal, Dr. Gopal pandi, Dr. Vasudeva reddy***, who cared much interest towards my research, and being involved in tackling all the technical problems during my research period. I am extremely grateful to my lovable brother,* **Dr. Vijay Selvaraj***,* **Mr. Cheran***, for there constant encouragement, and affectionate help throughout the study. I express my special thanks to my pleasant and cheerful lab mates cum friends' viz.,* **Bettina, Ida, Ilana, Neta, Shoshi, Tami, Yaacov** *and* **Daniel***, for their timely helps, adjustments and assistance rendered throughout the research work.*

I wish to register my indebtness to **Dr. Moshe Coll***, Programme Co-ordinator, and to* **Mrs. Nina Rosenthal***, for their parental care and continuous encouragement.*

I convey my respectful and heartfelt gratitude to Peers foundation, England, for their partial funding in the beginning of this year, and generous funding in the first year of my Master studies.

Finally, yet importantly, I thank everybody who directly and indirectly helped me in completing my research work.

Srivignesh .S

TABLE OF CONTENTS

LIST OF ABBREVIATIONS

ABA = Abscisic acid

ARF = Auxin responsive factor

AZ = Abscission zone

CaMV 35S = Cauliflower mosaic virus

DZ = Dehiscence zone

ERF = Ethylene responsive factor

EST = Expressed sequence tag

FAZ = Flower abscission zone

FNAZ = Flower non-abscission zone

GUS = β-Glucuronidase

hpRNA = Hairpin RNA

IAA = Indole-3-acetic acid

LAZ = Leaf abscission zone

LNAZ = Leaf non -abscission zone

LePHAN = PHANTASTICA ortholog of *Lycopersicum esculentum*

MS = Murashige and Skoog

1-MCP = 1-methylcyclopropene

NsPHAN = PHANTASTICA ortholog of *Nicotiana sylvestris*

NtPHAN = PHANTASTICA ortholog of *Nicotiana tabacum*

PG = Polygalacturonase

PEG = Polyethylene glycol

qPCR = Quantitative real-time PCR

RNAi = RNA interference-based gene silencing

SAM = Shoot apical meristem

sq-PCR = Semi-quantitative PCR

TAPG = Tomato abscission polygalacturonase genes

TF = Transcription factor

TPG = Tomato polygalacturonase genes

VIGS = Virus-induced gene silencing

ABSTRACT

Abscission, the separation of organs from the parent plant, results in pre-harvest and postharvest losses of quality and longevity in many fresh produce. To overcome this problem, many crops are treated after harvest with various chemicals to delay or prevent abscission.

The abscission process is initiated by changes in the auxin gradient across the abscission zone (AZ), is triggered by ethylene, and may be accelerated by postharvest stresses. Although changes in gene expression have been correlated with the ethylene-mediated execution of abscission, there is almost no information on the molecular and biochemical basis of the increased AZ sensitivity to ethylene. The molecular mechanisms that drive the acquisition of abscission competence and its modulation by auxin gradients are still unknown. Organ abscission is accompanied by a modified expression of various types of genes, including ethylene-inducible, auxin-responsive, pathogen-related (PR) genes, as well as genes encoding for cell-wall degrading enzymes. Our study used leaf and flower AZs of tomato (*Solanum lycopersicum* Mill, cvs. 'Shiran 1335' and 'VF-36') as a model system, to examine the spatial and temporal expression pattern of the genes, which control molecular mechanisms regulating the abscission process, in the flower AZ (FAZ) and in the leaf AZ (LAZ).

We examined, using semi-quantitative (sq) and quantitative (q) PCR, transcriptome changes in tomato flower and leaf AZs during the acquisition of ethylene sensitivity following flower removal or leaf deblading, which deplete the AZs from auxin. In addition, we have followed pedicel or petiole abscission induced by flower removal or leaf deblading, respectively. We have studied changes in gene expression in the tomato FAZ and LAZ, as compared to flower non-AZ (FNAZ) and leaf non-AZ (LNAZ), during 0, 2, 4, 8, and 14 h after flower removal or during 0, 12, 24, 48, and 72 h after leaf deblading. In addition, we examined the expression the various genes in other plant tissues, such as young and mature shoots, young and mature leaves and roots. Based on these expression studies, we selected some genes for stable transformation into tomato plants. For this purpose, the RNAi (hpRNA) vectors, PGSA 1285 and pHANNIBAL, driven by the CaMV 35S constitutive promoter or by the isolated tissue-specific *TAPG4* promoter, were used to silence the selected genes for their further functional analysis.

The present study was performed according to the following stages:

1) We have validated the microarray (Affymetrix Tomato GeneChip) transcriptome results in the FAZ and FNAZ by means of sq-PCR and qPCR. The genes encoding for abscission-related cell-wall hydrolases, *TAPG1, TAPG2, TAPG4, Cel1, XET-BR1*, were examined in order to validate the abscission system. The genes which were highly regulated shortly (within 2 h) after flower removal were also selected, including ethylene signal transduction-related genes - *ERF2*, *ERF1c*, *ERT10, JERF3*; regulatory genes - *Protein phosphatase-like*; early-modified transcription factors (TFs) - *MybSt1*; novel AZ-specific genes - *PHANTASTICA*, *TAGL12* (MADS-box), Knotted protein - *TKN4, OVATE*, *KD1,* and *TPRP-F1*. The results of the sq-PCR and qPCR analyses were in full agreement with the microarray results except for *MybSt1*. This shows that the microarray results truly reflect the events occurring in the FAZ and FNAZ.
2) The above-mentioned genes showed different kinetics of expression levels in the LAZ and LNAZ following leaf deblading, as well as in the other plant tissues examined to study their tissue specificity.
3) We have studied the kinetics of petiole abscission in response to leaf deblading (auxin removal) and exogenous ethylene. The results indicate that ethylene was effective in inducing petiole abscission only in debladed plants.
4) We identified potential candidate genes from the validated genes tested above, that might regulate abscission of tomato flowers or leaves for their detailed functional analysis by silencing their expression by means of RNA interference-based gene silencing (RNAi) in transgenic tomato plants. The selection was based on genes, which were specifically and significantly up- or down-regulated in the FAZ within 2 h after flower removal, or in the LAZ within 24 h after leaf deblading.
5) We have used the RNAi (hpRNA) vectors, PGSA 1285 and pHANNIBAL, driven by the CAMV 35S promoter, to silence the following six selected genes in the entire plant system for studying their functional role: *ERF2, Protein phosphatase-like, JERF3,* and *TKN4*, *Proline-rich protein* (*TPRP-F1*), and *KD1*. These genes are currently in the stage of transforming into plants (Phase V), and their modified phenotypes will be examined within few months.
6) We have isolated the *TAPG4* promoter from the genomic DNA and cloned it into the pGEMT vector by modifying the restriction sites to suit our vectors. We assembled the

RNAi constructs, driven by *TAPG4* as a promoter, to induce tissue-specific silencing in the FAZ, rather than silencing the entire plant system by using the constitutive CaMV 35S promoter. The constructs for two genes, *JERF3* and *TKN4,* with the *TAPG4* promoter, are ready, they are currently at Phase V. Similar constructs for TPRP-F1, and *KD1* genes are in Phase IV. Hence, we expect to see phenotypes within in a few months.

The findings of this study will shed light on the molecular mechanisms that drive the acquisition of abscission competence, and will facilitate novel approaches to the control and manipulation of abscission in horticultural and agricultural crops, in order to improve their postharvest quality.

CHAPTER 1

INTRODUCTION

Tomato (***Solanum lycopersicum* Mill., Solanaceae, South America)** is a valuable species for studying molecular systems, because it permits the integration of tools and concepts of genetics, physiology, developmental biology, host/pathogen interactions, molecular biology, and genetic engineering in studying and manipulating all the processes relevant to the vast store of genomic information available in public databases. We chose tomato as our model system in studying the regulation of foliar and flower abscission, because several studies that have addressed the related phenomenon of petal abscission in tomato (Osborne and Sargent, 1976; Tucker et al., 1984; Taylor et al., 1990) have found that it has typical abscission zone (AZ) characteristics, and it is easily transformed and regenerated. Moreover, tomato is an important horticultural crop. In addition, the tomato system offers the advantage of publicly available microarray chips, containing ESTs derived from cDNA libraries, and the entire genomic sequence is being processed.

The plants shed their tissues for numerous reasons: propagation or dispersal, protection against environmental stresses, effective pollination, as a defense mechanism, and when a particular organ loses its function in the plant system. Abscission is a process of detachment of plant organs, including leaves, flowers, fruits, and seeds, during plant development (Taylor and Whitelaw, 2001; Lewis et al., 2006), and it can result in postharvest quality loss in many ornamentals and other fresh produce. The domesticated food crops, rice, maize, and wheat, were selected based on aberrant AZ development (Patterson, 2001). Abscission can often result in a significant loss of quality and longevity (Beno-Moualem et al., 2004; Abebie et al., 2005, 2007). To overcome this problem, many crops receive postharvest chemical treatments to delay or prevent abscission (Van Doorn and Woltering, 1991). It is well established that treatments with various auxins or ethylene inhibitors significantly inhibit leaf and floret abscission in ornamentals (Michaeli et al., 1999; Gago et al., 2001). However, these chemical treatments provide an interim solution to the abscission problem in ornamentals; the long-term solution is

the development of cultivars, through conventional or molecular breeding, that are not prone to abscission.

The abscission process proceeds by means of cell-wall and middle-lamella breakdown in the separation-layer cells, and it may be influenced by environmental conditions and hormonal or developmental signals (Roberts et al., 2002; Lewis et al., 2006), pathogens, low light, and oxidative stresses, such as chilling, drought, and salinity (Gomez-Cadenas et al., 1996, 2003; Michaeli et al., 1999; Taylor and Whitelaw, 2001). Leaf abscission is accompanied by a distorted expression of various types of genes, including ethylene-inducible genes, auxin-responsive genes, pathogen-related (PR) genes, cell-wall degrading enzymes, and G proteins (Yuan et al., 2005; Meir et al., 2006; Agusti et al., 2008; Cai and Lashbrook, 2008).

Tomato has a swollen 'joint' on the pedicel, at the midway between the main shoot and the calyx. This structure encompasses the AZ where cell separation occurs (abscission layer), leading aborted flowers or ripened fruits to separate from the plant. The AZ is characterized by multiple layers of densely packed cytoplasmic cells, which are visually identical, but which contain several different classes of cells with different cell-wall chemistry, and which respond to abscission signals and various temporal patterns of cell-wall degradation (Sexton and Roberts, 1982; McKim et al., 2008). The AZ cells are small, have small vacuoles, contain no sclerenchyma fibers, exhibit localized vasculature disruption, and their tracheids are not fully lignified (Webster, 1968; Addicott, 1982; Osborne, 1989).

In many plants, the AZ contains ethylene-responsive tissues (Osborne, 1989). Plant development features unique changes in the behavior of cells, so that in different types of tissues the various factors that regulate the timing and position of AZ breakdown are unknown. There are several different AZs in the tomato plant, e.g., flower abscission zone (FAZ), leaf abscission zone (LAZ), pedicel-calyx abscission zone, fruit pedicel abscission zones, and corolla abscission zones (Hong et al., 2000). We have been interested in examining the spatial and temporal expression pattern of the genes, which control molecular mechanisms of the abscission process, in the FAZ and the LAZ.

Many changes occur during the execution phase of abscission. The abscission process is initiated by changes in the auxin flux across the AZ, triggered by ethylene, and it may be accelerated by preharvest and postharvest stresses. The generally accepted model is that IAA flux through the AZ, which originates in the growing parts of leaves, flowers and fruits, controls the sensitivity to ethylene. When the supply of IAA declines, ethylene-sensitivity of the AZ increases, leading to initiation of abscission signaling (Sexton and Roberts, 1982; Taylor and Whitelaw, 2001). Thus, the activities of cell-wall-degrading enzymes, including cellulase, polygalacturonase (PG), expansins and xyloglucan endohydrolase endotransglycosylase (XET) were shown to increase dramatically with the onset of abscission (Lashbrook et al., 1994; Kalaitzis et al., 1997; Agusti et al., 2008; Cai and Lashbrook, 2008; Roberts and Gonzalez-Carranza, 2009). Further evidence for the role of IAA was provided by Meir et al. (2006), who demonstrated that leaf deblading reduced IAA translocation from the leaf blade to the AZ, resulting in petiole abscission. Analysis at the promoter level revealed that ethylene up-regulated, cellulases and PGs, whereas IAA strongly inhibited their expression (Hong et al., 2000; Tucker et al., 2002). Although changes in gene expression have been correlated with the ethylene-mediated execution of abscission, there is almost no information on the initiation of abscission as the AZ becomes sensitive to ethylene.

Genetic evidence for the role of auxin in regulating floral-organ shedding in Arabidopsis has been elusive. Recently, functional studies of Auxin Response Factors (ARF) including *ARF*2, *ARF*1, *ARF*7 and *ARF19* suggested that these transcriptional regulators acted with partial redundancy to promote senescence and floral abscission (Ellis et al., 2005; Okushima et al., 2005a,b). The ethylene-insensitive mutant's *etr1* and *ein2* showed delayed floral senescence and organ shedding (Patterson and Bleecker, 2004). Enzymes such as chitinase and cellulase and PR-like proteins were detected during or after ethylene-induced abscission (Del Campillo and Bennett, 1996). The phytohormones auxin and ethylene are the most important regulators of the abscission process, even though the abscission mechanisms differ among plant parts (Patterson, 2001; Taylor and Whitelaw, 2001; Lewis et al., 2006). Moreover, other proteins are also involved or modulate abscission of flowers and seeds. They include MADS-box proteins, jasmonic acid synthesizing enzyme, and a receptor- like kinase (Jinn et al., 2000; Mao et al., 2000). Furthermore, other factors are indirectly associated with abscission; they include reactive oxygen species (ROS), peroxidases, and ozone. For example, increases in ROS–scavenging

enzymes are associated with delayed abscission of tomato flowers and fruits (Djanaguiraman et al., 2004).

The developmental genetics of leaf abscission, arguably the most widespread abscission phenomenon, remains largely untouched, likely because the most accessible plant genetic models, Arabidopsis and Maize, do not undergo leaf abscission. Even though the sequence of morphological, cytological and biochemical events associated with activation of the AZ have been extensively studied, the developmental processes leading to differentiation of the AZ have not yet been clearly elucidated. The abscission process is described as four phases (Roberts et al., 2000; Taylor and Whitelaw, 2001). In phase A, undifferentiated cells differentiate into an anatomically discrete AZ. In phase B, the AZ acquires competence to respond to the abscission signal/s. In phase C, the 'execution phase', the abscission signal (ethylene) induces production of cell wall-degrading and other enzymes and proteins, that activate the cells of the AZ and result in cell and organ separation. In phase D, the retained portion of the AZ differentiates to provide a protective layer for the plant. Very little is known about the physiology, biochemistry and molecular basis of phase A, and there is a relatively little knowledge about the critical phase B, in which the differentiated cells of the AZ acquire competence to respond to ethylene. The 'execution phase' C has been thoroughly studied (Sexton et al., 1985; Sexton, 1997). It is well known that the ethylene sensitivity of the AZ is responsive to the strength of the basipetal gradient of IAA through the zone (Bangerth, 1989). However, the molecular mechanisms that drive the acquisition of abscission competence and its modulation by auxin gradients are still unknown. We have aimed to use genomic approaches, including modern techniques for gene identification and functional analysis of identified genes, to investigate how auxin depletion renders the AZ ethylene-sensitive. Our study used leaf and flower AZs of tomato as a model system. The findings of this study might facilitate novel approaches to the control and manipulation of abscission in horticultural and agricultural crops, in order to improve their postharvest quality.

It should be noted that the present research is a part of a BARD project entitled: Molecular Studies of Postharvest Leaf and Flower Abscission. Therefore, apart of presenting my own data in the thesis, I have also presented in Appendixes 1- 4 part of the data obtained in this system by other participants of this binational project. I referred to these data in my Discussion section, in order to bring a more comprehensive picture of the system.

CHAPTER 2

OBJECTIVES

The general objective of the research

The main objective of the present research was to use the established microarray expression analysis to study the regulation and function of genes, which have been found to be associated with flower and leaf abscission in tomato. For this purpose, we plan to identify potentially relevant genes (early-regulated genes) that are specifically up- or down-regulated in the FAZ within 2 h after flower removal, or in the LAZ within 1 day after leaf deblading. Preparing the constructs for the functional study of the selected genes based on silencing their expression by means of RNA interference-based gene silencing (RNAi) in transgenic tomato plants.

Specific objectives

1. To study the kinetics and the expression patterns of the selected genes in the LAZ and FAZ vs. those in the corresponding non-AZ tissues, by using semi-quantitative PCR (sq-PCR) and/or quantitative real time PCR (qPCR), inorder to gain a more detailed understanding of their regulation during abscission. The PCR results of the FAZ and FNAZ will serve as a validation of the results previously obtained by microarray.
2. To study the general expression patterns of the selected genes in various tissues and organs.
3. Based on these studies, to evaluate and select suitable genes for functional analysis by RNAi.
4. To isolate and clone the tomato polygalacturonase promoter 4 *(TAPG4*), and prepare the construct for specific silencing of the selected genes in the FAZ and LAZ.
5. To prepare hpRNAi constructs of the selected genes with CaMV 35S and *TAPG4* promoter for *Agrobacterium tumifaciens*-mediated stable transformation into the plant.

CHAPTER 3

LITERATURE REVIEW

Microarray analysis of the tomato flower abscission zone (FAZ) tissues with the Affymetrix gene chip (Affymetrix GeneChip® Tomato Genome Array- Affymetrix- UK Ltd) revealed many genes that were more highly expressed in the FAZ than in the flower non-abscission zone (FNAZ) at various time points (Appendix 1). We selected several genes (Table 1) that are highly modified in the AZ, are abscission-specific, and whose expressions are associated with the regulation of flower abscission. In the following section, we review the genes that are relevant to the abscission process and that were analyzed in the present MSc thesis.

Table 1: Grouping of genes according to their functional roles in the plant system

Group type	**Gene name**	**Transcript identity**
Cell-wall degrading genes	*TAPG1*	U 23053
	TAPG2	U 70480
	TAPG4	U 70481
	Cel1	U 13054
	XET-BR1	AW 033252
Ethylene signal transduction-related genes	*ERF2*	TC 179207
	ERF1c	TC157961
	ERF4	AY192370
	JERF3	AY383630
Ethylene-responsive genes	*ERT10*	X72730
Regulatory genes	*Protein Phosphatase-like*	TC 171978
Transcription factors	*MybSt1*	TC163103
	PHANTASTICA	AF148934
	TAGL12	AY098737
	TKN4	AF533597
	OVATE	AY140893

3.1. Cell-wall degrading genes

3.1.1. *Tomato abscission polygalacturonase* (*TAPGs*) genes

Growth and development in higher plants often requires changes in the cell-wall structure and cell adhesion properties. Polygalacturonase (PG) hydrolyzes pectin in the cell-wall and middle lamella of plant cells (Carpita and Gibeaut, 1993), which leads to breakage of the primary attachment area between the cells and allows the cells to separate from each other. So far, nine tomato PGs have been deposited in public-domain databases. Expression of *PGs* increases during many developmental processes such as: fruit ripening (Fischer and Bennett, 1991), weakening of the AZs of leaves, flowers and sepals (Tucker et al., 1984; Hong and Tucker, 1998, 2000), pod dehiscence (Jenkins et al., 1996), pith autolysis (Huberman et al., 1993), lateral root emergence (Peretto et al., 1992), root cap cell detachment (Hawes and Lin, 1990), and also as a result of wounding (Bergey et al., 1999) or activity of plant pathogens (Cote and Hahn, 1994).

The cDNA clones encoding PG have been identified in avocado fruits (Kutsumai et al., 1993), peach (Lester et al., 1994), maize pollen (Niogret et al., 1991), and *Oenothera* spp (Brown and Crouch, 1990). Many studies have demonstrated the correlation between PG activity and abscission in, e.g., citrus fruits (Greenberg et al., 1975), *Sambucus nigra* (Taylor et al., 1993), and tomato (Tucker et al., 1984). In contrast, transgenic plants with antisense tomato-fruit PGs did not show any reduction in PG activity in the AZ (Taylor et al., 1990). In tomato *TAPG* activity was primarily restricted to the AZ, in contrast to cellulase, whose activity extended to adjacent distal and proximal tissues. The tomato fruit PG is encoded by a 1.9-kb mRNA coding for 457 amino acids, whereas *TAPG* is encoded by a 1.5-kb mRNA coding for 392 amino acids. In its promoter region, the *TPG3* gene has a sequence similarity with that of the potato wound-induced gene (*win2*), but in tomato it is not induced by wounding (Hong and Tucker, 1998).

The PG synthesis activity in the leaf and petiole AZs is enhanced by ethylene (Sexton and Roberts, 1982; Sexton, 1995) but inhibited by IAA and silver thiosulfate (STS), an ethylene action inhibitor (Kalaitzis et al., 1995). The *TAPG1, TAPG2, TAPG4* and *TAPG5* were abundantly expressed in AZs of the leaf, flower and pistils in response to ethylene exposure for 0, 6, 12, 24, and 48 h (Kalaitzis et al., 1995, 1997; Hong and Tucker, 1998), and exhibited 72% nucleotide sequence identity, but none of these transcripts were detected in stems, petioles, or fruits. *TAPG1* is a member of a small sub-family of PG genes that distinctly differ from the

tomato fruit PG, and whose transcripts are several fold higher in the FAZ than in the LAZ. IAA inhibited expression of *TAPG1* transcripts (Kalaitzis et al., 1995).

The temporal patterns of *TAPG1* and *TAPG2* expression were very similar, but *TAPG4* transcripts accumulated much earlier than those of *TAPG1* and *TAPG2* in AZs and pistils. *TAPGs* in the FAZ and LAZ showed a similar expression kinetics, i.e., GUS **[***TAPG4: GUS***]** staining revealed that GUS accumulated earlier and attained a higher maximum in *TAPG4:GUS* transformants than in those of *TAPG1*. The first 247 bp of the promoter or 73 bp of 5'-upstream UTR of *TAPG1* transcript was responsible for the tissue-specific hormone responsiveness (Hong et al., 2000). *TAPG5* transcripts were expressed in the FAZ and LAZ, whereas *TPG3* and *TPG6* were not detected (Hong and Tucker, 1998).

3.1.2. *Cellulase* genes

Cellulase activity increased during the abscission of tomato leaves (Roberts et al., 1989) and flowers (Tucker et al., 1984). The roles of two cellulases, *Cel1* in floral abscission (Lashbrook et al., 1998) and *Cel2* in fruit abscission (Brummell et al., 1999), had previously been demonstrated by means of antisense suppression. *Cel1* and *Cel5* were highly expressed in tissues that are undergoing cell separation, specifically in the later stages of flower abscission, and they were down-regulated by auxin (Del Campillo and Bennett, 1996, Kalaitzis et al., 1999). *Cel3* expression was high in developing vegetative tissues rather than in abscising tissues and it was found to be localized in the Golgi and plasma membranes (Brummell et al., 1997a). *Cel4* expression was associated with hypocotyls, pistils, and young leaves rather than in mature tissues (Brummell et al., 1997b). *Cel6* was highly expressed in flowers prior to abscission, and was slightly upregulated by auxin (Del Campillo and Bennett, 1996). *Cel7* expression was low in young growing tissues and fruits, and was induced by auxin (Catala et al., 1997, 2000). The *Cel8* C-terminal region resembles a bacterial carbohydrate binding site, a characteristic that is unique among the tomato endo-1,4-β-glucanases (Catala and Bennet, 1998).

3.1.3. *XET* genes

A novel cell wall-related gene, *XET-BR1*, is regulated by brassinosteroid treatment (Koka et al., 2000). BRI1 is a receptor kinase that transduces steroid signals across the plasma membrane, and has an extracellular domain containing 25 leucine-rich repeats (LRRs) (Wang et al., 2001). The activities of cell-wall degrading enzymes, including cellulase, PG, expansins and XET have been

shown to increase dramatically with the onset of abscission (Lashbrook et al., 1994; Kalaitzis et al., 1997; Agusti et al., 2008; Cai and Lashbrook, 2008; Roberts and Gonzalez-Carranza, 2009).

The expression of cell-wall metabolism-related genes was also studied by means of qPCR and Affymetrix GeneChip hybridization in the soybean LAZ from explants exposed to ethylene (0, 1 or 2 days): there was significant up-regulation of the *cellulase* genes, *XET1* and *XET2*, and strong down-regulation of *EXP1*, *PG7* and *PG16*. In both tomato (Catala et al., 1997) and Arabidopsis (Xu et al., 1995), *XET* expression was found to be restricted to expanding tissues; it was up-regulated by treatments with auxin and brassinosteroids, and down-regulated by ethylene (Catala et al., 1997; Campbell and Braam, 1999).

3.2. Transcription factors

It is well understood that genes are tightly regulated through differential expression of hundreds of transcription factors (TFs) in the plant system. TFs are proteins that bind upstream of the DNA coding region (promoter), activate the RNA polymerase to start transcription, and regulate expression of genes. TFs may bind directly or indirectly through other, already bound TFs, and they regulate gene expression by starting or repressing transcription. Repressor TFs inhibit transcription by blocking attachment of the activator protein (Nath et al., 2005). The whole-genome sequencing analysis of Arabidopsis reveals that 6% of the genome (1,500 genes) encodes for TFs, of which 45% are plant specific (*AP2/ERF, WRKY, NAC* families) (Chen et al., 2002). The numbers of TF families in plants are higher than those found in *Caenorhabditis elegans* and *Drosophilla*. In plants, ethylene signaling is mediated by various TFs, which belong to the ethylene responsive factor (ERF), ethylene insensitive 3 (*EIN3*), ethylene-insensitive-like (*EIL*), MADS-box, and *WRKY* families, which have pleiotropic effects in ripening, abscission, and senescence.

3.2.1. *ERF*-related genes

Ethylene is an important phytohormone that plays a vital role in plant growth and development processes (Osborne, 1990), including germination, stem and root elongation, fruit ripening, abscission, and organ senescence (Abeles et al., 1992). Regulation of ethylene can occur at the levels of synthesis, uptake, and turnover of the hormone; it can also occur at the levels of

perception or signal transduction. At the end of the signaling pathway are the transcription factors, including ERFs

ERF proteins such as ERF1, ERF2, ERF3, and ERF4, are plant-specific TFs, that belong to the AP2/ERF family, which regulates ethylene-dependent gene expression via binding to the GCC motif of the promoter regions of ethylene-regulated genes and various stress-responsive pathways. These comprise 139 genes in rice and 122 ERF genes in Arabidopsis (Nakano et al., 2006a,b). The ERF proteins also act as regulators in cross-talk between ethylene and abscisic acid (ABA) pathways (Yang et al., 2005; Wu et al., 2007). It is well known that some ERF proteins are transcriptional activators or repressors (Ohta et al., 2001). Over-expression of ERF genes constitutively activates ethylene responses, and causes dwarfism in seedlings (Solano et al., 1998; Gu et al., 2002).

The ERF family comprises four different classes, which exhibit differential expression in a tissue- and development-specific manner (Tournier et al., 2003). ERF proteins have been shown to regulate plant tolerance to both biotic and abiotic stresses, as exemplified in connection with plant defense (Zhou et al., 1997; Chang et al., 2003), osmotic stress tolerance (Zhang et al. 2004), and seed germination (Song et al., 2005). The ERF genes are induced not only by ethylene, but also respond to jasmonate, ABA, NaCl (Zhang et al. 2004), wounding (Tournier et al., 2003), salicylic acid, and biotic stress (Fujimoto et al., 2000; Lorenzo et al., 2003).

The regulatory functions of ERF proteins differ significantly from one another, because of their different interactions with specific *cis*-acting elements, such as bZIP transcription factors (Xue and Loveridge, 2004) or other proteins (Onate-Sanchez et al., 2007). The *Nicotiana sylvestris* plants expressing the dominant mutant of the Arabidopsis ethylene receptor *ETR1* exhibited delayed onset of leaf and flower abscission (Yang et al., 2007). *Sl-ERF2* is expressed in all plant tissues, but especially in germinating seeds and ripening fruits. Its over-expression in tomato transgenic lines resulted in premature seed germination and hook formation, indicating increased ethylene sensitivity through induction of the *Mannase2*. The accumulation of *EFR2* transcripts in flowers and stems was similar, but it exhibited very low expression in the roots. The alternative splicing in the ERF family, *Sl-ERF2* responds to transcripts corresponding to spliced and unspliced versions (Julien et al., 2006).

ERF2 proteins have a highly conserved AP2 DNA binding domain consisted of 58-59 amino acids, which binds to the GCC-box with a conserved GCCGCC core domain, and thereby modulates gene transcription (Allen et al., 1998); for example *PDF1, PDF2 or NtChitinase* harbor such *cis* elements on their promoter regions (Gu et al., 2002). Thus, the regulation of ERF proteins is expected to be an important factor in regard to analysis of the interaction of ethylene and ABA pathways.

3.2.2. *Myb*-related genes

Myb-like proteins control plant-specific processes, act as DNA-binding transcription factors, and have been widely found in eukaryotes (reviewed by Lipsick, 1996). They were first identified in the *v-myb* oncogene (Klempnauer *et al*., 1982). The known extent of the MYB family of regulatory proteins is much higher in plants than in animals (Rabinowicz et al., 1999; Jiang et al., 2004). The MYB proteins have a conserved 1-3 N-terminal sequence that binds target DNA and non-conserved C-terminal regions. They have in common a myb-homologous DNA-binding domain (myb domain), which consists of two or three imperfect repeats (R1, R2, and R3), containing approximately 50 amino acids, but in plants several DNA-binding myb-like proteins contain only a single myb repeat (Wang et al., 1997). The third helix is responsible for the sequence-specific DNA binding (Gabrielsen et al., 1991). The novel plant-specific short SANT/MYB-like gene, *Lefsm1* (fruit *SANT/MYB-like* 1), is expressed specifically during the very early stages of tomato fruit development (Rivkabarg et al., 2005). Myb1 and Myb2 were named after two LeMYBI domains. The DNA-binding activity of LeMYBI is located in the Myb2 domain.

Several small Myb TFs, Tryptichon (TRY), Caprice (CPC) and Enhancer of Try, Cpc1, 2 (Wada et al., 1997, 2002; Schellmann et al., 2002), were identified. Myb2 is similar to the MybSt1 protein, with a single myb domain from potato (Baranowskij *et al*., 1994), as well as to the recently identified single-myb proteins CCA1 and LHY from Arabidopsis (Schaffer *et al*., 1998). *MybSt1* acts as a transcriptional activator. *Mybst1* is not an isolog of LeMYBI, even though they exhibit similarity in their myb domains, which are located near the N-termini (Baranowskij et al., 1994). Even though M*ybst1* is expressed in potato, its specific role in plant systems is yet to be identified. The Arabidopsis database contains 13 ORFs similar to the Myb2 domain, but the

functional proteins have yet to be characterized (Williams and Grotewold, 1997). *LeMYBI* specifically binds to the I-box, and the protein activates transcription in both yeasts and plants.

3.2.3. The *PHANTASTICA*

PHANTASTICA (PHAN) was first identified in the cDNA library of tomato giant cells; it encodes for MYB-related TFs, such as those observed in tomato roots that were infected by root knot nematodes (Bird and Wilson, 1994). *PHAN* orthologs have been identified in other plants; *ROUGH SHEATH2* (*RS2*) in *Zea mays* (Timmermans et al., 1999), *ASYMMETRIC LEAVES* (*AS1, AS2*) in Arabidopsis (Sun et al., 2002), and *CRISPA* (*CRI*) in Pea (Lamm, 1949). Leaf morphology is determined by the differential expression of *PHAN*, *KNOX*, *LEAFY* (Geeta Bharathan and Neelima, 2001), *YABBY*, *STM*, *PHAB* and *LFY* (Hareven et al., 1996; Chen et al., 1997; Koltai and Bird, 2000).

LePHAN RNA was detected in the shoot apical meristem (SAM), the leaf and stem vascular tissues, and along the whole adaxial surface of the primordium of pinnate compound leaves by Minsung et al. (2003), whose observations agreed with those of Koltai and Bird (2000) but contrudicted those of Pien et al. (2001). *PHAN* mRNA was limited to leaf initials, and persisted in developing leaves, but was undetectable in the later stages of leaf development (Waites et al., 1998). It was also detected in stamens and carpel initials and primordia, in which *PHAN* mutants were shown to be required only in the developmental stages of leaves, bracts, and petal lobes (Waites et al., 1998).

Loss of *PHAN* function leads to an adaxial identity in the leaf primordia that forms radialized, bladeless leaves in *Antirrhinum* (Waites and Hudson, 1995), tomato (Kim et al., 2003), and *Nicotiana* (Neil and Ross, 2004). Other genes with a similar function in generating leaf blade growth in Arabidopsis are the *YABBY* (Sawa et al., 1999), *PHABULOSA* (*PHAB*), and *PHAVOLUTA* gene families (McConnell et al., 2001). The abaxial side is marked by the expression of the *KANADI* (Kerstetter et al., 1997; Emery et al., 2003) and *YABBY* (Siegfried et al., 1999; Golz et al., 2004) gene families. Down-regulation of *PHAN* affects the primordial leaf adaxial domain and changes pinnate compound leaves into palmate compound leaves (Minsung et al., 2003).

The expression of *Le-PHAN* is insufficient for repression of *Tkn2 TKN2* (*KNOX*) in tomato, which indicates an expanded role for either gene in the establishment of cell identity in plant development (Koltai and Bird, 2000). In maize and *Antirrhinum*, *PHAN* acts as an epigenetic regulator that suppresses *KNOX* genes (Schneeberger et al., 1998; Waites et al., 1998).

3.2.4. *KNOTTED* domain (*KNOX*) genes

Phylogenetic analyses revealed that homeobox genes are present in the common ancestor of plants, animals, and fungi (Bharathan et al., 1997). Therefore, the study of their function should increase our understanding not only of plant development but also of that of multicellular eukaryotic organisms in general.

Homeodomain genes play a major role in establishing cell identities (Sentoku et al., 1999). Class 1 *KNOTTED* domain (*KNOX*) genes play a pivotal role in formation and maintenance of SAM and development of lateral organs in Arabidopsis, such as *STM1*, *RS1*, knotted1-like (*KNAT2)* and *KNAT6* (Long et al., 1996), and *LeT6* in *Antirrhinum* (Waites et al., 1998). The homeobox genes of the 3-aa loop extension (TALE) superfamily – class I and II *KNOX* and *BELL* genes – play a central role in plant developmental processes. The tobacco and potato TALE proteins bind the regulatory sequences of *GA20-oxidase1*, which is a gibberellins synthesizing gene and negatively regulate GA biosynthesis by interacting with KNOX proteins in meristems (Sakamoto et al., 2001). The Class1 *KNOX* gene expression in tomato leaf primordium maintains the meristematic activity required for compound leaf formation (Janssen et al., 1998a,b) through partial mediation of gibrellins (Hay et al., 2002). Cytokinin levels were strictly correlated with *KNOX* gene expression, suggesting that cytokinins may regulate *KNOX* expression or act as a secondary signal regulated by KNOX (Frugis et al., 1999; Rupp et al., 1999), and that aberrant polar auxin transport is correlated with ectopic expression of *KNOX* in maize (Tsiantis et al., 1999).

Over-expression of *KNOX* resulted in ectopic apical meristem formation in Arabidopsis (Chuck et al., 1996) and in development of ectopic meristems in tobacco leaves, forming leaves with lobes (Sinha et al., 1993). In contrast, in the complex-leaved tomato, *KNOXI* genes were found to be expressed in the apical meristem and in leaf primordia, and their over-expression resulted in increased ramification of the complex morphology (Hareven et al., 1996; Chen et al., 1997;

Janssen et al., 1998b). These differences in *KNOXI* expression and effects in leaves that express contrasting morphology suggest that *KNOXI* genes might provide a degree of indeterminacy to the leaf primordia in tomato, thereby leading to an extended stage of morphogenesis and a more complex leaf form. Loss of KNOX functional mutations leads to failure to develop SAM in Arabidopsis embryogenesis (Long et al., 1996) and abnormalities in leaves and flowers in maize (Kerstetter et al., 1997). The expression of *LePHAN* is insufficient for the repression of *Tkn2* (*KNOX*) in tomato, which suggests an expanded role for either gene in the establishment of cell identity in plant development, and that their expression temporally and spatially is coincidental (Koltai and Bird, 2000). *In situ* localization of the tomato *KNOX* transcripts *Tkn1* and *Tkn2* (*LeT6*) showed that they are expressed not only in SAM, but also in pre-primordium sites, leaf and floral meristems (Janssen et al., 1998a, b).

3.2.5. The *TAGL12* (MADS-box domain)

The *MADS*-box genes are among the most extensively studied transcription gene families in plants (Parenicova et al., 2003; de Folter et al., 2006). MADS-domain proteins act as potential TFs, whose putative DNA-binding function is conserved, and which play important roles in many biological processes of plants from root development to fruit ripening. TM6 and TM3 were the first MADS-box lineage discovered in tomato (Pnueli et al., 1991, 1994), and 36 tomato *MADS*-box genes are presently available in public-domain databases (Hileman et al., 2006).

The *AGAMOUS* (*AG*) sub-family comprises four members: *TAG1, TAGL1, TAGL11,* and *SLMBP3*. It was shown that *MADS*-box genes are involved in the complex ripening process of tomato (Pnueli et al., 1994). Development of the pedicel AZ requires the activity of the *MADS*-box *JOINTLESS* (*J*) (Mao et al., 2000), and mutations in *J* affect the inflorescence determinacy and flowering time (Quinet et al., 2006). The variations in flower structures are mainly due to the radiation of $MIKC^C$-type *MADS*-box genes (Becker and Theissen, 2003), and it has been reported that Arabidopsis and rice genomes carry 39 and 47, respectively, $MIKC^C$-type *MADS*-box genes (Kofuji et al., 2003; Leseberg et al., 2006).

In Arabidopsis, expression of *AGAMOUSE*-like 12 (*AGL12*), a member of the MADS domain family of regulatory factors 12 MADS-box protein (*TAGL12*), was reported to encode a MADS-box TF, that was found to be involved in abscission (Fernandez et al., 2000). Over-expression of

AGL15, under the *35S* promoter, resulted in delayed abscission of petals and sepals, but did not block the development of a functional AZ in the flower or the dehiscence zone (DZ). On the other hand, the MADS-box TF *JOINTLESS* has a central role in coordinating gene expression, that underlies differentiation of the pedicel AZ in tomato (Mao et al., 2000). *STK* (*SEEDSTICK*), which encodes a MADS domain TF, is closely related to an *AGAMOUS SHATTERPROOF* - *SHP1* and *SHP2* (Pinyopich et al., 2003).

3.3. Regulatory genes

3.3.1. The *OVATE*

The *Arabidopsis thaliana OVATE* family proteins (AtOFPs) are a plant-specific protein family, with close functional connections to TALE homeodomain proteins. The *OVATE* domain is also known as the DUF623 domain (domain of unknown protein 623). There are 18 genes in Arabidopsis, which code for the putative *OVATE* domain. *AtOFP1* is required for gametophyte or sporophyte development, and it acts as an essential regulator of pleiotropic development. *AtOFP1* and *AtOFP5* were shown to associate with the cytoskeleton and to regulate sub-cellular localization of TALE homeodomain proteins, which suggests a previously unrecognized control mechanism in plant development.

AtOFPs have the characteristic conserved C-terminal domain found in the tomato *OVATE* protein. The *OVATE* over-expressing lines lead to abnormal genotypes, such as slow plant growth, and abnormal phenotypes such as extended stigmas, reduced stamens and petals, less apparent serration, smaller compound leaves, and changed vegetative and floral architecture (Liu et al., 2002). Transgenic plants of *Arabidopsis thaliana* over-expressing *AtOFP1* also exhibit pleiotropic genotypes and phenotypes, such as stunted growth and delayed development, irregular heart-shaped leaves, thickened stems, style and stigma that protrude from the flower, and thickened aerial parts (Hackbusch et al., 2005). Transgenic tobacco plants also display similar phenotype alterations (Hackbusch et al., 2005).

In tomato, a single non-sense mutation at the *OVATE* locus (second exon of *ORF6*), led to a premature stop codon, that resulted in 75-aa truncation in the C terminus of the predicted protein to initiate the transition from round to pear-shaped fruit (Liu et al., 2002). *OVATE* leads to a negative class of proteins, which are important for plant development. It is expressed in early

development of flowers and fruits, and it is the major quantitative trait: QTL controls the development of pear-shaped tomato and eggplant fruits (Ku et al., 1999; Doganlar et al., 2002).

In Arabidopsis, *OVATE* is expressed in very low levels during plant development, and it could not be detected in leaf, flower, and fruit RNAs by means of northern blots. It is expressed mainly in the reproductive organs, i.e., flowers, from 10 days before anthesis to 8 days after anthesis, and in almost undetectable levels in young shoots and leaves (Liu et al., 2002). *AtOFP1* is expressed in roots, shoots, inflorescences, stems, flowers, and siliques (Wang et al., 2007). It is localized to the nucleus and functions as an active transcription repressor, reducing cell elongation by acting in conjunction with the *AtGA20x1* gene, which encodes a key enzyme in GA biosynthesis (Wang et al., 2007), that is essential for male transmission and pollen function (Hackbusch et al., 2005). AtOFP proteins may also have some similarities to Aux/IAA proteins with regard to their mode of action, which involves repression of gene expression via dimerization with ARF proteins. For example, no AtOFP proteins or Aux/IAA proteins contain an apparent DNA binding domain.

However, very little is known about the function of *OVATE* in plants, and their molecular mechanisms of action are unknown. *OVATE* is regulated at the transcriptional level and by developmental cues. Thus, studying the spatial and temporal expression patterns of *OVATE* will provide more understating of *OVATE* expression, its specific function in AZs, and its role in plant development.

CHAPTER 4

MATERIALS and METHODS

4.1. Plant material and growth conditions

For FAZ and FNAZ studies, cherry tomato (*Solanum lycopersicum* Mill, cv. 'Shiran 1335') (Hazera Genetics Ltd., Israel) inflorescences were harvested from 7-month-old plants in a commercial tomato greenhouse in Israel.

For leaf abscission and other plant-tissue expression studies, seeds of tomato cv. 'VF-36' (kindly supplied by Dr. Amnon Lers, ARO, The Volcani Center) were sown in perlite and kept in a dark incubation room for 3 days. Germinated seedlings were then transferred to a growth room under conditions of 23°C and 14/10 h day/night. Three-week-old seedlings were transplanted in a growth medium (Arabidopsis medium) and moved to a long-day greenhouse under conditions of 25°C and 16/8 h day/night. Samples for studying LAZ and other plant tissues were collected from three-month-old plants.

The tomato cultivars 'Moneymaker' and 'VF-36' were chosen for *Agrobacterium*-mediated stable transformation.

4.2. Leaf petiole abscission experiment

Plants from the long day greenhouse were used in these experiments. The 3rd and 4th leaves above the cotyledons were debladed by leaving a subtended petiole of 2 cm long from the AZ. The level of petiole abscission was determined by counting the number of petioles detached from the LAZ at 0, 24, 48, 72, and 96 h after deblading. The same procedure was followed for the ethylene-treated plants (see below, Section 4.3).

4.3. Ethylene-induced leaf petiole abscission experiment

After deblading, the plants were exposed to ethylene to enhance petiole abscission. The plants were placed in an air-tight chamber at 20°C, through which a continuous flow of ethylene (5 μL/L) was maintained for 24 h. Air samples of 5 mL were withdrawn from the chamber with a gas-tight syringe, and the ethylene concentration was determined with a Varian 3300 gas chromatograph equipped with a flame ionization detector and a C-5000 alumina-packed column,

with helium as the carrier gas. The rate of petiole abscission was determined as detailed above for the leaf-petiole abscission experiments (Section 4.2).

4.4. Flower sample preparation

Cherry tomato (*Solanum lycopersicum* Mill, cv. 'Shiran 1335') inflorescences were harvested from a commercial greenhouse in Israel, between 09:00 and 11:00. Bunches containing at least two to four fresh open flowers were brought to the laboratory under high-humidity conditions. Senesced flowers and young (unopened) buds were removed, and the stem ends were trimmed. The flowers were immediately sorted by removing all but two or three fresh flowers from each stem. Bunches of five flower stalks were placed in vials with 10 mL of 50 μL L^{-1} organic chlorine as TOG-6 (Milchan Bros, Ltd., Israel) in water, to prevent microorganism development. They were then placed in an observation room under conditions of 20 ± 1°C, 60 ± 10% RH, and 12 h light at intensity of 14 μmol m^{-2} s^{-2}, provided by cool white fluorescent tubes. Groups of 15 vials, containing about 50 explants with ~120 flowers, were used for each treatment.

4.5. Sample collection for RNA extraction

At each time point, FAZ tissues were collected from each side of the abscission fracture, by excising 0.5 mm tissue from each side of the AZ. Tissue from the flower non-abscission zone (FNAZ) was obtained by excising 3-mm-long pedicel tissue from the proximal part of the pedicel, 1 cm from the AZ. The samples were collected at 0, 2, 4, 8, and 14 h after flower removal. The samples for 0 h time were taken from explants before flower removal. LAZ tissues were collected by removing 1 mm of the AZ from the base of the petiole, which was still attached to the main stem. Tissues from the leaf non-AZ (LNAZ) were obtained by excising 0.3-cm-long leaf petiolar tissue sections from the distal part of the petiole, 1 cm from LAZ, at 0, 12, 24, 48 and 72 h after deblading. Old shoot (OS) tissue samples were obtained by excising about 7-mm-long sections from the basal internodal stem region, 5 cm above the ground level. Young shoot (YS) tissue was excised from the tender growing region of the shoot, 5 cm below the top expanding leaf. Young leaf (YL) tissue was obtained from the second fully opened leaves from the plant top. Old leaf (OL) tissue was obtained from fully mature green leaves. The total root system (R) was harvested and washed with water until all the adhering medium was completely removed. For each time point, at least 40 FAZ/ LAZ segments, 20 FNAZ/LNAZ segments, and

10 samples of each of YL, OL, YS, OS, and R were collected. All tissues collected for further analyses were immediately frozen with liquid nitrogen and stored at -80°C.

4.6. Total RNA extraction

Total RNA was isolated with the Spectrum Plant Total RNA Kit (Sigma-Aldrich, St. Louis, MO, USA). For each extraction, 40 mg of frozen tissues were pulverized with liquid nitrogen, in a prechilled porcelain pestle and mortar, to prevent thawing of the tissues. The RNA was cleared of both double-stranded and single-stranded DNA and of other impurities by using RQ1 RNase-Free DNase (Promega Corp., Madison, WI, USA) in a total volume of 10 µL, according to the manufacturer's protocol (http://www.promega.com/tbs/9pim610/9pim610.pdf). The final concentration of the purified RNA was determined in a 1.5-µL aliquot with a Nanodrop spectrophotometer (Thermo Fisher Scientific, USA). The RNA purity was determined by the A260:A230 wavelength ratio, and was further confirmed by running the samples on a non-denaturing gel.

4.7. cDNA first-strand synthesis

Total RNA was converted to complementary DNA (cDNA) by using the Reverse Transcription System (Promega Corp., Madison, WI, USA). A total of 2 µg of RNA were used for the cDNA construction from each sample. In a sterile RNase-free micro centrifuge tube, 1 µL of the random primer and 1 µL of Oligo$(dT)_{15}$ primer were added to the 2 µg of the RNA sample in a total volume of ≤15 µL in double-distilled water (DDW). The tube was then heated to 70°C for 5 min, to melt secondary structures within the template. The tube was then immediately cooled on ice, to prevent re-formation of secondary structures, and the following components were added: 5 µL of Moloney Murine Leukemia Virus (M-MLV) 5X reaction buffer; 5 µL of 10 mM dNTP Mix; 200 units (1 µL) of M-MLV Reverse Transcriptase (RT); and 25 units (1.5 µL) of Recombinant RNasin Ribonuclease Inhibitor. These components were mixed gently with the samples by flicking the tube, and incubated for 60 min at 37°C. The synthesized cDNA was stored at -20°C for future use.

4.8. Semi-quantitative PCR (sq-PCR)

The concentrated cDNA was diluted to 1:20 with DDW and normalized against *Betatubulin2*. The gene-specific primers were designed with the aid of IDT Primerquest tools (http://www.idtdna.com/Scitools/Applications/Primerquest/). The annealing temperatures (Table 2), extension time, and number of cycles were specific for each gene. The number of PCR cycles was optimized according to the amplification of the final product, for easy comparison in agarose gel. We used Ampliqon Taq DNA Polymerase Master Mix 2.0 Master Mix Kit – (1.5 mM $MgCl_2$) (Genetech supplier, Israel) for PCR. The PCR amplifications were carried out in a peqSTAR 96 Universal Gradient Thermal Cycler (PEQLAB, Germany). The PCR product was runned on 0.8% agarose gel in 0.5% TAE buffer for 25 min at 110 V. The total time varied according to the size of the PCR product, and it was recorded with the Image Master VDS 1208 system. The optimal number of cycles for expression analysis of genes was determined when the amplification level was in the lag phase (Fig. 1).

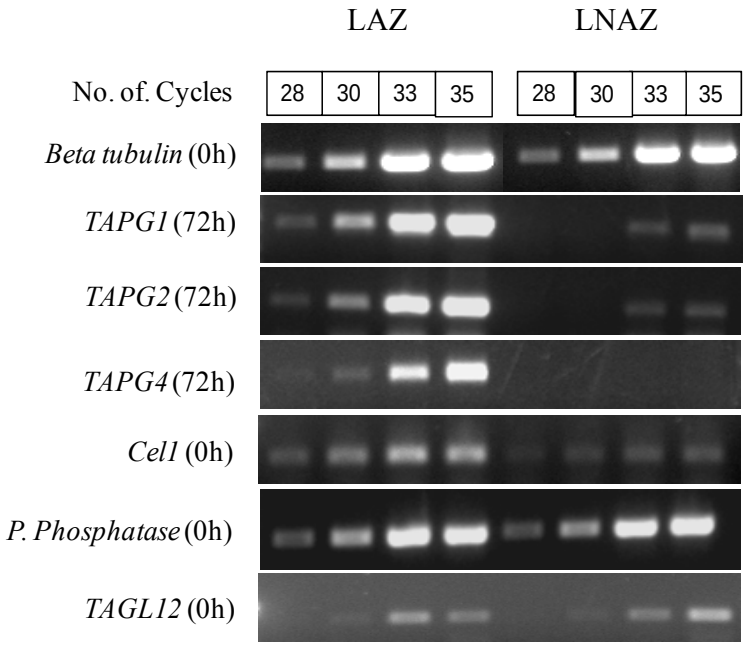

Figure 1: sq-PCR cycle calibration showing the amplified expression levels of various genes isolated from different leaf zones, LAZ and LNAZ, at the indicated time points (numbers in parenthesis) after leaf deblading.

Table 2: Genes and primer sequences used for semi-quantitative PCR analyses.

Serial no	Gene name	Transcript identity	RT-PCR primer sequence	Product size (bp)	Annealing Temperature (°C)
1.	*PHANTASTICA*	AF148934	**F-** ACAAACTCTTCTTCCTCCGTGGCT **R-** CTTAGCAAGGCGCATGTGTTTGGA	532	62
2.	*TAGL12*	AY098737	**F-** ACTAGTGGGAGGTTGTCTGCCAAA **R-** TCTAGTGTCATTGTTCCTGCGCCT	435	58
3.	*TKN4*	AF533597	**F-** AAGGTTGGAGCACCGCAAGAAATG **R-** AGTGATTCTTCCACCAGTCCAGCA	508	62
4.	*OVATE protein*	AY140893	**F-** ACAATGAGGCGTCGTCACAAGAGA **R-** TCTCCCAAATGTCTGAGAACGCCT	376	62
5.	*ERF2*	TC 179207	**F-** GGCCGACTGATTTCTGGCCAATTT **R-** ACTGATTGCCCGTCAACATACGGT	604	62
6.	*ERF1c*	TC157961	**F-** AAGATG TCA AGC CCA CTA GAG A **R-** CCCATGGCCTCTTTCTAACTCCAA	319	60
7.	*PROTEIN PHOSPHATASE*	TC 171978	**F-** AACTGTGGATCAGGAGCTGGAACA **R-** CGTTTCCAAGCACGAACAGCACAT	534	62
8.	*MybSt1*	TC163103	**F-** TGCTGGTTCTTCATCTAGCCGTGA **R-** AGGAGGCAACGGATTGTTGCTTTG	331	61
9.	*TAPG1*	U 23053	**F-** GGGCTTGCAAGAACTCCAACAACA **R-** CATTGCTAGGCCTTGCCCAAGTTT	459	60
10.	*TAPG2*	U 70480	**F-** TGCATCTCTATTGGCCCTGGAACT **R-** ACACCTTCAAGTGTTATGCCGCTG	428	62
11.	*TAPG4*	U 70481	**F-** TTGCCCTAAAGGAACTACGGCACT **R-** ACCAGAAGCTCTTCCTCCAGCATT	730	62
12.	*Cel1*	U 13054	**F-** AATTCTCCAGGATCTGAGGTGGCA **R-** GTTTGGGCTCCAGCAAACTTGTCA	335	61
13.	*XET-BR1*	AW 033252	**F-** GTGGACAACACACCAATAAGAGT **R-** GGCTAAAGCTTTGGGCCATGTAGT	200	60
14.	*BETA TUBULIN2*	TC 171630	**F-** AGGGCATTATACTGAAGGCGCTGA **R-** TCTGTATTGCTGTGAACCACGGGA	538	61

4.9. Quantitative real-time PCR (qPCR)

The qPCR reaction was carried out with the SYBR Green/ROX fluorescence detection method. Primers were designed with optimal GC nucleotides content of 50%, and differences between the Tm values of the two primers did not exceed 2°C. The presence of more than two G or C nucleotides was avoided among the last five nucleotides at 3'- end, to reduce the risk of nonspecific priming, in such a way as not to form hairpins, self-dimers and hetero-dimers. The gene-specific primers were designed with the aid of IDT Primerquest tools (http://www. idtdna.com/Scitools/Applications/Primerquest/) and Fermentas Oligo tools (http: //www. fermentas. com/reviewer/app?page=DesignPrimers&service=page), and were analyzed for secondary structures with the aid of the Oligo analyzer (http://eu.idtdna.com/analyzer/ Applications/ Oligo Analyzer/). Serial dilutions of the primer ranging from 1 to 20 pmol were run to ensure that the concentration was within the linear range of the graph, in order to prevent a primer dimerization effect that could lead to a nonspecific reaction. A concentration of 8 pmol

gave good results, both for the housekeeping genes (*Betatubulin2, Actin and GAPDH*) and the genes of interest.

A different cDNA dilution of 1:100 was prepared for creating a linear standard curve with efficiency of 1 and M = – 3.3 ± 0.1, and this dilution was used for all samples. Reaction mixtures contained forward and reverse primers (Table 3) and Absolute QPCR SYBR Green ROX Mix (AB Gene Company, Epson, UK) in a 10-µL total sample volume. ROX is a passive internal-reference dye used to normalize the fluorescent reporter signal generated in QPCR. The ROX concentration in the final volume was 500 nM. Reactions were run in triplicates and analyzed with the Rotor-Gene 3000 PCR instrument (Corbett Life Research, Sydney, Australia). All reactions were performed with non-template control (NTC) and RT-minus (RNA) controls. The results were validated with the delta-delta Ct method ($2^{-\Delta\Delta Ct}$). The results were obtained from two biological replicates and six technical replicates. The presented results were obtained after attainment of constant responses. The three-step PCR program comprised of 40 cycles: initial enzyme activation at 95°C for 15 min, denaturation at 95°C for 15 s, annealing at 65°C for 15 s, and extension at 72°C for 20 s.

Table 3: Genes and primer sequences used for quantitative real-time PCR analyses.

Serial no.	Gene name/ Transcript identity	Primer sequence	Product size (bp)	Annealing temperature (°C)
1	*SL-Actin* (U60481)(Q96483)	F- TGTCCCTATTTACGAGGGTTATGC R- AGTTAAATCACGACCAGCAAGAT	115	65
2	*JERF3*-Realtime-153F (AY383630)	F -TCA GAC AAG GAT GCT GCT GCT GAT R- TGC AGT ATT GAA GGT TCC CAG CCA	153	65
3	*TKN4*-realtime	F- TAT CGA TGG CCT TAT CCC ACG GAA R- TCG ATC CAG CAC TTA CAC CTT CCA	166	65
4	*KD1*-Realtime (AF375969)	F- CCTACTTCTACTTCCACTCCATC R- CAATCATCTAGCTTCCTCATG	159	65
5	*Prolinerichprotein- TPRP-F1* (BI206022, X57076.1)	F- GAATCGGTGGAAGTGCTAAG R- CCTGTAGAGCAATGGGAAGA	138	65
6	*Betatubulin*2-Realtime	F- AGC ACG AAA GAG GTC GAT GAG CAA R- TCA CGC GCC TAA ACA TCT CCT GAA	181	65
7	Homeobox-Leucine zipper (HB-13) - AF011556	F- GCCTTCATGCAGAGATAATGTCAC R- GCTGTGAATGGCTGGTGTTCTTGA	149	65
8	*ERF4* (AP2 transcription factor) - AY192370	F- AATCTCCGCTCCGATTTCCCTGAA R- TGGATCTCTTATCTCCGCCGCAAA	165	65
9	Homeobox-Leucine zipper (CK715706)	F- TTCCTCCGCTAGCAGATTTGAGCA R- TTCAGAGGGTTGCTTTGGCTCTCT	162	65
10	*TAGL12* MADS-box protein - (AY098737)	F- AGGCGCAGGAACAATGACACTAGA R- CAGCTTCCAGTATCCCTCCCTTAT	190	65
11	*ERT10* – Ripening-related burst oxidase protein D (*RbohD*) - (X72730)	F- TGCATATGCGCGCTGCTAATCAAG R- GAGGGCCAACACCT TTGTAATGCT	149	65

4.10. PGSA 1285 RNAi vector

The RNAi vector PGSA1285 (9948 bp) (Fig. 2) was obtained from the Chromatin Database (http://www.chromdb.org/rnai/pGSA1285.html), which carries the CaMV 35S promoter, the bacterial chloramphenicol resistance gene (bacterial selection), the bacterial kanamycin resistance gene (plant selection), and a 360-bp fragment from the GUS (*Escherichia coli* beta-glucuronidase gene) as intron. Primers were designed so that they could clone in both sense and antisense orientations, as mentioned in the Chrombd, Primer design strategy for RNAi constructs (Fig. 3). The list of gene primers and other sequencing primers used is presented in Table 4.

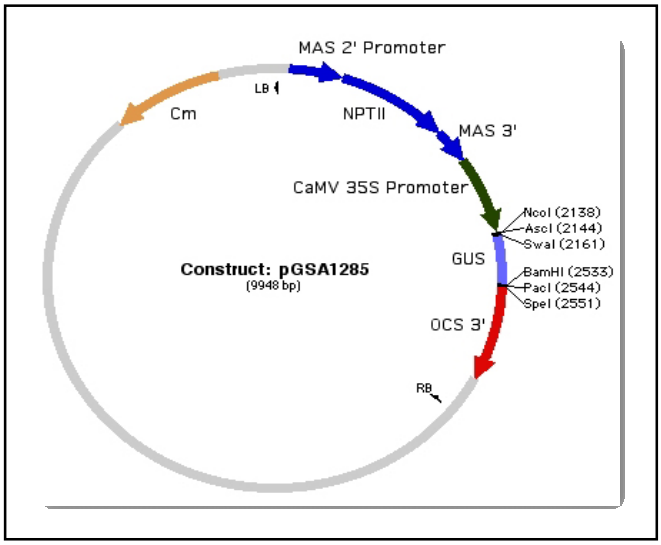

Figure 2: Plasmid restriction map of the RNAi vector PGSA1285.

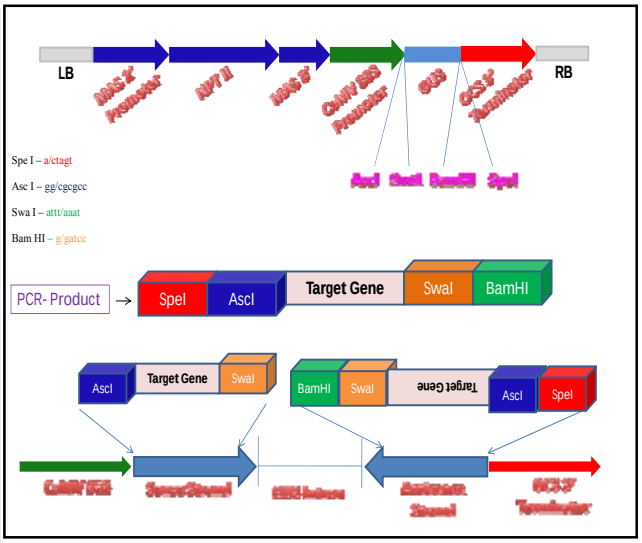

Figure 3: Schematic diagram describing the cloning strategy and methods adopted for PGSA1285.

Table 4: Genes and primer sequences used to clone into the PGSA1285- RNAi vector.

Serial no.	Gene name	PGSA- primer	Product size (bp)	Annealing temperature (°C)
1	*ERF2*- RNAi	F:GGACTAGTGGCGCGCCGGCCGACTGATTTCTGGCCAATTT R:ACGGATCCATTTAAATACTGATTGCCCGTCAACATACGGT	604	72
2	*P. PHOSPHATASE*-RNAi	F: GGACTAGTGGCGCGCCAACTGTGGATCAGGAGCTGGAACA R: ACGGATCCATTTAAATCGTTTCCAAGCACGAACAGCACAT	534	66
3	*PHANTASTICA*- RNAi	F-GGACTAGTGGCGCGCCACAAACTCTTCTTCCTCCGTGGCT R-ACGGATCCATTTAAATCTTAGCAAGGCGCATGTGTTTGGA	532	71.5
4	*OVATE* protein-RNAi	F-GGACTAGTGGCGCGCCACAATGAGGCGTCGTCACAAGAGA R- AC GGATCCATTTAAATTCTCCCAAATGTCTGAGAACGCCT	376	71
5	PGSA (2483-2684)	F- TGT AAT GTT CTG CGA CGC TCA CA R- AGA ATG AAC CGA AAC CGG CGG TAA	201	58
6	PGSA (2051-2219)	R-GCC GAC AGC AGC AGT TTC ATC AAT	169	60
7	PGSA-R-559	R-TAT CAT GCG ATC ATA GGC GTC TCG		59

Restriction sites: Spe I – a/ctagt *Asc I – gg/cgcgcc * Swa I – attt/aaat * Bam HI – g/gatcc

4.11. pHANNIBAL RNAi vector

The hairpin RNAi vector pHANNIBAL (5824 bp – AJ 311872.1) (Fig. 4), which have widely been used for constructing the hairpin RNAi in plants, was obtained from CSIRO, Australia (http://www.pi.csiro.au/RNAi/). This vector carries the CaMV 35S promoter, with the bacterial ampicillin-resistance gene for bacterial selection and an 800-bp PDK intron. The primers were designed so that they could be cloned in both sense and antisense orientations, as mentioned by CSIRO (Fig. 5). The gene primers and sequencing primer pairs used are listed in Tables 5 and 6.

The binary plasmid vector pART27 (Gleave, 1992) (Fig. 6), in which the NotI fragment (entire hairpin structure including introns) from the primary vector pHANNIBAL was cloned into the NotI site of pART27, also obtained from CSIRO. The vector pART27 contains *NPTII* selection marker gene for plant selection within the T-DNA borders, and a spectinomycin-resistance gene for bacterial selection.

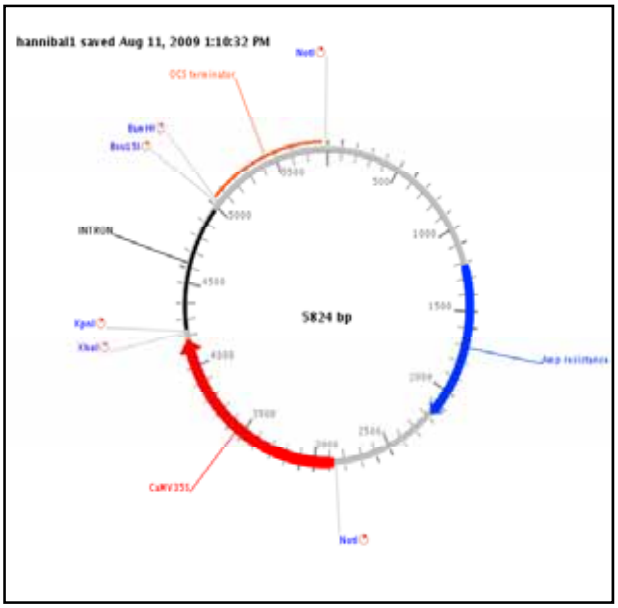

Figure 4: Plasmid restriction map of the primary vector pHANNIBAL.

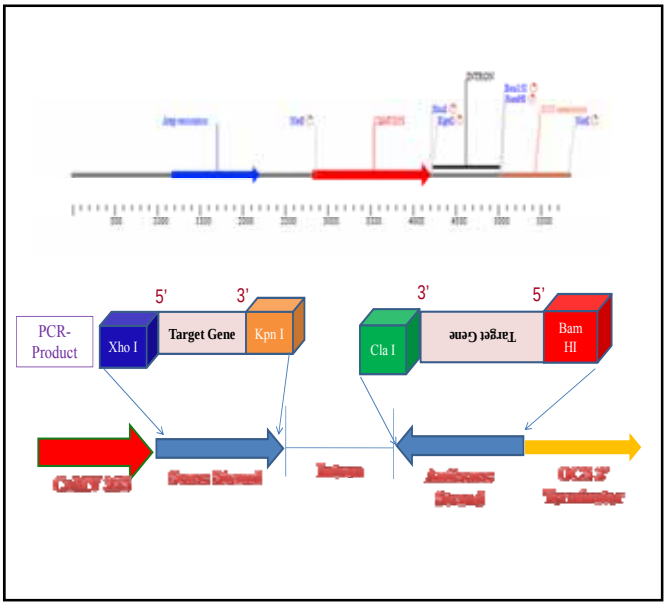

Figure 5: Schematic diagram describing the cloning strategy and methods adopted for the primary vector pHANNIBAL.

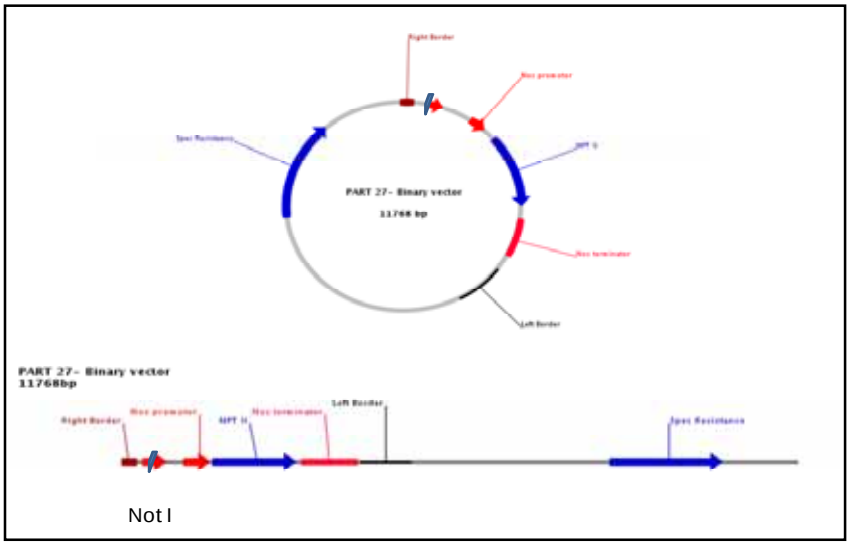

Figure 6: Plasmid restriction map of the binary vector pART27.

Table 5: Genes and primer sequences used to clone into the primary vector pHANNIBAL (AJ311872.1).

Serial No.	Gene name/ Transcript identity	Custom design for pHANNIBAL	Product size (bp)	Annealing temperature (°C)
1	*TKN4* (AF533597)	**Sense** F- CCCTCGAGGGTGGAGCTGATCCAGAACTTG R- CGGGGTACCCCTTCCACCAGTCCAGCAATACA **Antisense** F- CGGGATCCCGTGGAGCTGATCCAGAACTTG R- CCATCGATGGCTTCCACCAGTCCAGCAATACA	409	66 65
2	*JERF3* (AY383630)	**Sense** F-CCCTCGAGGGGAAATACGTGACCCAAGGAAAGGG R-GGGGTACCCCAGATGATATCTCTGGAGTCCTGGAGC **Antisense** F- CGGGATCCCGAAATACGTGACCCAAGGAAAGGG R- CCATCGATGGAGATGATATCTCTGGAGTCCTGGAGC	468	67 65
3	*KD1* (AF375969)	**Sense** F- CCCTCGAGGG TATGTTGTCACTCTTTGTATGGTC R- CGGGGTACCCCATGAGCTTATAGAATCTTGGCTCT **Antisense** F- CGGGATCCCGTATGTTGTCACTCTTTGTATGGTC R- CCATCGATGGATGAGCTTATAGAATCTTGGCTCT	450	65 65
4	*Proline rich-protein TPRP-F1* (BI206022,X57076.1)	**Sense** F- CCCTCGAGGG TACTCCACCCATAGTTCCAACACC R- CGGGGTACCCCTGCCTTCAACTATGACAATGCGGC **Antisense** F- CGGGATCCCG TACTCCACCCATAGTTCCAACACC R- CCATCGATGG TGCCTTCAACTATGACAATGCGGC	411	69 66

Restriction sites: XhoI- CTCGAG * KpnI- GGTACC * BamHI- GGATCC * ClaI- ATCGAT

Table 6: Primer sequences used to sequence the primary vector pHANNIBAL (AJ311872.1) for conformation and sequencing.

Serial No.	Vector name	Primer sequences	Product size (bp)	Annealing temperature (°C)
1	Hannibal 4136-A	**F-** TGACGCACAATCCCACTATCCTTC	275	60
2	Hannibal 4136-B	**R-** TTCGTCTTACACATCACTTGTCA		
3	Hannibal 4923-C	**F-** AGTCGAACATGAATAAACAAGG	200	61
4	Hannibal 5122-D	**R-** TTTACAACGTGCACAACAGAATTG		
5	Hannibal-2791-X	**F-**TAT GAC CAT GAT TAC GAA TT	1482	60
6	Hannibal-4272-Y	**R-**ATA CTA AAA GGA AAA AAG AAA A		
7	CaMV 35S	**F-** CAC AAC AAG TCA GCA AAC AG **R-** TGT CAC ATC AAT CCA CTT GC	1017	55
8	*NPT II*	**F-** CCTATTTCCGCCCGGATCCG **R-** GTCAAGAAGGCGATAGAAGGCG	800	60

Restriction sites: Sac I-GAGCTC * Not I- GCGGCCGC * Xho I- CTCGAG

RNAi constructs

Phase 0 - Empty plasmid of the vector.

Phase I - Gene cloned at sense orientation into the primary vector.

Phase II - Gene cloned at antisense orientation into the primary vector.

Phase III - Entire RNAi construct into destination vector/ binary vector.

Phase IV - Transforming into *Agrobacterium tumefaciens.*

Phase V - Transforming into plants ('Moneymaker' and 'VF-36').

4.12. pGEM-T: PGSA constructs

Because of the technical difficulties in dealing with such a large (11 kb) plasmid of the vector PGSA1285, we used primers from PGSA1285 (Table 7) to clone the hairpin-cloning site (MCS) into pGEM-T Easy for easy transformation. After Phase I and Phase II of cloning, they were restricted by using specific restriction sites to maintain the hairpin constructs intact, and were cloned back into PGSA1285 in specific orientation, and the process entered Phase IV, as mentioned above.

Table 7: Primer sequences used to clone part of the PGSA1285 into pGEMT-Easy vector.

Serial No.	Name	Primer sequence	Product size (bp)	Annealing temperature (°C)
1	pGEM-PGSA-F	F-AGG ACA CGC TCG AGT ATA AGA G R-TAT CAT GCG ATC ATA GGC GTC TCG	559	57

4.13. Gene cloning

The PCR product was further purified from the gel using the Wizard SV Gel and PCR Clean-Up System (Promega Corp., Madison, WI, USA) according to the manufacturer's instructions (www.promega.com). The purified products were evaluated for quantity and quality with a Nanodrop Spectrophotometer (Thermo Fisher Scientific, USA), prior to further use.

Purified PCR products/vectors were double digested overnight at 37°C with specific restriction enzymes, i.e., a different one for each cloning vector/gene, according to the manufacturer's protocol. Most of the restriction enzymes were in fast-digest format, unless otherwise stated (www.fermentas.com). The restricted products were again gel purified with the Wizard SV Gel and PCR Clean-Up System (Promega Corp., Madison, WI, USA). The purified products were ligated with T4 DNA ligase (Promega Corp., Madison, WI, USA) according to the manufacturer's protocol, unless a different ligase was used for a specific clone. In some special circumstances, pART 27 was restricted with NotI enzyme overnight, and again treated with FastAP Thermosensitive Alkaline Phosphatase for dephosphorylation, i.e., release of 5'- and 3'-phosphate groups from the NotI site to prevent recirculation of the vector. Cloning the NotI fragment into pART 27 gave a low yield of positive colonies when T4 DNA-ligase (3u) (Promega Corp., Madison, WI, USA) was used, therefore we used the T4 ligase (5u) with PEG from (Fermentas, Canada). All the ligation reactions were performed in accordance with the producers' protocols.

The cloned vectors were transformed into bacterial (*E. coli*) competent cells, JM109 (Promega) and DH5α (RBC Bioscience, Taiwan), by means of the heat-shock method in accordance with the manufacturers' protocols (www.rbcbioscience.com). Then, they were transferred to agar media with selective antibiotics (ampicillin at 100 mg/mL, kanamycin at 50 mg/mL, spectinomycin at 30 mg/mL, and chloramphenicol at 30 mg/mL), and incubated overnight at 37°C. The transformed colonies were screened by PCR for the presence of inserts, with specific primers being used before plasmid purification.

The selected transformed colonies were grown overnight in luquid broth (LB) medium at 37°C with shaking. Different volumes were used for the various stages of cloning and/or various vectors and selective antibiotics were included, which differed for the various vectors. The plasmids were purified with the Wizard plus Minipreps DNA Purification System and the

PureYield Plasmid Midiprep System (Promega Corp., Madison, WI, USA), depending on the quantity of plasmid required for further study. The extracted plasmids were sequenced by using specific primers from various positions and with various orientations with respect to each vector system (Tables 3, 5). The clones and PCR products were sequenced at Hylabs Laboratories Ltd, Rehovot, Israel.

4.14. Isolation of the *TAPG4* gene promoter

Genomic DNA was isolated from the flower AZ tissues with the GenElute Plant Genomic DNA Miniprep Kit (Sigma Aldrich, St. Louis, MO, USA) in accordance with the manufacturer's instructions. The promoter region was identified by using the PLACE program (http://www.dna.affrc.go.jp/PLACE/). The specific primer with restriction sites (Table 8) was used to amplify the 2.4-kb upstream promoter region of the *TAPG4* gene. The PCR reaction was executed with the pfu DNA polymerase enzyme (Fermentas, Canada) to reduce the error rate in the long template. The PCR product was cloned into pGEMT- Easy Vector (Promega Corp., Madison, WI, USA) for further use. The *TAPG4* promoter was used in the RNAi system for tissue-specific silencing; the strategic design is shown in Figure 7. Cycling conditions for PCR comprised of 30 cycles: initial denaturation at 94°C for 5 min, denaturation at 94°C for 40 s, annealing at 65°C for 30 s, and extension at 72°C for 6 min.

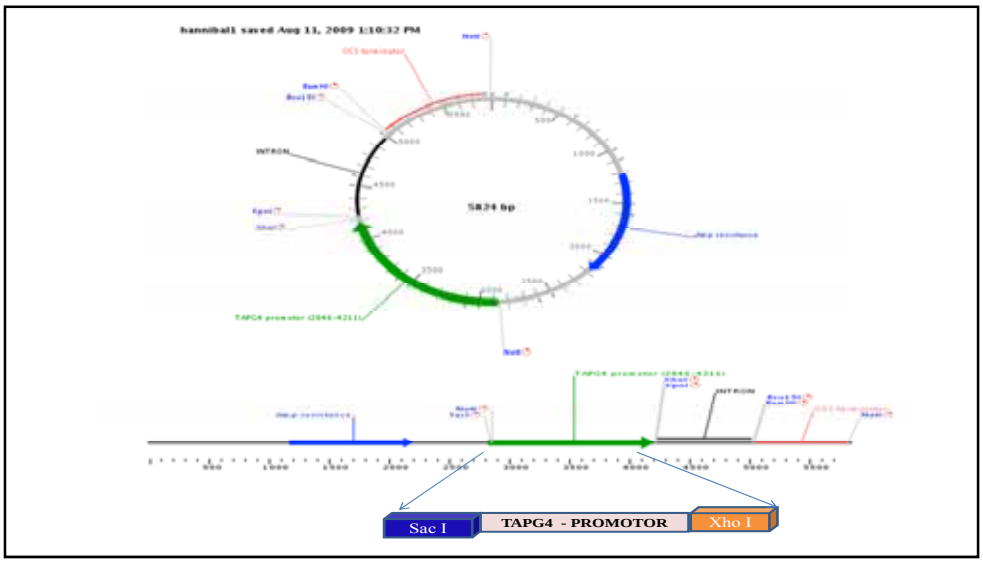

Figure 7: Schematic diagram of creation of a new vector containing the *TAPG4* gene as a promoter.

Table 8: Primer sequences used to clone the *TAPG4* promoter into the primary vector pHANNIBAL (AJ311872.1), and the primer to sequence from middle region of the promoter.

Serial no.	Name	Primer sequence	Product size (bp)	Annealing temperature (°C)
9	UC-*TAPG4*	F- CCGAGCTCAGCGGCCGC TTTAGGCTCCCAAAGAGCTATAC R- CCCTCGAGGGAACATTGTAAATGGTGTTTGTTGC	1437-3817	2381
10	*TAPG4* Inner region	F- GCT ATC AAA TAC CTA GTG GCT AGA CT R-CAT GCC TCT TTG CAA CCC TCC TAT	1373-1927	554

4.15. *Agrobacterium*-mediated transformation

The selected genes that showed drastic changes in the AZ shortly (2 h) after flower removal – PGSA 1285- *ERF, Protein Phosphatase*; pHANNIBAL - *JERF3, TKN4, KD1,* and Proline-rich protein-*TPRP-F1* – were used for further stable transformation into plants. The reconstructed binary vectors were individually electroporated into *Agrobacterium tumefaciens* strain EHA105 according to Dower (1998), with the aid of a Biovolt Electroporator at 110 V for 20 ms. The plasmids where sequenced after each cloning from a different region, to confirm their orientation and to ensure that there were no mutations or deletions in the cloned genes. The tomato 'VF-36' and 'Moneymaker' lines were used for the transformations. The presence of the transgenes in *Agrobacterium* was confirmed by PCR in several different regions of plasmids. The individual gene primers were *NPTII* and CaMV 35S, and the primers used are listed in Table 5.

4.16. Analysis of the data

DNA sequences and cloning sequences results were analyzed with the Bio-Edit software program, version 7.0.9 (http://www.mbio.ncsu.edu/bioedit/bioedit.html). The SigmaPlot 2000 and Excel 2007 softwares were used to generate graphic depiction of the results.

4.17. Analytical chemicals and enzymes

- Absolute qPCR SYBR Green ROX Mix (AB Gene Company, Epson, UK; AB-1162/A).
- Ampliqon-Taq DNA polymerase Master Mix (1.5 mM $MgCl_2$) (Ampliqon- Genetech supplier).

- Kanamycin, Ampicillin, Chloromphenicol, NaCl, NaOH – Spectrum Plant Total RNA Kit Sigma-Aldrich, St. Louis, MO, USA).
- GenElute Plant Genomic DNA Miniprep Kit - G2N10 (Sigma-Aldrich, St. Louis, MO, USA).
- Agar, Bacto-tryptone and yeast extract (Becton, Dickinson and Co, France).
- Agarose (Biotechnology Grade)-(0710) (Amresco Inc., Solon, OH, USA).
- pGEM-T Easy vector (3015 bp), T4 DNA Ligase (3 u/µL) Blue/White Cloning Qualified (M180A), Reverse Transcription System, M-MLV Reverse Transcriptase (M170A), Oligo(dT)$_{15}$ Primer (C1101), Random Primers (C1181), dNTP Mix (U1511), RNasin Ribonuclease Inhibitor (N2111), Wizard SV Gel and PCR Clean-Up System, Wizard *Plus* Minipreps DNA Purification System, PureYield Plasmid Midiprep System, *E. coli* Competent Cells, JM109 Competent Cells, >108 cfu/µg* (L2001) (Promega Corp., Madison, WI, USA).
- T4 DNA Ligase (with PEG) **(**EL0334), *Pfu* DNA Polymerase (EP0501), FastAP. Thermosensitive Alkaline Phosphatase (EF0654), Restriction enzymes used were in fast digest format (Fermentas-www.fermentas.com).
- HIT Competent Cells, High 10^8 HIT-DH5a - (RH618) (RBC Bioscience Corporation 12F, Taipei county 235, Taiwan).

CHAPTER 5
RESULTS

5.1. Petiole abscission response to leaf deblading and ethylene treatments

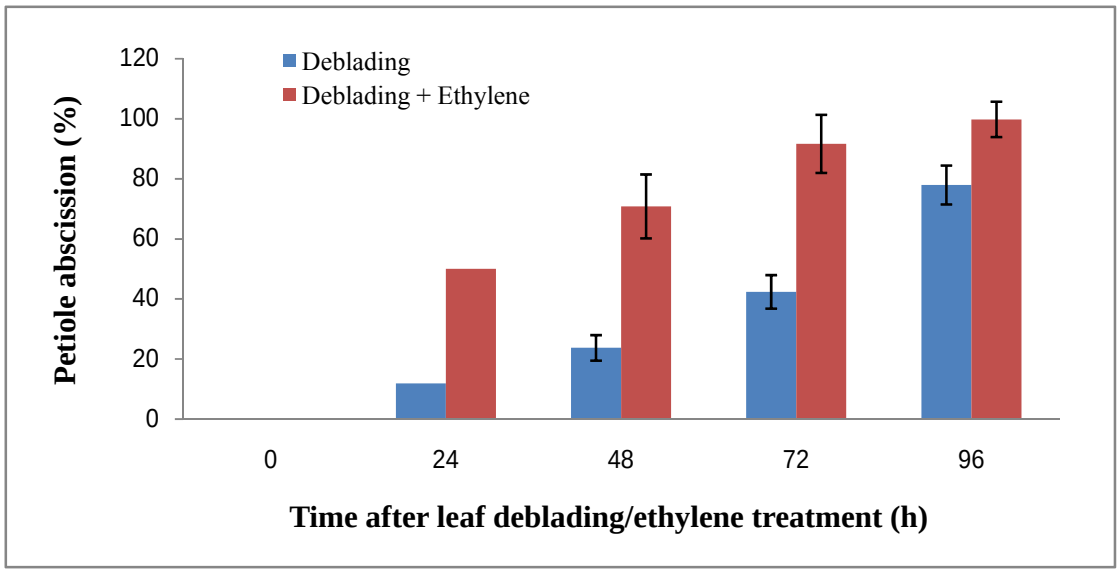

Figure 8: Effects of leaf deblading and ethylene treatment (5 µl/L for 24 h at 20°C) on petiole abscission of tomato cv. 'VF-36' explants. Immediately after leaf deblading, half of the explants were exposed to 5 µl/L ethylene for 24 h to enhance petiole abscission. The results are the means of three replicates (30 leaves each) ± SD.

Leaf petioles did not abscise upto 24 h after deblading, whereas the flower pedicels started to abscise 8 h after flower removal (Appendix 1, Fig. 2). Ethylene treatment applied for 24 h had no effect on leaf abscission in control (without deblading) plants during at least 96 h after application (data not shown). On the other hand, in debladed plants, the ethylene effect on petiole abscission was already pronounced 24 h after the treatment. Thus, 50% of the petioles abscised after 24 h in response to ethylene, whereas in untreated debladed plants, only 10% of the petioles abscised (Fig. 8). After 96 h, almost 100% of the petioles in the ethylene-treated plants abscised, whereas in debladed control plants only 80% of the petioles abscised. These results indicate that ethylene is effective in inducing abscission only in debladed plants.

5.2. Expression analysis of abscission-related cell-wall modifying genes

5.2.1. Expression analysis of *TAPG1*

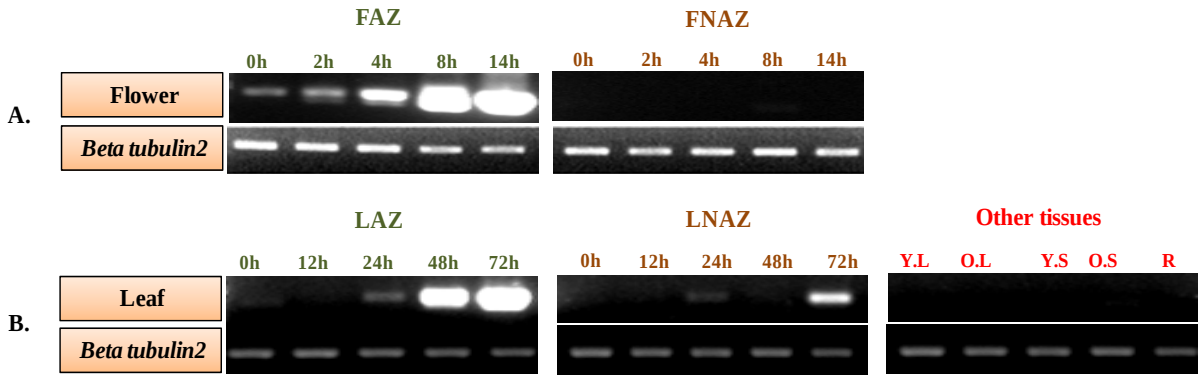

Figure 9: Effects of flower removal (A) or leaf deblading (B) on *TAPG1* expression in the FAZ and FNAZ (A), LAZ and LNAZ (B) at various time points (h) after organ removal, and in other tissues – young leaves (YL), old leaves (OL), young shoots (YS), old shoots (OS) and roots (R) – compared with *Beta tubulin2* as a reference gene. The data were validated by applying sq-PCR in two independent biological replicates and obtaining similar results.

The cell-wall hydrolyzing enzyme genes was used as a reference for analyzing and confirming the microarray results (Appendix 1, Fig. 4), because its expression pattern had been well studied. Our results show that tomato abscission *PG1* (*TAPG1*) gene was highly specific to AZs. *TAPG1* was highly expressed in the FAZs and LAZs in parallel with the abscission rate (Fig. 9 and Appendix 1, Fig. 2). The gene was not expressed in the FNAZ, but was weakly expressed in the LNAZ 24 and 72 h after deblading. In the FAZ, its expression was low at 0 h but increased gradually up to 14 h after flower removal (Fig. 9A). These results were consistent with the microarray results (Appendix 1, Fig. 4A). In the LAZ, expression was weaker than that in the FAZ; it followed the same pattern as in the latter, but started to appear at 24 h and attained a maximum 72 h after deblading (Fig. 9B). *TAPG1* was not expressed in young and old leaves, young and old shoots, and roots (Fig. 9).

5.2.2. Expression analysis of *TAPG2*

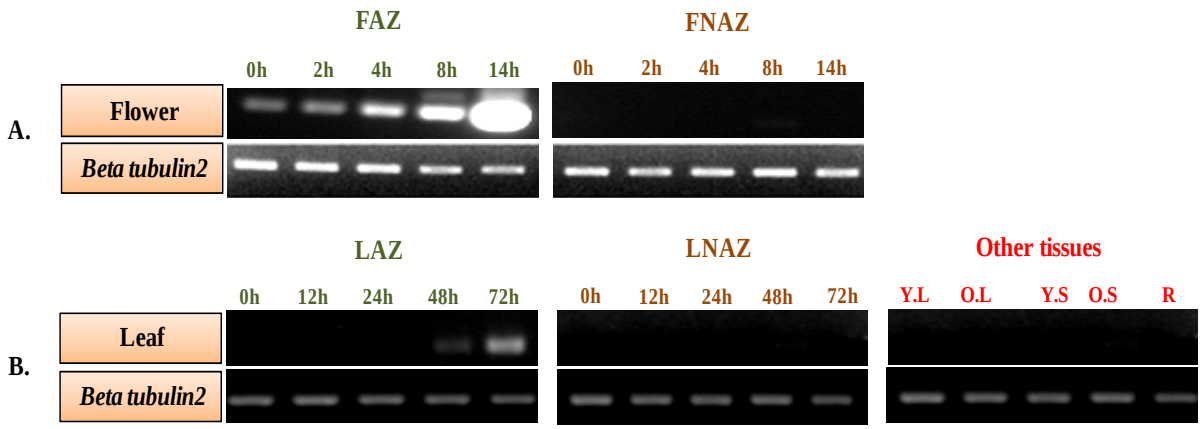

Figure 10: Effects of flower removal (A) or leaf deblading (B) on *TAPG2* expression in the FAZ and FNAZ(A), LAZ and LNAZ (B) at various time points (h) after organ removal, and in other tissues – young leaves (YL), old leaves (OL), young shoots (YS), old shoots (OS) and roots (R) – compared with *Beta tubulin2* as a reference gene. The data were validated by applying sq-PCR in two independent biological replicates and obtaining similar results.

The tomato abscission *PG2* (*TAPG2*) gene was highly specific to the AZs, and did not show any expression in the NAZs of flowers or leaves (Fig. 10). The gene was expressed at all times in the FAZ, at a low level at zero time, with a gradual increase to a maximum 14 h after flower removal (Fig. 10A). These results were consistent with the microarray results (Appendix 1, Fig. 4B). In the LAZ, *TAPG2* expression started to appear after 48 h and increased towards 72 h after leaf deblading (Fig. 10B). *TAPG2* expression in LAZ was lower than in the FAZ, and lower than that of other *TAPGs* in the LAZ. Similarly, to other tomato abscission *PGs*, *TAPG2* was not expressed in any other tissues, such as leaves, shoots, and roots (Fig. 10).

5.2.3. Expression analysis of *TAPG4*

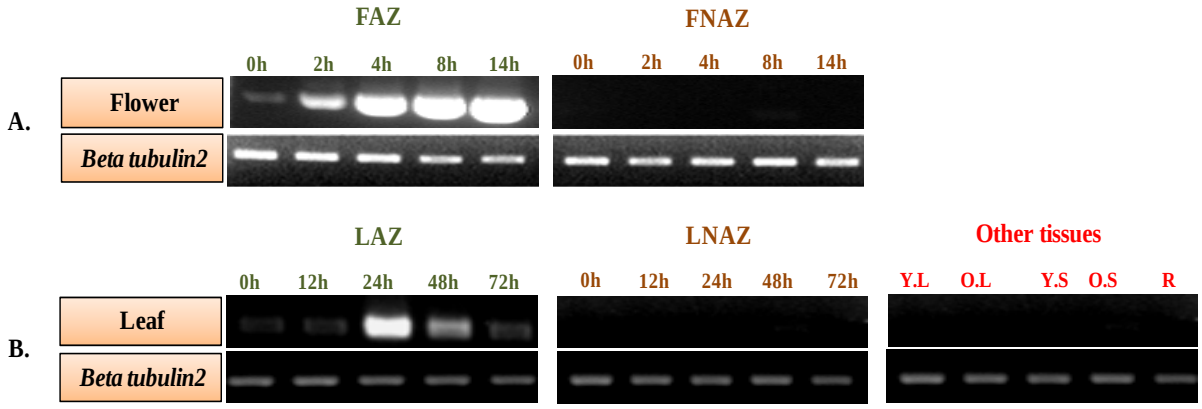

Figure 11: Effects of flower removal (A) or leaf deblading (B) on *TAPG4* expression in the FAZ and FNAZ (A), LAZ and LNAZ (B) at various time points (h) after organ removal, and in other tissues – young leaves (YL), old leaves (OL), young shoots (YS), old shoots (OS) and roots (R) – compared with *Beta tubulin2* as a reference gene. The data were validated by applying sq-PCR in two independent biological replicates and obtaining similar results.

The tomato abscission *PG4* (*TAPG4*) gene was highly specific to the AZs (Fig. 11): it showed higher and earlier expression in the AZs compared to other tomato abscission PGs, *TAPG1* and *TAPG2*. Its expression level in the FAZ was low at 0 h, but increased gradually to a maximum 14 h after flower removal (Fig. 11A). These results were consistent with the microarray results (Appendix 1, Fig. 4C). In the LAZ, *TAPG4* expression started at 0 h, reached a peak 24 h after deblading, and then decreased from 24 to 72 h (Fig. 11B). Expression in the LAZ was lower than in the FAZ, and there was no expression in the FNAZ, LNAZ, leaves, shoots, and roots (Fig. 11).

5.2.4. Expression analysis of *Cel1*

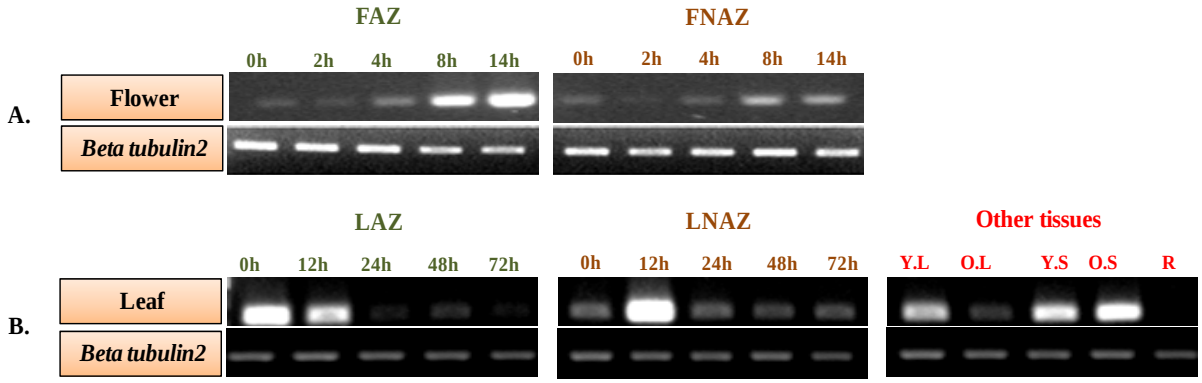

Figure 12: Effects of flower removal (A) or leaf deblading (B) on *Cel1* expression in the FAZ and FNAZ (A), LAZ and LNAZ (B) at various time points (h) after organ removal, and in other tissues – young leaves (YL), old leaves (OL), young shoots (YS), old shoots (OS) and roots (R) – compared with *Beta tubulin2* as a reference gene. The data were validated by applying sq-PCR to two independent biological replicates and obtaining similar results.

Cel1 was expressed in all the examined tissues, except roots (Fig. 12), unlike the other abscission-related cell-wall hydrolyzing enzymes, *TAPG1, TAPG2,* and *TAPG4,* which were specific to the AZs (Figs. 9A, 10A, 11A). *Cel1* was more highly expressed in FAZ than in the FNAZ: in the FAZ, the level of expression increased with time, and attained a maximum level 14 h after flower removal, whereas in the FNAZ it was expressed at a very low level, although it exhibited too an increasing trend (Fig. 12A). These results were consistent with the microarray results (Appendix 1, Fig. 4E). In the LAZ, *Cel1* expression was highest at 0 h and showed a slight decrease 12 h after deblading, a sharp decrease after 24 and 48 h, and no expression after 72 h (Fig. 12B). In the LNAZ, the expression level remained constant, except 12 h after deblading, when it attained its highest expression level, which was even higher than that in the FAZ. *Cel1* was more highly expressed in young than in old leaves, but its expression levels were very similar in young and old shoots; it was not expressed in roots (Fig. 12B).

5.2.5. Expression analysis of *XET- BR1*

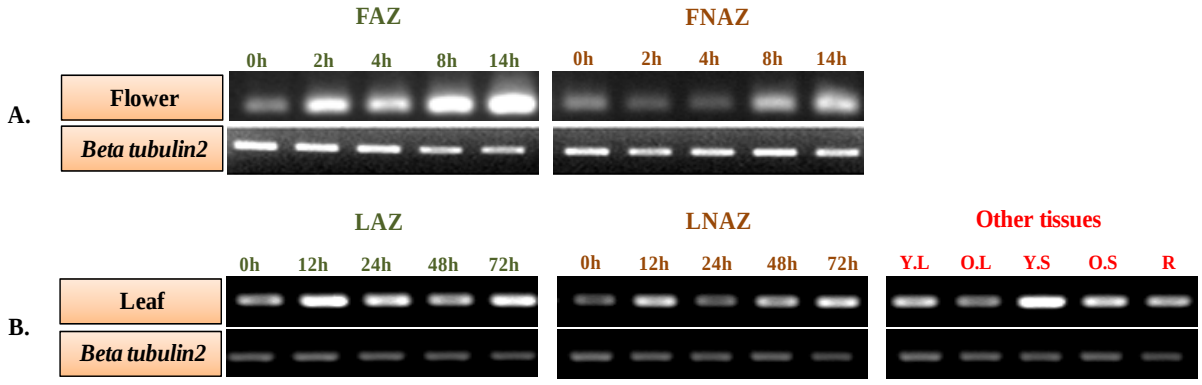

Figure 13: Effects of flower removal (A) or leaf deblading (B) on *XET-BR1* expression in the FAZ and FNAZ (A), LAZ and LNAZ (B) at various time points (h) after organ removal, and in other tissues – young leaves (YL), old leaves (OL), young shoots (YS), old shoots (OS) and roots (R) – compared with *Beta tubulin2* as a reference gene. The data were validated by applying sq-PCR to two independent biological replicates and obtaining similar results.

The activities of cell-wall degrading enzymes, including cellulase, PG, expansins and XET have been shown to increase dramatically with the onset of abscission (Lashbrook et al., 1994; Kalaitzis et al., 1997; Agusti et al., 2008; Cai and Lashbrook, 2008; Roberts and Gonzalez-Carranza, 2009). We regard *XET-BR1* as a novel FAZ-related gene (Appendix, 1 Fig. 4E); therefore, we were interested to study its expression levels in the LAZ and other plant tissues.

XET-BR1 was more highly expressed in the FAZ than in the FNAZ (Fig. 13A), although its expression patterns in both zones were similar to those of *Cel1* (Fig. 12A). In the FAZ, the expression level was low at 0 h, increased gradually as abscission progressed, and attained its maximum 14 h after flower removal (Fig. 13A). In the FNAZ, the expression levels at 2 and 4 h were the same, but lower than that at 0 h, and they showed an increasing trend from 8 to 14 h after flower removal. These results were consistent with the microarray results (Appendix 1, Fig. 4D). In the LAZ, *XET-BR1* was expressed in a low level at 0 h, attained a peak after 12 h after deblading and maintained more or less similar levels of expression thereafter (Fig. 13B). In the LNAZ, the expression level was low at 0 h, increased after 12 h, and decreased again after 24 h after deblading (Fig. 13B). Young leaves and shoots showed higher expression levels than old ones, and the expression level in roots was similar to that observed in old leaves and shoots (Fig. 13B).

5.3. Expression analysis of ethylene-related genes

5.3.1. Expression analysis of *ERF2*

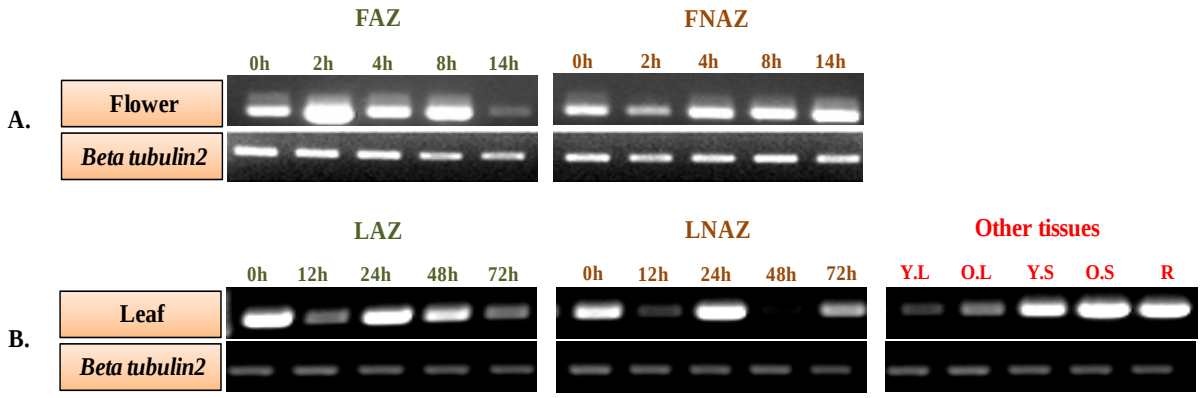

Figure 14: Effects of flower removal (A) or leaf deblading (B) on *ERF2* expression in the FAZ and FNAZ (A), LAZ and LNAZ (B) at various time points (h) after organ removal, and in other tissues – young leaves (YL), old leaves (OL), young shoots (YS), old shoots (OS) and roots (R) – compared with *Beta tubulin2* as a reference gene. The data were validated by applying sq-PCR to two independent biological replicates and obtaining similar results.

ERF2 expression pattern in the FAZ (Fig. 14A) was quite similar to that of the Myb transcription factor (*MybSt1*) in the microarray results (Appendix 1, Fig. 9C and Appendix 2, Fig. 1B). In the FAZ, *ERF2* expression was low at 0 h showed a transient increase during the 2 h period after flower removal, followed by a decline and a slight increase after 4 and 8 h, respectively, and expressed in a very low level after 14 h (Fig. 14A). This gene was one of the early up-regulated genes 2 h after flower removal. In the FNAZ, *ERF2* expression paralleled the microarray results at all time points, except at 2 h after flower removal, when it differed from the microarray results in showing increased expression after 2 h (Appendix 1, Fig. 9C). In the LAZ, *ERF2* was highly expressed at 0 h, after which its expression decreased sharply 12 h after deblading, started to increase again at 24 h, and again declined after 48 and particularly 72 h after deblading (Fig. 14B). The more or less similar expression pattern was obtained in the LNAZ. *ERF2* was more highly expressed in both young and old shoots than in leaves. Old leaves showed higher expression levels than young leaves, and the expression level in roots was similar to that observed in shoots (Fig. 14B).

5.3.2. Expression analysis of *ERF1c*

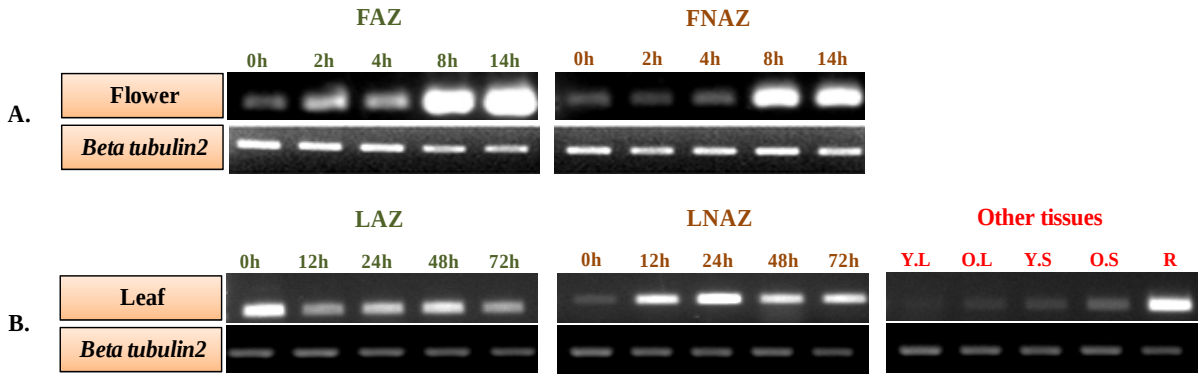

Figure 15: Effects of flower removal (A) or leaf deblading (B) on *ERF1c* expression in the FAZ and FNAZ (A), LAZ and LNAZ (B) at various time points (h) after organ removal, and in other tissues – young leaves (YL), old leaves (OL), young shoots (YS), old shoots (OS) and roots (R) – compared with *Beta tubulin2* as a reference gene. The data were validated by applying sq-PCR to two independent biological replicates and obtaining similar results.

The level of *ERF1c* expression was higher in the FAZ than in the FNAZ at all time points (Fig. 15A). In the FAZ, its expression increased gradually from 0 to 14 h after flower removal. The sq-PCR results (Fig. 15A) for the FAZ matched the microarray results, which showed a low expression at 0 h, a transient increase 2 h after flower removal, a decline starting at 4 h, and an increase between 8 and 14 h (Appendix 1, Fig. 9B). In the FNAZ, the sq-PCR results disagreed with the microarray results (Appendix 1, Fig. 9B): *ERF1c* expression levels remained fairly uniform from 0 to 4 h after flower removal, and rose after 8 and 14 h. The expression level in the LAZ was high at 0 h, declined 12 h after deblading, and remained constant between 24 and 72 h (Fig. 15B). The expression level in the LNAZ was low at 0 h, increased 12 h after deblading, reached a peak at 48 h, and declined slightly after 72 h (Fig. 15B). The expression levels in leaves and shoots were lower than in the LAZ and LNAZ; they remained constant in the leaves and shoots. *ERF1c* was highly expressed in roots (Fig. 15B).

5.3.3. Expression analysis of *JERF3*

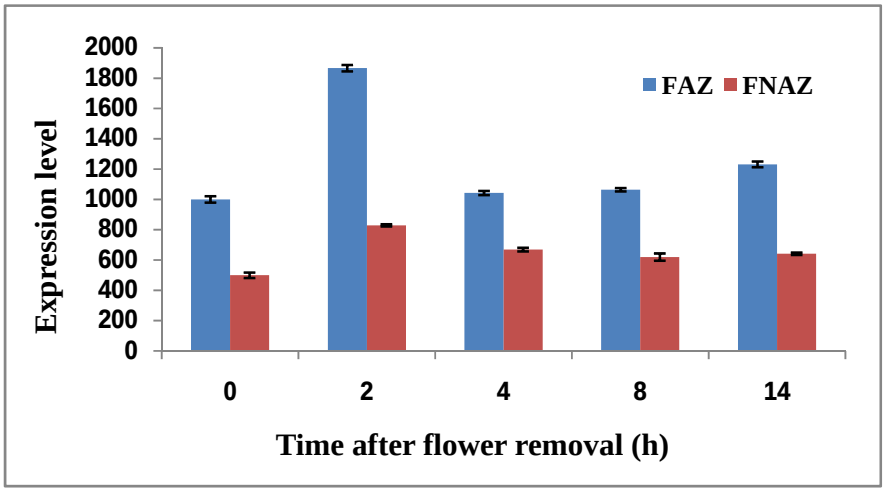

Figure 16: Effects of flower removal on *JERF3* expression in the FAZ and FNAZ at various time points (h) compared with *Actin* as a reference gene. The data were validated by applying real-time qPCR to two independent biological replicates and obtaining similar results.

JERF3 was more highly expressed in the FAZ than in the FNAZ before flower removal and at all times after flower removal (Fig. 16). In the FAZ, the expression level was low at 0 h and peaked 2 h after flower removal. A similar expression pattern of *JERF3* was obtained also in the FNAZ, but with lower levels than in the FAZ (Fig. 16). These results were consistent with the microarray results (Appendix 2, Fig. 1F). *JERF3* was among the early up-regulated genes, whose expression was transiently up- regulated within 2 h after flower removal.

5.3.4. Expression analysis of *ERF4* (AP2 transcription factor)

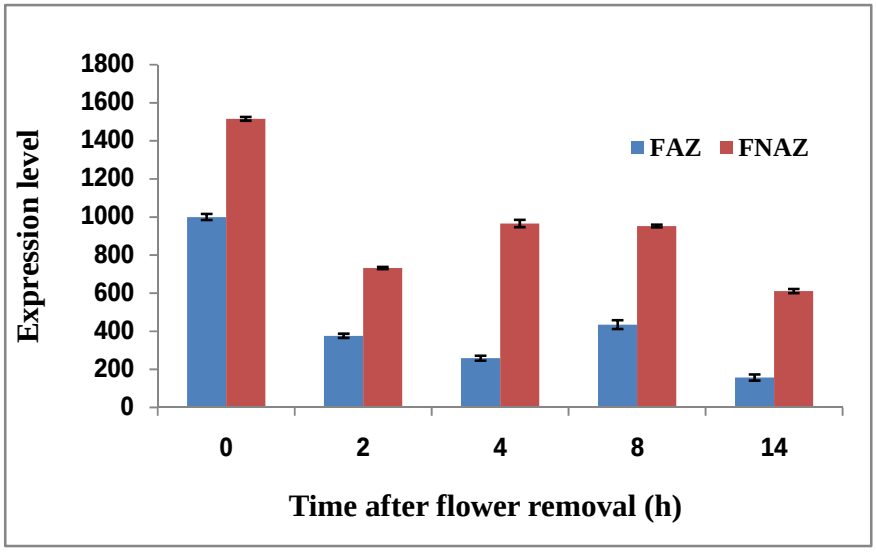

Figure 17: Effects of flower removal on *ERF4* expression in the FAZ and FNAZ at various time points (h) compared with *Actin* as a reference gene. The data were validated by applying real-time qPCR to two independent biological replicates and obtaining similar results.

ERF4 was more highly expressed in the FNAZ than in the FAZ (Fig. 17). In the FAZ, the maximum expression was at 0 h; it started to decline significantly within 2 h after flower removal, and remained low after 4, 8, and 14 h. In the FNAZ, the gene was also initially highly expressed, and its expression decreased significantly 2 h after flower removal, increased after 4 h, remained the same after 8 h, and decreased again after 14 h. *ERF4* was among the early down-regulated genes, whose expression in the FAZ was down-regulated within 2 h after flower removal (Fig. 17). These results were consistent with the microarray results (Appendix 1, Fig. 9E). All the other examined *ERF*s were up-regulated within 2 h after flower removal, while *ERF4* was the only one to be down-regulated within this time period (Appendix 1, Fig. 9).

5.3.5. Expression analysis of *ERT10 – Ripening-related burst oxidase protein D* (*RbohD*)

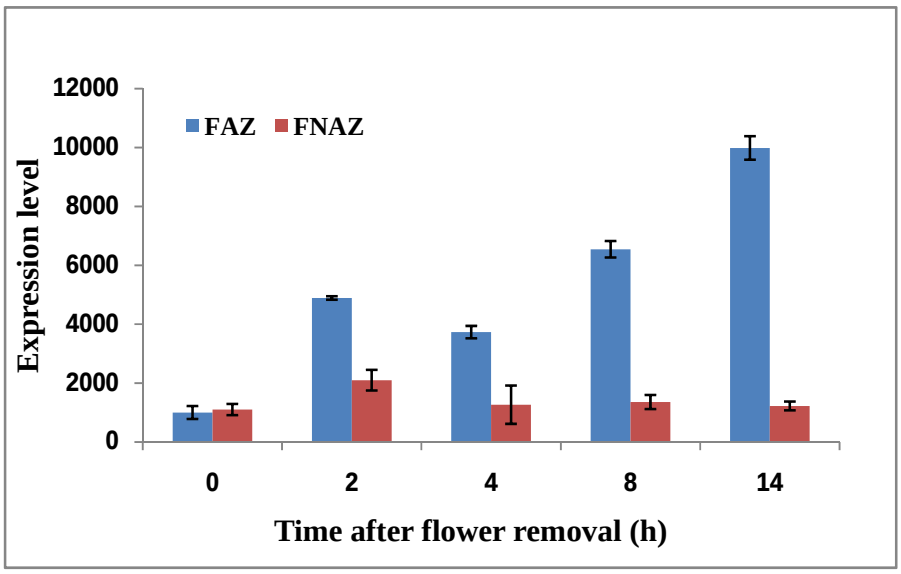

Figure 18: Effects of flower removal on *ERT10* expression in the FAZ and FNAZ at various time points (h) compared with *Actin* as a reference gene. The data were validated by applying real-time qPCR to two independent biological replicates and obtaining similar results.

ERT10 expression pattern (Fig. 18) was quite similar to that of *ERF1c* (Fig. 15). *ERT10* expression levels were similar in the FAZ and FNAZ at 0 h. In the FAZ, its expression showed a significant increase at 2 h, declined at 4 h, and then gradually increased toward a maximum at 14 h after the flower removal (Fig. 18). Its level in the FNAZ remained almost constant and lower than that observed in the FAZ at all time points (Fig. 18). *ERT10* was expressed specifically in the FAZ. These results were consistent with the microarray results (Appendix 1, Fig. 10D).

5.4. Expression analysis of other transcription factors and confirmation of the flower abscission microarray experiments

5.4.1. Expression analysis of *MybSt1* transcription factor

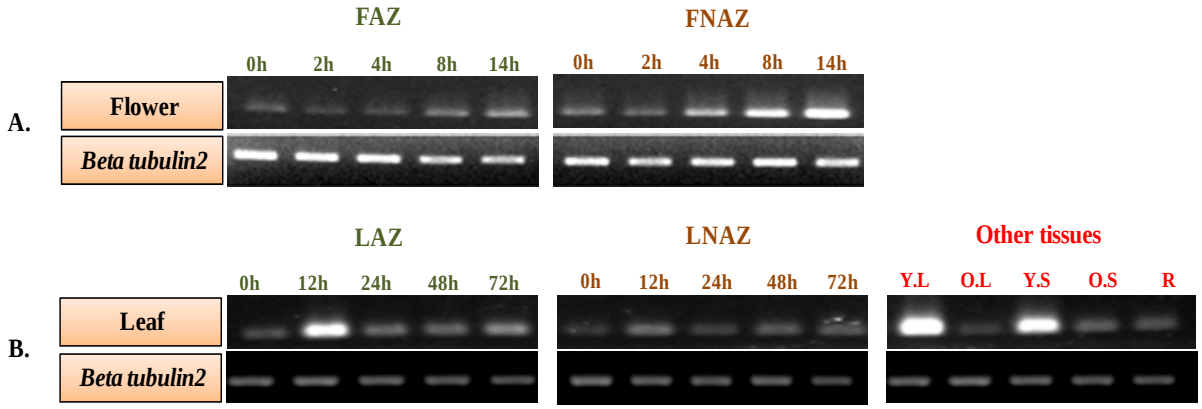

Figure 19: Effects of flower removal (A) or leaf deblading (B) on *MybSt1* expression in the FAZ and FNAZ (A), LAZ and LNAZ (B) at various time points (h) after organ removal, and in other tissues – young leaves (YL), old leaves (OL), young shoots (YS), old shoots (OS) and roots (R) – compared with *Beta tubulin2* as a reference gene. The data were validated by applying sq-PCR to two independent biological replicates and obtaining similar results.

The microarray (Appendix 2, Fig. 1B) and sq-PCR (Fig. 19) results for *MybSt1* did not agree with each other. The expression of *MybSt1* TF in the FAZ (Fig. 19A) maintained the same level 0, 2, 4 h after flower removal, and increased at 8 and 14 h, whereas in the microarray results *MybSt1* TF expression level transiently increased 2 h after flower removal in both the FAZ and the FNAZ (Appendix 2, Fig. 1B). On the other hand, a transient increase in *MybSt1* expression was observed in the LAZ (Fig. 19B). Overall, a higher expression was found in the FNAZ than in the FAZ, which match the microarray results. In the LAZ, the initial expression level was low; it maximized 12 h after deblading and then started to decline. The same expression pattern was observed in the LNAZ. The expression levels were higher in young leaves and shoots than in older ones, and were very low in old leaves, old shoots, and roots (Fig. 19B).

5.4.2. Expression analysis of *PHANTASTICA*

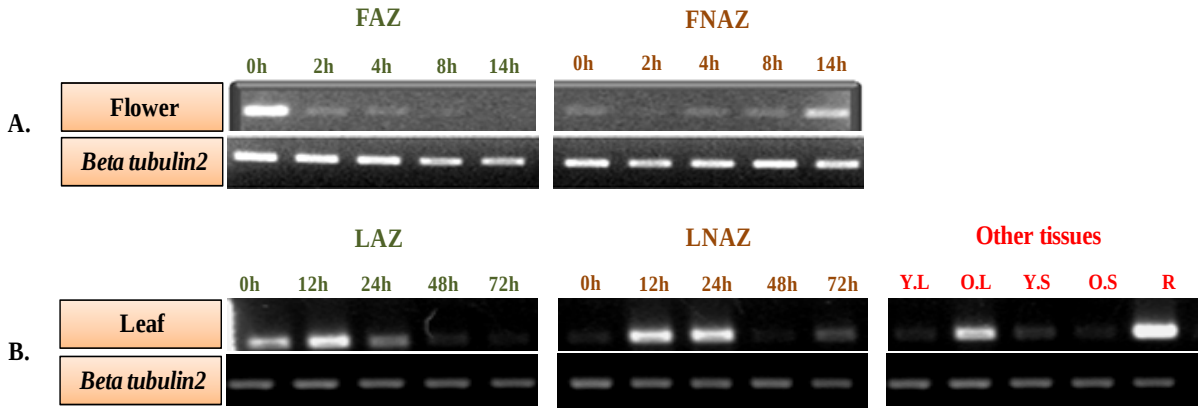

Figure 20: Effects of flower removal (A) or leaf deblading (B) on *PHANTASTICA* expression in the FAZ and FNAZ (A), LAZ and LNAZ (B) at various time points (h) after organ removal, and in other tissues – young leaves (YL), old leaves (OL), young shoots (YS), old shoots (OS) and roots (R) – compared with Beta tubulin2 as a reference gene. The data were validated by applying sq-PCR to two independent biological replicates and obtaining similar results.

PHANTASTICA (*PHAN*) was highly expressed in the FAZ at 0 h, and was down-regulated within 2 h after flower removal; it was one of the early down-regulated genes in the FAZ after flower removal (Fig. 20A). The expression level of *PHAN* in the FAZ was reduced drastically within 2 h after flower removal, it continued to decrease gradually, and completely disappeared after 14 h. Its expression level in the FNAZ was lower than that observed in the FAZ at 0 h, remained the same 2, 4, and 8 h after flower removal, and increased slightly after 14 h (Fig. 20A). These results were consistent with the microarray results (Appendix 2, Fig. 1C).

At 0 h the expression level of *PHAN* in the LAZ was higher than that obtained in the LNAZ (Fig. 20B). In the LAZ, the maximum expression was obtained 12 h after deblading, and then it decreased gradually towards 72 h. In the LNAZ, *PHAN* was highly expressed 12 h after deblading, remained the same after 24 h, and started to decrease towards 72 h (Fig. 20B). The expression level was higher in old than in young leaves. Young and old shoots had similar low expression levels, while the gene was highly expressed in roots (Fig. 20B).

5.4.3. Expression analysis of *KNOTTED*-like homeobox (*KNOX*) - *TKN4*

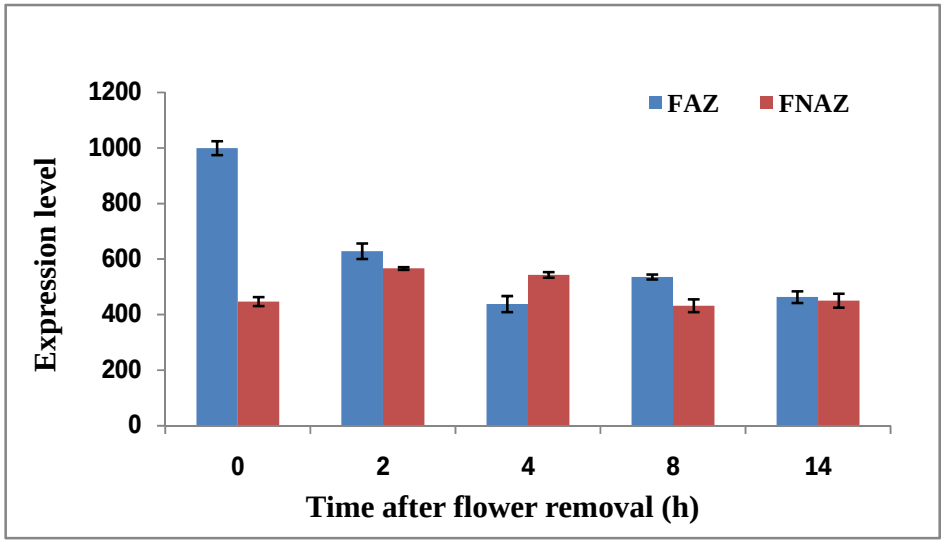

Figure 21: Effects of flower removal on *TKN4* expression in the FAZ and FNAZ at various time points (h) compared with *Actin* as a reference gene. The data were validated by applying real-time qPCR to two independent biological replicates and obtaining similar results.

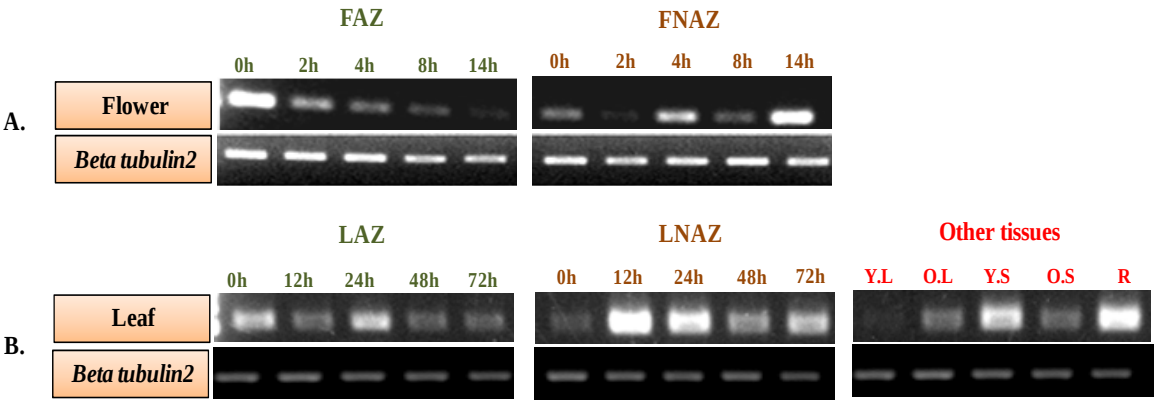

Figure 22: Effects of flower removal (A) or leaf deblading (B) on *TKN4* expression in the FAZ and FNAZ (A), LAZ and LNAZ (B) at various time points (h) after organ removal, and in other tissues – young leaves (YL), old leaves (OL), young shoots (YS), old shoots (OS) and roots (R) – compared with *Beta tubulin2* as a reference gene. The data were validated by applying sq-PCR to two independent biological replicates and obtaining similar results.

TKN4 was expressed more strongly in the FAZ than in the FNAZ, but it started to decline between 2 to 14 h after flower removal (Fig. 21A), and it was one of the early-expressed and early down-regulated genes in FAZ at 0 h, i.e. before flower removal. The results of both the real time-qPCR (Fig. 21) and the sq-PCR (Fig. 22A) analyses showed that at 0 h *TKN4* expression

was lower by a factor of two in the FNAZ than in the FAZ. *TKN4* expression level in the FNAZ was similarly low between 0 to 14 h according to the real-time PCR results (Fig. 21A), which were consistent with the microarray results (Appendix 1, Fig. 11B).

The expression pattern of *TKN4* in the LAZ was similar to that in the FAZ, except for a difference in transition times. In the control, i.e. at 0 h, the expression level in the LAZ was higher than that in the LNAZ, and resembled that obtained in flowers (Fig. 22B). In the LNAZ, the expression level was low at 0 h, reached a maximum 12 h after deblading, declined after 48 h, and increased again after 72 h. *TKN4* expression followed a declining pattern between 0 and 14 h in both the FAZ and the LAZ, i.e. it was one of the early down-regulated genes (Fig. 22B). *TKN4* showed much lower expression levels in young than in old leaves. It was more highly expressed in young than in old shoots, and showed the greatest expression in roots (Fig. 22B).

5.4.4. Expression analysis of *TAGL12*

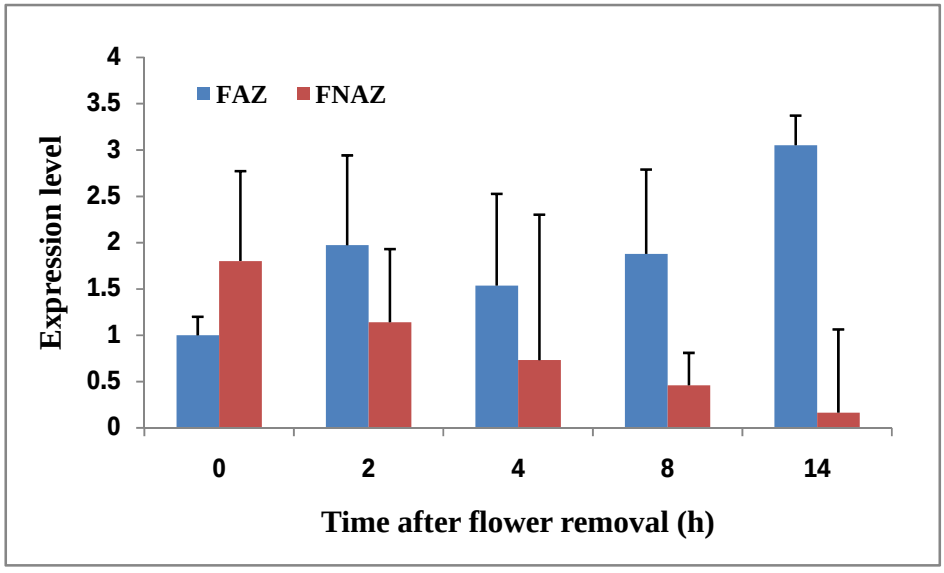

Figure 23: Effects of flower removal on *TAGL12* expression in the FAZ and FNAZ at various time points (h) compared with *Actin* as a reference gene. The data were validated by applying real-time qPCR to two independent biological replicates and obtaining similar results.

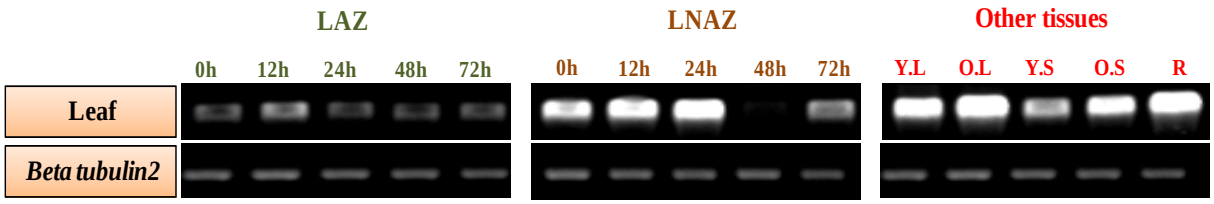

Figure 24: Effects of leaf deblading on *TAGL12* expression in LAZ and LNAZ at various time points (h), and in other tissues – young leaves (YL), old leaves (OL), young shoots (YS), old shoots (OS) and roots (R) – compared with *Beta tubulin2* as a reference gene. The data were validated by applying sq-PCR to two independent biological replicates and obtaining similar results.

The expression patterns of *TAGL12* in the FAZ and the FNAZ, as confirmed by sq-PCR (data not shown), did not agree with the microarray data (Appendix 1, Fig. 12C), but the real-time qPCR results (Fig. 23) matched the microarray data. This discrepancy could probably be due to the non-specificity of the primers used in sq-PCR for the experiments with flowers.

In the FAZ, the *TAGL12* expression level was low at 0 h, increased 2 h after flower removal, maintained a similar level after 8 h, and reached maximum at 14 h after flower removal (Fig. 23). It was one of the lately up-regulated genes after flower removal. In the FNAZ, *TAGL12* was more highly expressed at 0 h than in the FAZ and its expression declined gradually, reaching the lowest level 14 h after flower removal (Fig. 23).

In the LAZ, *TAGL12* expression remained at the same level except after 12 h, when it increased slightly (Fig. 24). In the LNAZ, the expression level was higher compared to that in LAZ, remained high 0, 12, and 24 h after deblading, declined after 48 h, and slightly increased after 72 h. The expression levels were higher in leaves, shoots, and roots than in the FAZ and LAZ, and were slightly lower in young leaves and shoots than in old ones (Fig. 24).

5.4.5. Expression analysis of *Homeobox-Leucine zipper* (*HB-13*)

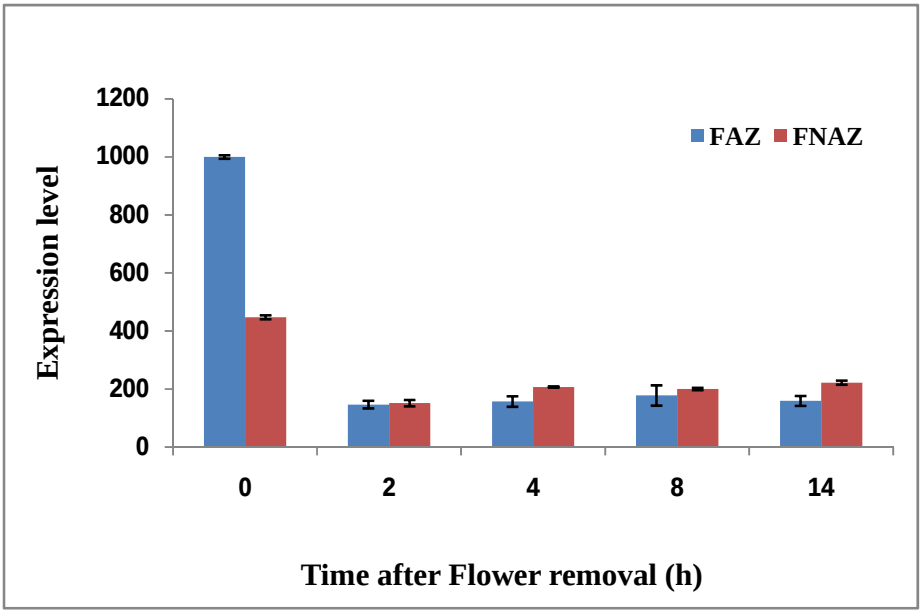

Figure 25: Effects of flower removal on *HB-13* expression in FAZ and FNAZ at various time points (h) compared with *Actin* as a reference gene. The data were validated by applying real-time qPCR to two independent biological replicates and obtaining similar results.

Homeobox-Leucine zipper (*HB-13*) TF was highly expressed in the FAZ at 0 h, was down-regulated within 2 h after flower removal, and remained low upto 14 h (Fig. 25). It was also expressed in the FNAZ, but the level of expression was only 40% of that in the FAZ at 0 h, but at all the other time points after flower removal, its expression level equaled that in the FAZ. It was one of the early down-regulated transcription factors in the FAZ. These results were consistent with the microarray results (Appendix 1, Fig. 11C).

5.4.6. Expression analysis of *Homeobox-Leucine Zipper* (CK715706)

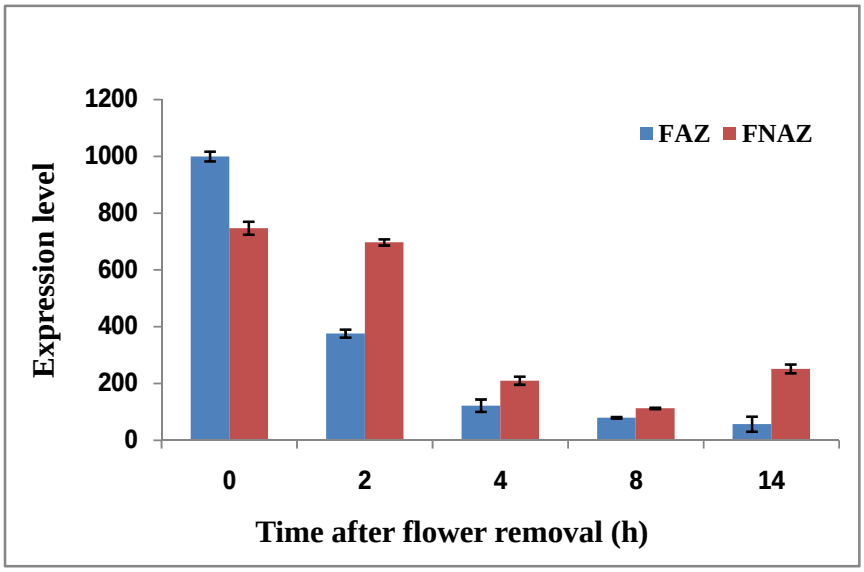

Figure 26: Effects of flower removal on *Homeobox-Leucine zipper* (CK 715706) expression in the FAZ and FNAZ at various time intervals points (h), compared with *Actin* as a reference gene. The data were validated by applying real-time qPCR to two independent biological replicates and obtaining similar results.

Homeobox-Leucine zipper gene (CK715706) was expressed in both the FAZ and the FNAZ. At 0 h, the expression level in the FAZ was higher than that in the FNAZ, and it declined linearly between 2 and 14 h after flower removal (Fig. 26). In the FNAZ, the expression at 0 h was lower than that in the FAZ, but its level was similar in both the AZs 4, 8 and 14 h after flower removal. *Homeobox-Leucine zipper* TF was among the early down-regulated TFs, whose expression in the FAZ was down-regulated within 2 h after flower removal. The real-time PCR results were in agreement with the microarray results (Appendix 1, Fig. 11E).

5.5. Regulatory genes

5.5.1. Expression analysis of the *Protein phosphatase-like*

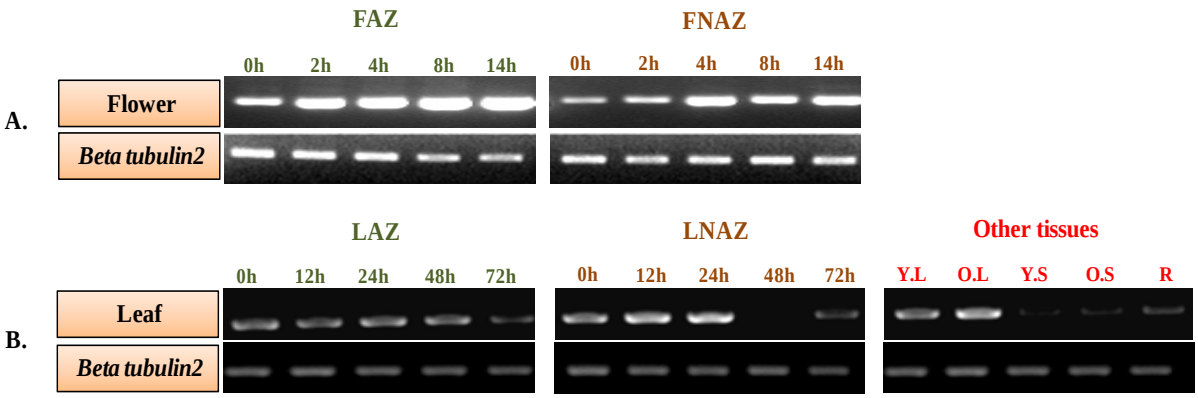

Figure 27: Effects of flower removal (A) or leaf deblading (B) on *Protein phosphatase-like* expression in the FAZ and FNAZ (A), LAZ and LNAZ (B) at various time points (h) after organ removal, and in other tissues – young leaves (YL), old leaves (OL), young shoots (YS), old shoots (OS) and roots (R) – compared with *Beta tubulin2* as a reference gene. The data were validated by applying sq-PCR to two independent biological replicates and obtaining similar results.

The *Protein phosphatase-like* gene was expressed in all the tissues examined. It was more highly expressed in the FAZ than in the FNAZ, and the expression levels in both the FAZ and the FNAZ increased gradually to a maximum level 14 h after flower removal (Fig. 27A). These results were consistent with the microarray results (Appendix 2, Fig. 1A).

The expression patterns in the LAZ and LNAZ were very different from those in the FAZ and the FNAZ (Fig. 27B). In the LAZ, the expression levels were constant between 0 to 48 h after deblading, and declined slightly after 72 h. In the LNAZ, the expression levels remained constant between 0 to 24 h after deblading, declined after 48 h, and showed a modest increase after 72 h (Fig. 27B). The *Protein phosphatase-like* gene was expressed more strongly in young and old leaves than in young and old shoots, and exhibited a very low level in the roots (Fig. 27B).

5.5.2. Expression analysis of *OVATE*

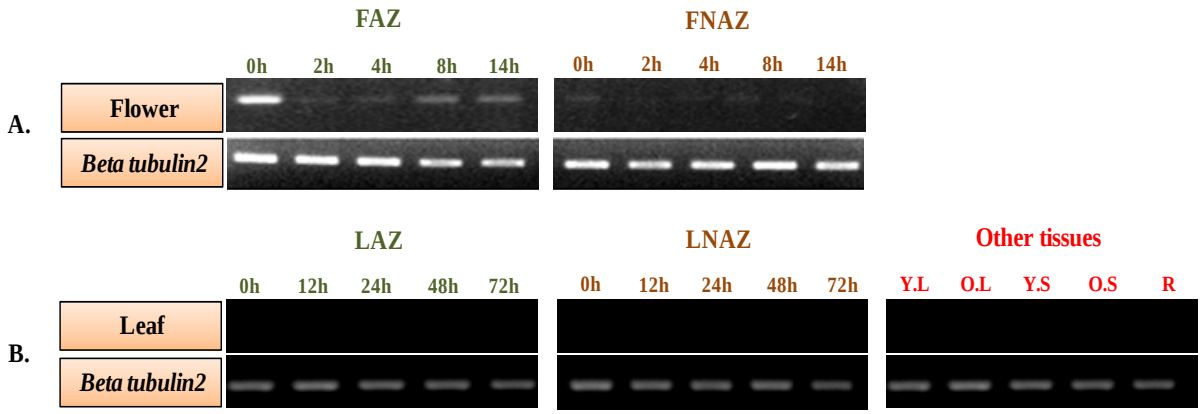

Figure 28: Effects of flower removal (A) or leaf deblading (B) on *OVATE* expression in the FAZ and FNAZ (A), LAZ and LNAZ (B) at various time points (h) after organ removal, and in other tissues – young leaves (YL), old leaves (OL), young shoots (YS), old shoots (OS) and roots (R) – compared with *Beta tubulin2* as a reference gene. The data were validated by applying sq-PCR to two independent biological replicates and obtaining similar results.

OVATE was highly expressed in the FAZ at 0 h, showed a sharp decline within 2 h after flower removal, increased slightly after 4 h, and again decreasaed slightly after 14 h (Fig. 28A). It was a specifically early down-regulated gene in the FAZ. In the FNAZ, there was a slight expression at 0 h, but none later, 4, 8, and 14 h after flower removal (Fig. 28A). These results were consistent with the microarray results (Appendix 2, Fig. 1D). There was no *OVATE* expression in the LAZ, the LNAZ, young and old leaves, young and old shoots, and roots (Fig. 28B).

5.5.3. Expression analysis of *TPRP-F1 - proline rich protein*

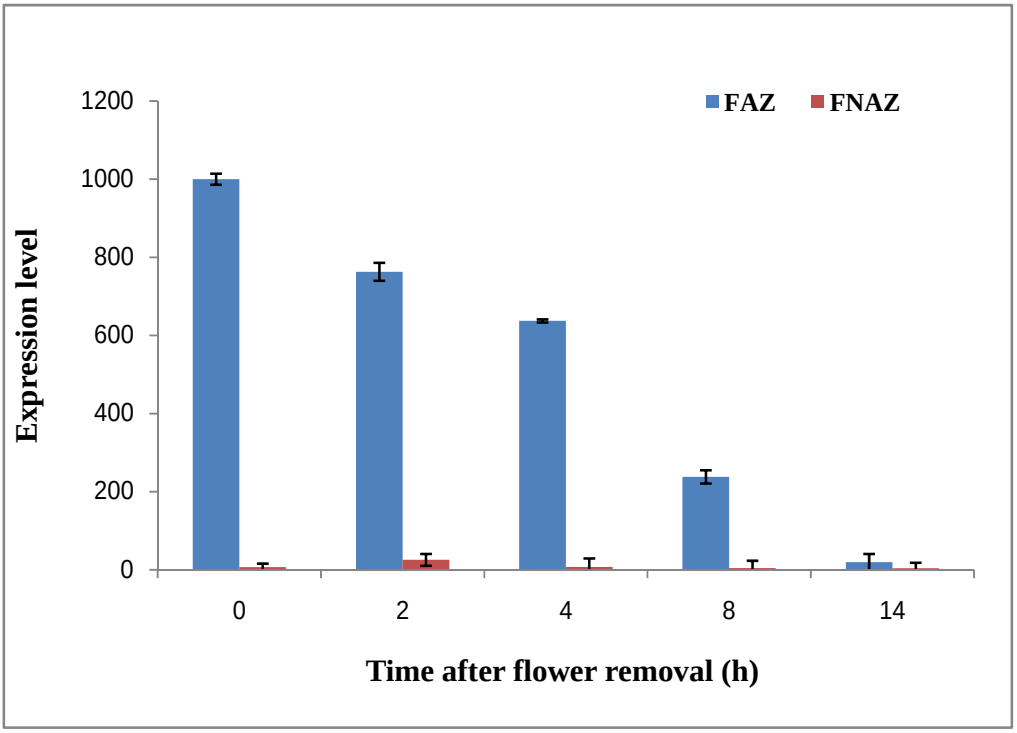

Figure 29: Effects of flower removal on *TPRP-F1* expression in the FAZ and FNAZ at various time points (h) compared with *Actin* as a reference gene. The data were validated by applying real-time qPCR to two independent biological replicates and obtaining similar results.

TPRP-F1 was highly expressed in the FAZ, in which it was highly specific (Fig. 29). It was highly expressed at 0 h, and its expression decreased gradually to a minimum level 14 h after flower removal. *TPRP-F1* expression was very low in the FNAZ, being negligible compared with that in the FAZ (Fig. 29). It seems therefore, that *TPRP-F1* is a FAZ-specific gene. These results were consistent with the microarray results (Appendix 1, Fig. 14D).

5.6. Sequence results of *JERF3* in the binary vector pART27

JERF3 was cloned into the pHANNIBAL vector in both sense and antisense orientations (each phase of cloning was proceeded after sequencing) within the NotI site. Then, the NotI fragment with the entire hairpin cassette was moved to the NotI site of the pART27 and sequenced from the different regions (4136thbp, 5122thbp of pHANNIBAL) with different primers (Table 6), in order to confirm that the entire hairpin structure was placed in the correct orientation, with no mutations. The final sequencing before transforming into *Agrobacterium* is presented in Figure 30.

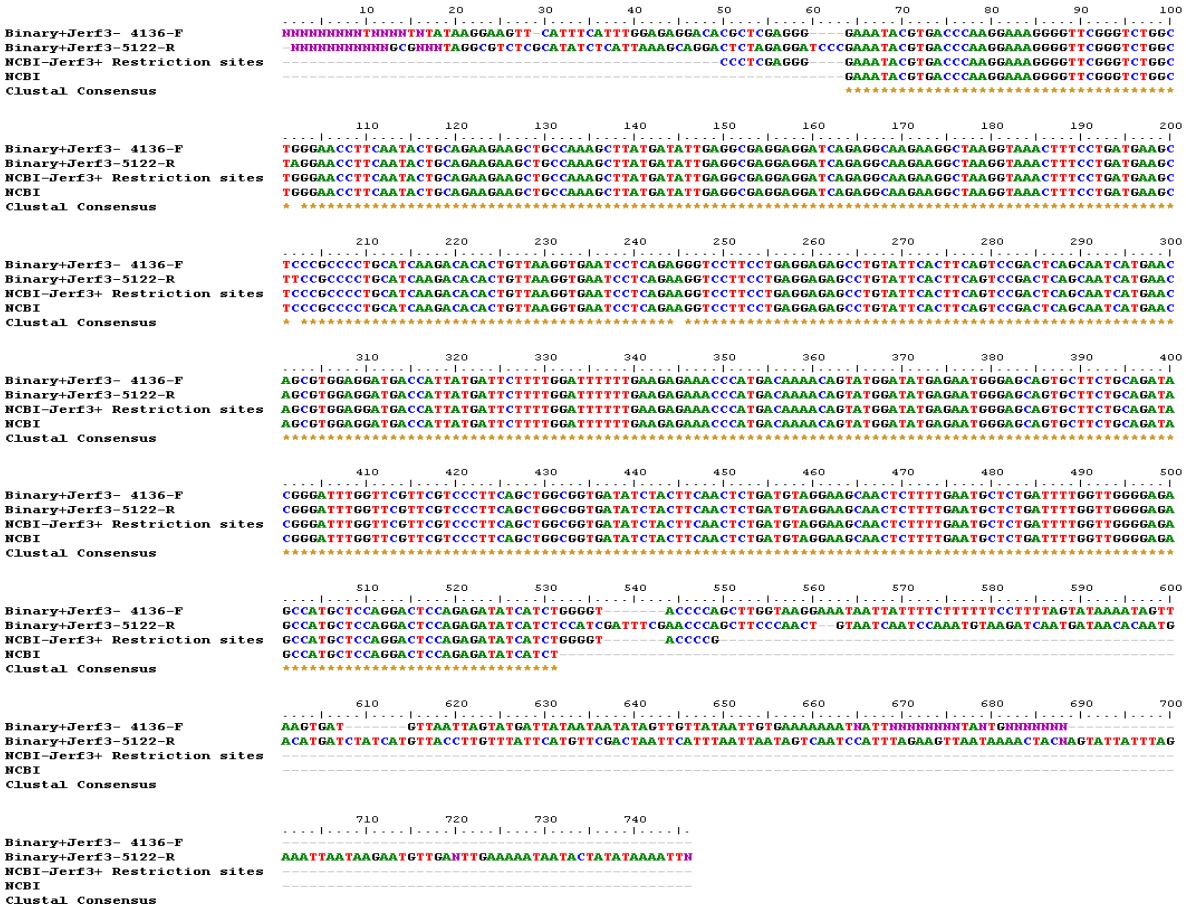

Figure 30: Sequence analysis of hairpin structure of *JERF3* in the pART27 vector before its transformation into *Agrobacterium*. Alignment of sequences obtained by sequencing pART27 vector with the sequences from: forward sequencing primer (4136 bp-F), reverse sequencing primer (5122 bp-R) (Table 6), sequence of cloned region of the *JERF3* (AY383630) from NCBI database, sequence of cloned region of the *JERF3* with restriction sites to identify the orientation of cloning.

XhoI- CTCGAG * KpnI- GGTACC * BamHI- GGATCC * ClaI- ATCGAT

5.7. Sequence results of *TKN4* in the binary vector pART27

TKN4 was cloned into the pHANNIBAL vector within the NotI site, in both sense and antisense orientations (each phase of cloning was proceeded after sequencing), within NotI site. Then, the NotI fragment, with the entire hairpin cassette, was moved to the NotI site of the pART27 and sequenced from the different regions (4136th, 5122th bp of pHANNIBAL) with different primers (Table 6), in order to confirm that the entire hairpin structure was placed in correct orientation, with no mutations. The final sequencing before transforming into *Agrobacterium* is presented in Figure 31.

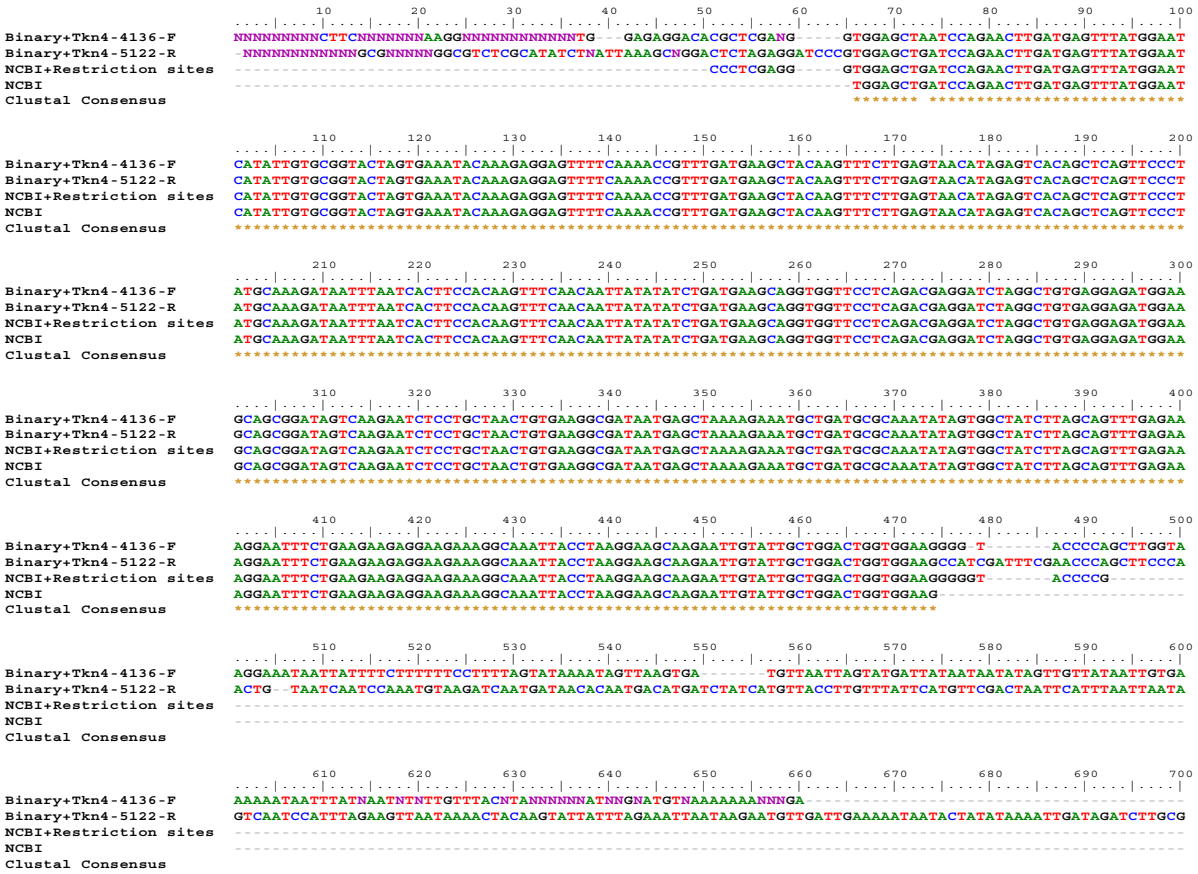

Figure 31: Sequence analysis of hairpin structure of *TKN4* in the pART27 vector before its transformation into *Agrobacterium*. Alignment of sequences obtained from sequencing of the pART27 vector with the sequences from forward sequencing primer (4136 bp-F), reverse sequencing primer (5122 bp-R) (Table 6), sequence of cloned region of the *TKN4* (AF533597) from NCBI database, sequence of cloned region of the *TKN4* with restriction sites to identify the orientation of cloning.
XhoI- CTCGAG * KpnI- GGTACC * BamHI- GGATCC * ClaI- ATCGAT

5.8. Sequence results of *ERF2* in the binary vector PGSA 1285

ERF2 was cloned into the PGSA 1285 vector in both sense and antisense orientations (each phase of cloning was proceeded after sequencing) and directly transferred into *Agrobacterium* because it served as both primary and binary vectors. The final sequence results before transforming into *Agrobacterium* with different primers (Table 4) from different regions is presented in Figure 32.

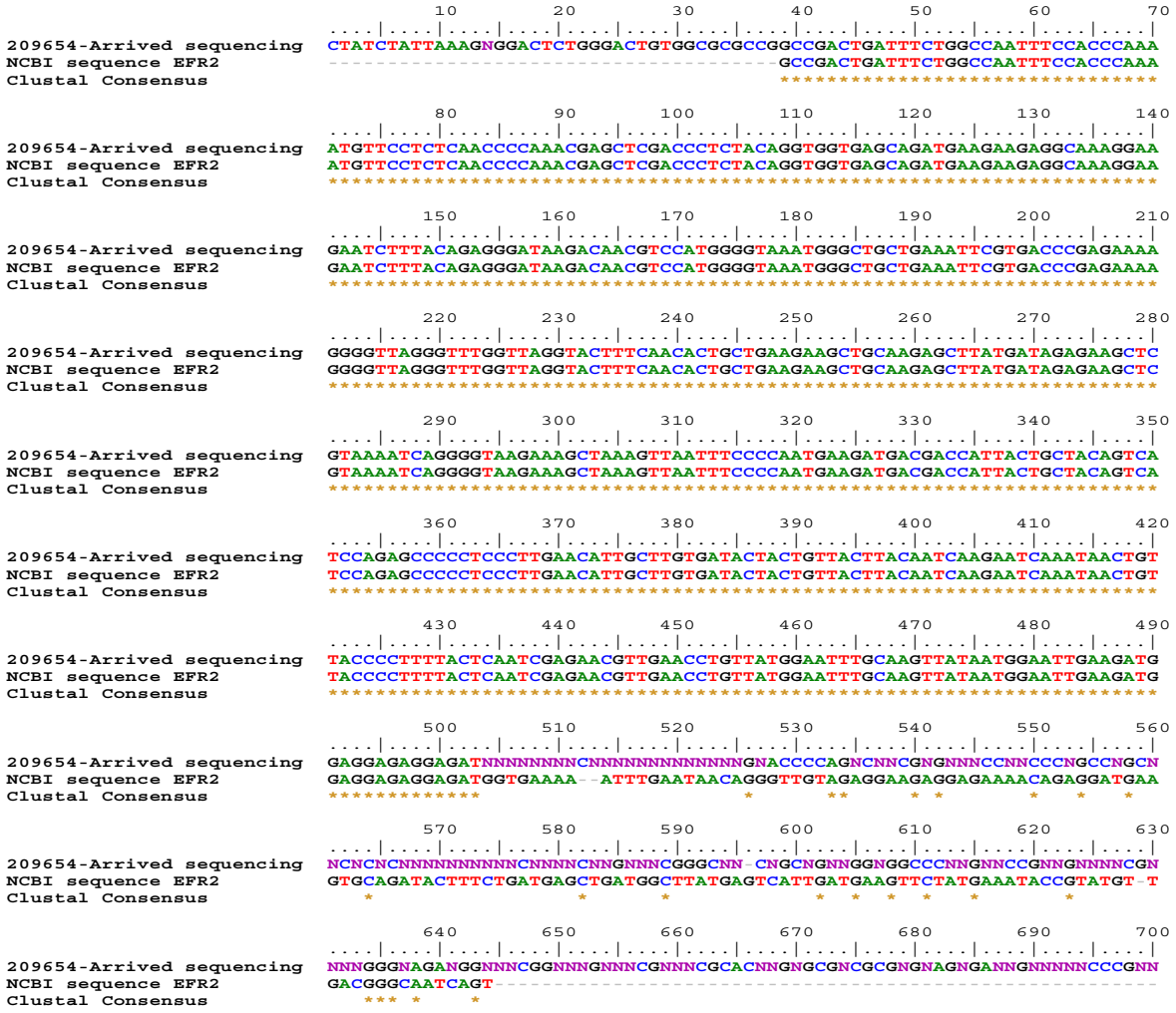

Figure 32: Sequence analysis of hairpin structure of *ERF2* in the PGSA 1285 vector before its transformation into *Agrobacterium*. Alignment of sequences obtained from sequencing of the PGSA 1285 vector with the sequences from forward sequencing primer (PGSA 2051-2219), reverse sequencing primer (PGSA 2483-2684 -R) (Table 4), and sequence of cloned region of the *ERF2* (TC 179207) from NCBI database.

5.9. Sequence results of *Protein phosphatase-like* in the binary vector PGSA 1285

Protein phosphatase-like was cloned into PGSA 1285 vector in both sense and antisense orientations (each phase of cloning was proceeded after sequencing) and directly transferred into *Agrobacterium* because it served as both primary and bianry vector. The final sequence results before transforming into *Agrobacterium* with different primers (Table 4) from different regions is presented in Figure 33.

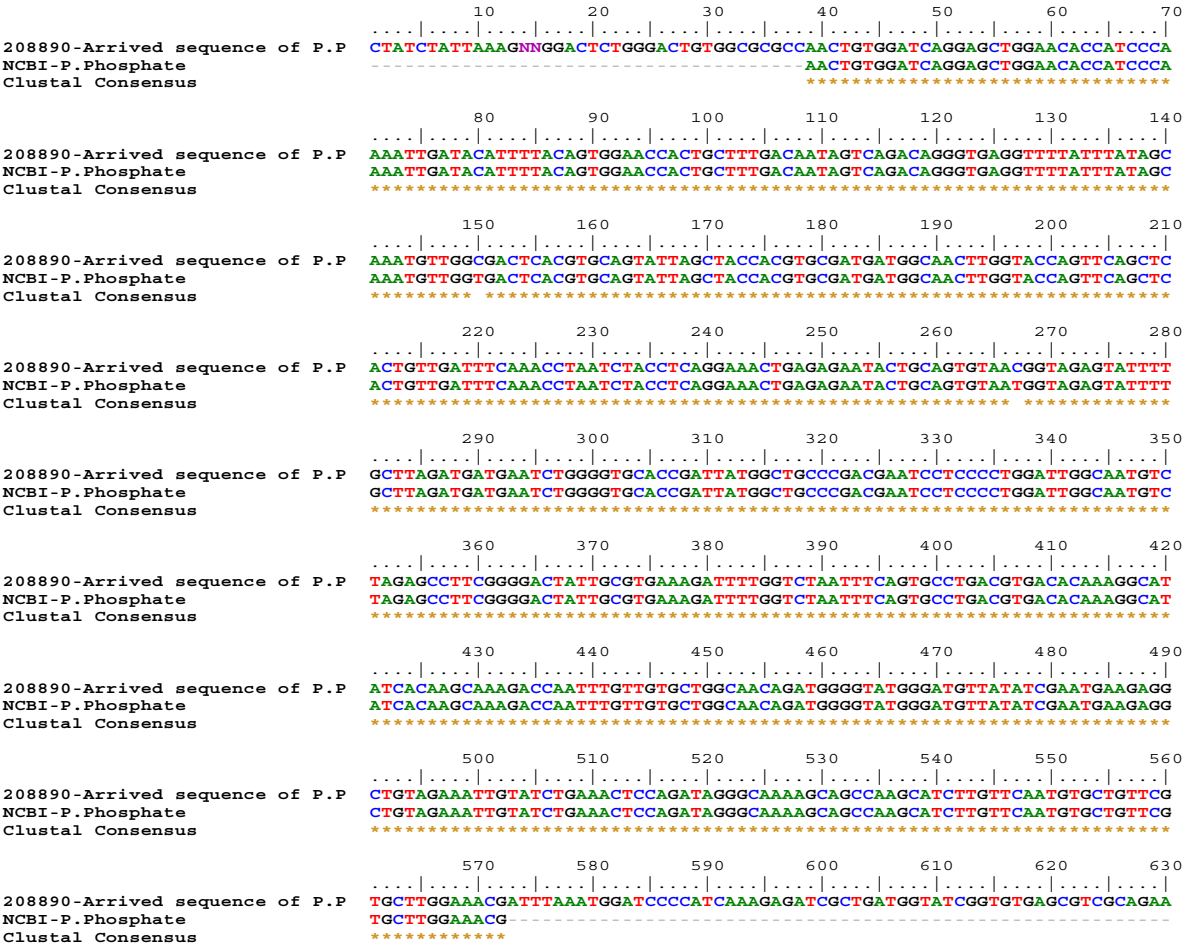

Figure 33: Sequence analysis of hairpin structure of *protein phosphatase-like* in the PGSA 1285 vector before its transformation into *Agrobacterium*. Alignment of sequences obtained from sequencing of the PGSA 1285 vector with the sequences from forward sequencing primer (PGSA 2051-2219), reverse sequencing primer (PGSA 2483-2684 -R) (Table 4), sequence of cloned region of the *Protein phosphatase* (TC 171978) from NCBI database.

5.10. Isolation of the *TAPG4* promoter and using it for RNAi constructs

In our expression studies, we noted that *TAPG4* was specifically expressed in the FAZ quiet early, 2 h after flower removal (Fig. 11A), and at higher levels than other *TAPG* genes (Figs. 9A, 10A). This suggests that the *TAPG4* promoter is a strong AZ-specific promoter, and therefore, it can be used for specific silencing of genes in the AZ to enable functional analysis. We cloned *TAPG4* from genomic DNA, using specific primers with restriction sites (Table 8) appropriate for our RNAi vectors. We assembled the RNAi constructs, driven by *TAPG4* as promoter, to induce tissue-specific silencing in the FAZ rather than in the entire plant, which would result from using the constitutive CaMV 35S promoter. The constructs for two genes, namely *JERF3* and *TKN4*, with *TAPG4* as promoter are now ready for transformation, and they are at phase IV (see Section 4.11). Hence, we expect to obtain phenotypes in a few months. The *proline-rich protein* (*TPRP-F1*) and *KD1* genes are in phase III of RNAi constructs. The sequence results after cloning the *TAPG4* promoter is presented below in Figure 34.

Continued Figure 34

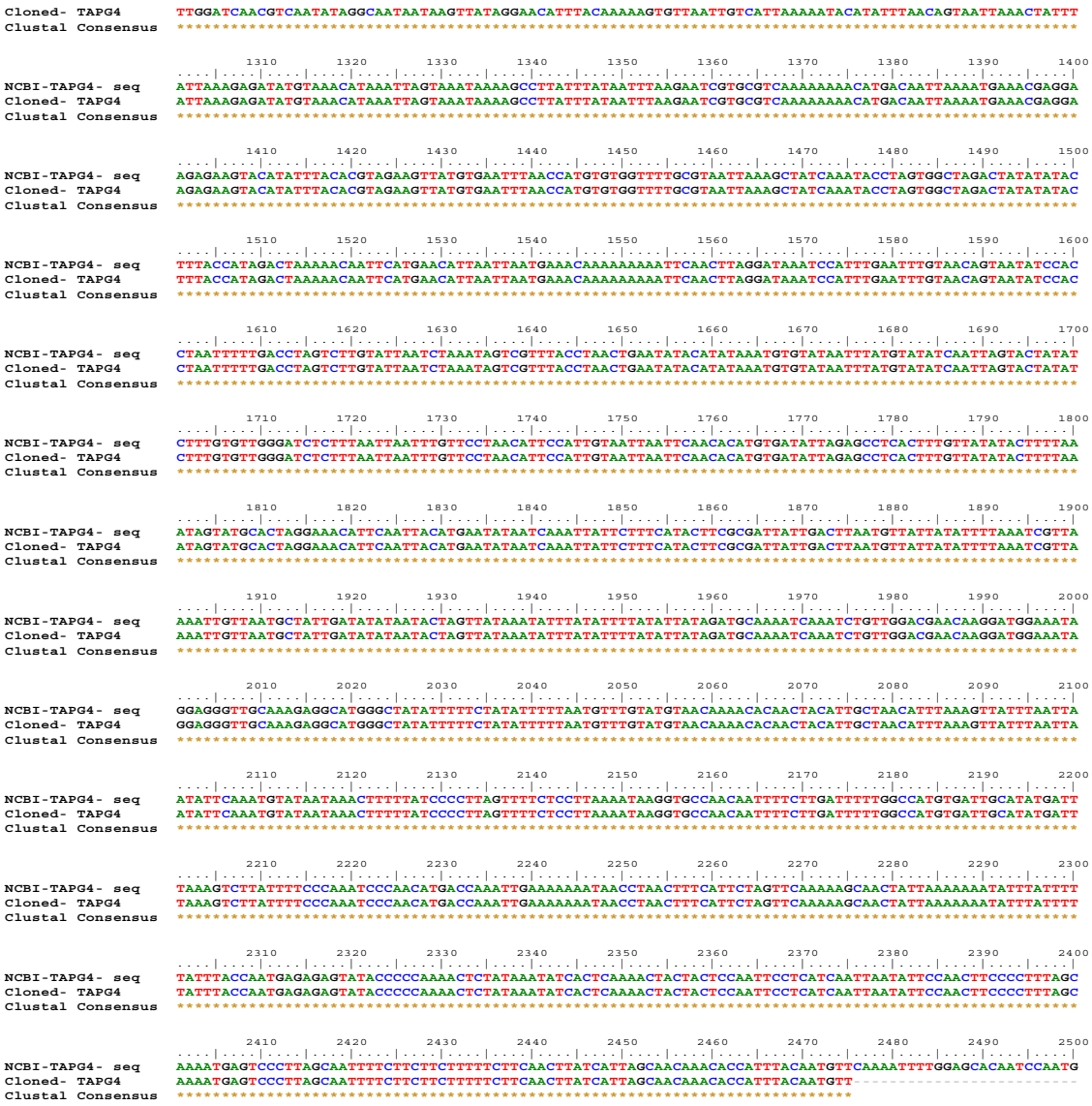

Figure 34: Isolation of *TAPG4* promoter: region from genomic DNA using the selected primers (Table 8) and alignment of cloned sequence with NCBI database *Lycopersicon esculentum TAPG4* (AF001002.1), complete cds sequence cloned by Hong and Tucker (1998).

CHAPTER 6

DISCUSSION

The main goal of the present study was to identify potential candidate genes that might regulate the abscission of tomato flowers or leaves for their detailed functional analysis. Our hypothesis suggests that following leaf deblading or flower removal, which eliminates IAA source, the hormone levels in the AZs would decline. This has two major consequences: firstly, the levels of a subset of genes (IAA-induced genes), whose expression is normally maintained by IAA, might decrease; secondly, the levels of a second subset of genes (IAA-repressed genes), whose expression is normally repressed by IAA, might be induced. The IAA-repressed genes, some of which may be related to ethylene sensitivity, can be induced either directly, as a result of reduction of IAA levels, or indirectly, as a result of the decline in *Aux/IAA* genes. This is possible since the *Aux/IAA* products can interact with *ARF* gene products, thereby affecting a wide range of IAA responses (Kim et al., 1997; Ulmasov et al., 1997). Because of up-regulation of ethylene sensitivity-related genes, the AZ becomes sensitive to ethylene, and the pedicels or petioles abscise in response to endogenous or exogenous ethylene.

We can separate the molecular events that occur during tomato flower abscission after flower removal into two phases (Appendix 1, Fig. 15). Phase I comprises of early events occurring between 0 to 4 h after flower removal, that probably lead to acquisition of ethylene sensitivity and abscission competence. This phase involves genes that were calssified in three groups: Group 1 includes genes that are directly down-regulated after IAA depletion, such as *Aux/IAA* (Appendix 1, Fig. 6), and some of the TFs, that were observed to be down-regulated as early as 2 h after flower removal, such as *Knotted-TKN4* (Fig. 21A and Appendix 1, Fig. 11B), *bHLH* (Appendix 1, Fig. 11F), *ERF4* (Fig. 17) that belongs to the *AP2* family (Appendix 1, Fig. 9E), and *AGO1* (Appendix 1, Fig. 14C), *PHANTASTICA* (Fig. 20A and Appendix 2, Fig. 1C), and *OVATE* (Fig. 28A and Appendix 2, Fig. 1D); Group 2 includes genes that are directly repressed by IAA, which were observed to be up-regulated soon after IAA depletion; such as *AP2* TF (Appendix 1, Fig. 12B); Group 3 includes genes of other TF and/or post transcription regulators, such as *LRR-RLK*, *AGO1* (Appendix 1, Fig. 14A,B,C) and *TPRP-F1* (Fig. 29 and Appendix 1,

Fig. 14D). It should be noted that not all genes hypothesized to be involved in either Group 1 or 2 are necessarily directly regulated by IAA. Their differential regulation could be a result of a secondary effect of the initial response.

Phase II comprises late events that occur between 8 to 14 h after flower removal, when an active abscission processes already occurs, leading to the execution of pedicel abscission and development of the protective layer (Appendix 1, Fig. 15). This phase involves genes included in Group 4 that can be classified into three sub-groups, based on their putative functions: I – TF genes or genes belonging to ethylene signal transduction or abscission regulators, such as: *ETR4* (Appendix 1, Fig. 8B), *CTR1* (Appendix 1, Fig. 8C), *ERF1c* (Fig. 15A and Appendix 1, Fig. 9B), *TAGL12* (Fig. 23 and Appendix 1, Fig. 12C), *LRR* receptor PK (Appendix 1, Fig. 14A) and *PK7* (Appendix 1, Fig. 14B); II - Genes encoding cell-wall modifying proteins (Figs. 9-13 and Appendix 1, Fig. 4); III– Genes involved in the PR and development of the defense layer such as *WRKY* TFs (Appendix 1, Fig. 13), *ERT10* (Fig. 18 and Appendix 1, Fig. 10D), and *Chitinase* (Appendix 1, Fig. 10E, F). The later events, which are ethylene-induced, were inhibited by 1-MCP pretreatment, whereas the early events were not always inhibited by 1-MCP. The transition from the early to the late events probably happens between 4 to 8 h after flower removal.

The data presented in Appendixes 1, 2 and 4 support the hypothesis that auxin depletion by means of flower removal affected various regulatory genes, including auxin-inducible genes and genes related to ethylene biosynthesis and regulation. The data presented in the present work confirmed by means of sq-PCR and/or real-time qPCR analyses the microarray results presented in the Appendixes, and expanded this hypothesis also to the AZ of leaves using leaf deblading. Alltogether, this study sheds light on our understanding of the events involved in regulation of flower and leaf abscission, and the role of IAA in the process.

6.1. IAA affects AZ sensitivity to ethylene during induction of abscission

Application of IAA to tomato explants following flower removal prevented pedicel abscission (Roberts et al., 1984; Del Campillo and Bennett, 1996), so that these explants resembled those explants whose flowers had not been removed, and their pedicels did not abscise (Appendix 3, Fig. 1). Further evidence for the active role of auxin was observed in leaf-debladed plants, in

which IAA application inhibited petiole abscission (Appendix 3, Fig. 2). This clearly indicates that the main effect of flower removal or leaf deblading in inducing abscission is due to auxin depletion. 1-MCP pretreatment before flower removal or leaf deblading completely prevented pedicel or petiole abscission, respectively, for at least 20 h (Appendix 1, Fig. 2; Appendix 3, Figs. 1, 2), which again demonstrates the involvement of ethylene in tomato organ abscission. After about 30 h (Appendix 1, Fig. 2; Appendix 3, Fig. 2) the inhibitory effect of 1-MCP was no longer maintained, probably because of the synthesis of new ethylene receptors in the AZ. This shows that most of the regulatory events and reactions occurring up to 14 h after flower removal or up to 72 h after leaf removal were not affected by 1-MCP, and are probably not regulated by ethylene. It should be noted that samples for the RNA extraction for the microarray, sq-PCR, and real-time qPCR experiments were taken only when 1-MCP completely inhibited pedicel or petiole abscission, i.e., up to 14 h after flower removal or 24 h after leaf deblading, respectively.

6.2. Assessment of the microarray data

For validation of the microarray data, we first compared our microarray results for cell-wall-related genes in the FAZ and the FNAZ with the well-known published findings regarding *TAPG1, TAPG2, TAPG4* (Kalaitzis et al., 1997) and *Cel1* (Lashbrook et al., 1994) in the FAZ and other tissues. The microarray results regarding these AZ-related cell-wall modifying genes (Appendix 1, Fig. 4) were in full agreement with the published data. A second validation approach, which was based on sq-PCR and real-time qPCR using various randomly chosen primer pairs, detected expression levels of selected genes in the FAZ and FNAZ. The selected genes were: ethylene signal transduction-related genes*, ERF2*, *ERF1c*, *ERT10, JERF3*; regulatory genes, *Protein phosphatase-like*; early-modified TFs, *MYBSt1*; novel AZ-specific genes, *PHANTASTICA*, *TAGL12* (MADS-box), Knotted protein in *TKN4, OVATE*, *KD1, TPRP-F1*; genes encoding for abscission-related cell-wall hydrolases, *TAPG1, TAPG2, TAPG4, Cel1, XET-BR1*. The results of the sq-PCR and real-time qPCR analyses (Figs. 9 to 29) were in full agreement with the microarray results (Appendixes 1 and 2), except for *MybSt1*. This shows that the microarray results truly reflect the events occurring in the FAZ and the FNAZ. After obtaining data for the FAZ and the FNAZ, we also examined the expression levels of the above mentioned genes in the LAZ and the LNAZ and other plant tissues, YL, OL, YS, OS, and R, to study their expression patterns and kinetics.

6.3. Changes in the expression of the abscission-related cell-wall modifying genes in the AZ

We have identified many genes, whose expressions were changed specifically in the AZ, and those that were up- or down-regulated following the 1-MCP pretreatment. Some genes that conformed to this pattern belong to the group of genes coding for cell-wall hydrolyzing enzymes related to the abscission process, such as various PGs, *TAPG1*, *TAPG2, TAPG4* (Figs 9, 10 and 11) and cellulose, *Cel1* (Fig. 12). These groups of genes are involved in the execution phase, which comprises the late events that occur between 8 to 14 h after flower removal, when an active abscission process occurs (Appendix 1, Fig. 15).

Cel1 and *Cel2* transcripts showed increased accumulation in abscising flower pedicels and in ripening tomato fruits (Lashbrook et al., 1994; Beno-Moualem et al., 2004). In our system, *Cel1* was more highly expressed in the FAZ than in the FNAZ, and attained its maximum level of expression in the FAZ 14 h after flower removal (Fig. 12A), while pedicel abscission progressed (Appendix 1, Fig. 2). Pretreatment with 1-MCP completely inhibited *Cel1* expression in the FAZ between 0 to 14 h after flower removal (Appendix 1, Fig. 4E). Supplementation with IAA after flower removal drastically reduced its expression level (Appendix 4, Fig. 1E). It seems, therefore, that IAA negatively regulated *Cel1* expression in the FAZ. Our data for *Cel1* expression in the FAZ were in line with published data, showing that *Cel1* was expressed in all cells that underwent cell separation (Lashbrook et al., 1994).

Unlike in the FAZ, *Cel1* was highly expressed in the LAZ at 0 h, declined sharply within 12 h after leaf deblading, and exhibited no expression between 24, 48, and 72 h (Fig. 12B). In contrast, in the LNAZ, *Cel1* expression was low at 0 h, peaked after 12 h, and maintained a low level of expression during the subsequent 24 to72 h (Fig. 12B). Unlike these results, other researchers suggest that *Cel1* is not involved in tomato leaf abscission (Jiang et al., 2008). In our system, *Cel1* expression was higher in young leaves and stems than in old ones, and no expression was detected in roots (Fig. 12B). These findings are similar to those reported by Shani et al. (2006), who showed that *Cel1* was more highly expressed in young leaves than in old ones, and showed no expression in roots.

The activities of cell-wall degrading enzymes, including cellulase, PG, expansins, and XET, were shown to increase dramatically with the onset of abscission (Lashbrook et al., 1994; Kalaitzis et al., 1997; Agusti et al., 2008; Cai and Lashbrook, 2008; Roberts and Gonzalez-

Carranza, 2009). In our system, *XET-BR1* was highly expressed in the FAZ, with a continuous gradual increase to maximal expression 14 h after flower removal (Fig. 13A), whereas other *XET* genes were not up-regulated (Data not shown). In contrast, *XET-BR1* expression in the LAZ increased sharply 12 h after leaf deblading and remained almost constant up to 72 h (Fig. 13B). These results are in line with those of a soybean leaf AZ hybridization study for other XFTs, obtained by using the Affymetrix GeneChip (Tucker et al., 2007. *XET-BR1* was more highly expressed in young leaves and shoots than in old ones (Fig. 13B). Pretreatment with 1-MCP inhibited *XET-BR1* expression in the FAZ between 0 to 14 h after flower removal, but not as strongly as that of *TAPG*s (Appendix 1, Fig. 4D). Supplementation with IAA after flower removal similarly inhibited the expression level (Appendix 4, Fig. 1D). These observations are different from the results of Catala et al. (1997) and Campbell and Braam (1999), who found that *XET*s gene expression was restricted to expanding tissues, and was up-regulated by auxin and brassinosteroid treatments and down-regulated by ethylene.

The positive correlations between PG activity and abscission in citrus fruits (Greenberg et al., 1975) and tomato flowers (Tucker et al., 1984) are well documented. PG accumulation was also found after exogenous ethylene treatment of tomato plants: *TAPG1, TAPG2*, and *TAPG4* mRNA started to accumulate in the LAZ and FAZ, which were exposed to ethylene for 0, 6, 12, 24, and 48 h (Kalaitzis et al., 1995). In the present study, *TAPG*s were expressed at high levels in the FAZ even at 0 h and increased gradually thereafter, reaching a peak 14 h after flower removal (Figs. 9A, 10A and 11A), which corresponded to pedicel abscission development without exogenous ethylene treatment (Appendix 1, Fig. 2). *TAPG1* transcripts were previously found to be several times higher in the FAZ than in the LAZ (Kalaitzis et al., 1995), and our present research showed a similar expression pattern (Fig. 9). Pretreatment with 1-MCP completely inhibited *TAPG1* expression in the FAZ after flower removal (Appendix 1, Fig. 4A). Similarly, application of IAA after flower removal also inhibited *TAPG1* expression (Appendix 4, Fig. 1A). The temporal expression patterns for *TAPG1* and *TAPG2* were very similar to those reported by Hong et al. (2000). Pretreatment with 1-MCP completely inhibited *TAPG2* expression in the FAZ after flower removal (Appendix 1, Fig. 4B). Similarly, supplementation with IAA after flower removal also inhibited *TAPG2* expression (Appendix 4, Fig. 1B). Activity of TAPGs in tomato was primarily restricted to AZs, in contrast to that of cellulase, which was extended to adjacent distal and proximal tissues (Del Campillo and Bennett, 1996). We also showed that

*TAPG*s expressions were restricted to the AZs of flowers and leaves (Figs. 9, 10 and 11), whereas *Cel1* was expressed in all tissues, including the LNAZ, leaves and shoots, except for roots (Fig. 12B). It was previously reported that *TAPG4* mRNA was detected much earlier than mRNAs of *TAPG1* and *TAPG2* (Kalaitzis et al., 1997) or *Cel1* (Lashbrook et al., 1994) during both leaf and flower abscission in tomato. However, to the best of our knowledge, no one has examined the spatial and temporal aspects of their expression. Our microarray and sq-PCR results also showed that *TAPG4* accumulated much faster than any other *PG* genes in the FAZ, exhibiting an increased expression 2 h after flower removal and thereafter (Fig. 11A). It should be noted that this sharp increase in gene expression in the AZ is very significant in the light of the fact that AZ cells represent only a small proportion of the cells in the sampled tissue. Pretreatment with 1-MCP reduced *TAPG4* expression in the FAZ to a very low level, but this inhibition was weaker than that observed with other tomato abscission *PGs*, *TAPG1* and *TAPG2* in the FAZ after flower removal (Appendix 1, Figs 4A, B, C). Supplementation with IAA after flower removal reduced the expression levels between 4 and 14 h after flower removal, but had no effect on expression between 0 to 4 h after flower removal (Appendix 4, Fig. 1C).

Taken together, the increase in expression of all four cell-wall modifying genes induced by flower removal was highly specific to the AZ, and was completely prevented by IAA treatment and 1-MCP pretreatment (Appendix 1, Figs. 4A to 4E; Appendix 4, Figs. 1A to 1E). These findings, showing that treatments that inhibited pedicel abscission, such as 1-MCP and IAA, reduced expression of these cell-wall modifying genes, further support their involvement in the execution of the abscission process.

6.4. Analysis of genes, whose expression in the FAZ was changed by flower removal, as possible candidates for functional analysis

The microarray analysis revealed that the expression of many IAA-related genes in the FAZ was changed after flower removal (Appendix 1, Figs. 5, 6). We did not choose any of these auxin-related genes for functional analysis, because of functional redundancy. The single, double, and triple *Aux/IAA* mutants do not show any detectable phenotypic differences related to aberrant auxin levels (Overvoorde et al., 2005); therefore, it would be difficult to identify which gene is solely responsible for any given action. For this reason, we addressed other potential regulators, i.e. early-modified genes that can sense the IAA depletion signals in the AZ. The second reason

was that none of the *Aux/IAA* genes whose expression was modified in the FAZ was AZ-specific, i.e. the same pattern of expression occured also in the FNAZ (Appendix 1, Fig. 6).

6.4.1. Assessment of ERFs as abscission regulators

Our hypothesis postulates that acquisition of ethylene sensitivity in the AZ is associated with alteration of the expression of auxin-regulated genes. Therefore, we examined the effect of flower removal, which leads to auxin depletion, on expression of genes operating in the ethylene signal transduction pathway. Potential candidates for such effects comprise of the receptors for ethylene. However, our results (Appendix 1, Fig. 2) demonstrated that 1-MCP, which binds irreversibly to the available ethylene receptors, prevented pedicel abscission for a relatively long period following flower removal. This suggests that the acquisition of ethylene sensitivity in the AZ, in response to flower removal, could not be due to changes in the ethylene receptors levels. The expression of only one ethylene receptor, *ETR4* was modified by flower removal, being transiently upregulated after 2 h, and increased again 8 and 14 h after flower removal (Appendix 1, Fig. 8B). According to the currently accepted model (Klee, 2004), the presence of more receptors for ethylene mean less sensitivity to ethylene. Thus, higher expression of *ETR4* induced by flower removal cannot account for the increase in ethylene sensitivity after flower removal.

Analysis of the promoters of several *ERF*s revealed a common *cis*-acting ethylene-responsive element called the GCC-box (Fujimoto et al., 2000), which was shown to be necessary for ethylene regulation in various plant species. A highly conserved DNA binding domain, known as the ERF domain, is the unique feature of this protein family. We found five different expression patterns of *ERFs* following flower removal (Figs. 14A, 15A, 16, 17, 18). The linkage between *ERF*s and auxin signaling has further been indicated by results obtained in tomato, which demonstrated that *ERF*s and the *Aux/IAA* genes mediate the active ethylene and auxin signaling crosstalk throughout fruit development and ripening (Audran et al., 2006).

The expression levels of the *ERF*s tended to increase after flower removal. In the present study the expression of *ERF2*, which was higher in the FAZ than in the FNAZ, increased early and transiently between 0 and 2 h after flower removal (Fig. 14A), and was not affected by 1-MCP pretreatment neither in the FAZ nor in the FNAZ (Appendix 1, Fig. 9C). Supplementation with IAA after flower removal had no effect on the *ERF2* expression levels in the FAZ between 0 to 8

h after flower removal, but it increased the expression level slightly after 14 h (Appendix 4, Fig. 2C). The expression patterns of *ERF2* in shoots and roots (Fig. 14B) were similar to those found by Pirrello et al. (2006). In addition, *Sl-ERF2* exhibited a ripening-associated pattern of expression (Tournier et al., 2003).

JERF3 was more highly expressed in the FAZ than in the FNAZ at all time points; it was strongly up-regulated within 2 h after flower removal (Fig. 16), and was significantly down-regulated by 1-MCP pretreatment in the FAZ at all time points (Appendix 2, Fig. 1F), suggesting a response to ethylene. *ERF1c* expression increased between 2 to 14 h after flower removal in a high AZ-specific manner (Fig. 15A), and was down-regulated at 2 h, up-regulated at 4 h, and unaffected between 8 to 14 h after flower removal by 1-MCP treatment (Appendix 1, Fig. 9B). Supplementation with IAA after flower removal significantly reduced *ERF1c* expression in the FAZ at all time points after flower removal, except at 4 h (Appendix 4, Fig. 2B). We believe that for abscission studies we should select *ERF*s that are affected by IAA depletion rather than those affected by abiotic stresses, such as wounding, which can also affect *ERFs* expression independently of ethylene action (Fujimoto et al., 2000**)**. Therefore, *ERF2, ERF1c,* and *JERF3,* whose expression levels increased specifically and significantly in the FAZ 2 h after flower removal (Figs 14A, 15A, 16), are good candidates to serve as abscission regulators, and were therefore chosen for further functional analysis by their silencing.

Another ripening-related gene, *ERT10,* was more highly expressed in the FAZ than in the FNAZ. It was up-regulated transiently after 2 h and peaked after 14 h, well after flower removal (Fig. 18). These early and late increases were inhibited by 1-MCP pretreatment, and the second increase was highly AZ-specific (Appendix 1, Fig. 10D). Supplementation with auxin after flower removal also inhibited the increase in *ERT10* expression (Appendix 4, Fig. 4C), but with a slight down-regulation. Thus, *ERT10* exhibited almost the same response to both 1-MCP and IAA. These observations were similar to those observed for the *ACC synthase (ACS)* gene in response to 1-MCP (Appendix 1, Fig. 7D). Therefore, studying the function of *ERT10* might be extremely interesting to us with regard to ethylene sensitivity in the AZ, since it appears to be a good marker for ethylene responses. It is interesting to note that the development of the competence of tomato fruits to ripen and to respond to ethylene while undergoing the transition from a green fruit (which does not respond to ethylene) to a mature-green fruit (which does respond), is very similar to that of the abscission process (Li et al., 2007). Therefore, genes

associated with tomato ripening, and which are modified during the transition between these two ripening stages, might be significant for the general phenomenon of acquisition of ethylene sensitivity manifested in these two systems.

Expression of the *ERF*s tended to decrease after flower removal. The repressor *ERF4* was more highly expressed in the FNAZ than in the FAZ; in the FAZ its expression was down-regulated early, i.e. 2 h after flower removal, remained low, and was even further down-regulated after 4 h (Fig. 17). It was little affected by 1-MCP pretreatment only 14 h after flower removal (Appendix 1, Fig. 9E). Supplementation with IAA after flower removal did not change the expression pattern of *ERF4* between 0 to 2 h after flower removal, but it increased the expression level, which remained highly constant between 4 to 14 h (Appendix 4, Fig. 2A). Since *ERF4* expression was up-regulated by auxin application, this gene could also serve as a good candidate for regulating early events after auxin depletion.

6.4.2. Assessment of transcription factors (TFs) as abscission regulators

Regulation of gene expression at the level of transcription influences or controls many biological processes, including abscission. TFs act as switches of regulatory cascades during development, and alterations in the expression of genes coding for transcriptional regulators may affect various developmental processes (Riechmann et al., 2000). Thus, studying the effect of flower removal on expression of TFs could be highly relevant for understanding the control of the abscission process. Our results show that the expression of five TF genes, *MybSt1, PHAN, TKN4, TAGL12* and *HB-13* (Figs. 19A, 20A, 21, 22A, 23 and 25), was early and transiently modified following flower removal. The microarray data show an early up-regulation of *MybSt1* 2 h after flower removal, which was completely inhibited by 1-MCP pretreatment (Appendix 2, Fig. 1B). Supplementation with IAA after flower removal down-regulated *MybSt1* expression in the FAZ between 0 to 4 h after flower removal (Appendix 4, Fig. 3B). Thus, *MybSt1* could be a downstream transcriptional regulator in the auxin pathway in the FAZ. However, the sq-PCR results (Fig. 19A) were quite contrary to these findings, demonstrating that the expression level of *MybSt1* in the FAZ was down-regulated 2 h after flower removal, and it increased gradually upto 14 h after flower removal. Three technical replicates were performed with a single biological sample for the sq-PCR analysis (Fig. 19A), and it might be that other biological replicates will confirm the microarray results presented in Appendix 2, Fig. 1B.

TAGL12 belongs to the MADS-box domain, which is a transcription gene family in plants and is involved in the complex ripening process of tomato (Parenicova et al., 2003). The gene coding for the Tomato *AGAMOUS*-Like 12 MADS-box protein (*TAGL12*) was highly up-regulated between 8 to 14 h, specifically in the AZ (Fig. 23), and this induction was inhibited by 1-MCP pretreatment, again specifically in the AZ between 8 to 14 h (Appendix 1, Fig. 12C). Supplementation with IAA after flower removal reduced the expression level of *TAGL12* in the FAZ 14 h after flower removal (Appendix 4, Fig. 4D). TFs that were modified by flower removal, particularly if they are AZ-specific, might be considered as good candidates to function as effectors of ethylene responsiveness. *TAGL12* was more highly expressed in the FAZ than in the FNAZ; its expression in the FAZ started to increase gradually between 0 to 14 h, whereas in the FNAZ it started to be down-regulated 2 h after flower removal and thereafter, and reached a very low expression level after 14 h (Fig. 23). *TAGL12* was highly expressed in the LNAZ, as well as in leaves, old shoots and roots (Fig. 24). To the best of our knowledge, this is the first report that *TAGL12* was expressed in the LAZ, LNAZ, leaves, shoots, and roots. These results suggest that *TAGL12* is a good candidate for functional studies of the abscission process.

PHAN, *KNOX,* and *LEAFY* genes play major roles in regulation of leaf morphology (Bharathan and Neelima, 2001), apical meristems, bracts, and petal lobes of *Antirrhinum majus* (Waites et al., 1998). In tomato, we observed that *PHAN* was more highly expressed in the FAZ than in the FNAZ, except for 14 h after flower removal; it was expressed in the FAZ at 0 h, was down-regulated within 2 h after flower removal, and then maintained a lower expression level (Fig. 20A). *PHAN* was one of the early-down-regulated genes, whose expression was down-regulated 2 h after flower removal. *PHAN* expression in the FAZ was unaffeted by 1-MCP pretreatment at all time points (Appendix 2, Fig. 1C). However, supplementation with IAA after flower removal gradually increased *PHAN* expression to a maximum level after 14 h (Appendix 4, Fig. 3D). *PHAN* seems, therefore, to be an IAA-induced gene in the FAZ. These results indicate that *PHAN* responds to auxin rather than to ethylene. *PHAN* was more highly expressed in old than in young leaves of tomato (Fig. 20B), which is contrary to the data reported for *Antirrhinum majus* (Waites et al., 1998), in which *PHAN* was highly expressed in young leaves, but was undetectable at the later stages of leaf development. These differences could be due to differential expression patterns in the two different plant systems. *PHAN* expression was low in both young and old shoots of tomato (Fig. 20B), and these results are different from those of

Minsung et al. (2003), who observed an expression of *PHAN* in the vascular tracts of leaves and shoots. Our data show that *PHAN* was highly expressed in roots (Fig. 20B), and to the best of our knowledge, this is demonstrated for the first time. *PHAN* was shown to encode a *Myb*-related TF in tomato roots after infection by root knot nematodes (Bird and Wilson, 1994).

TKN4 was expressed at much higher levels in the FAZ than in the FNAZs at 0 h, and it showed a rapid down-regulation in the FAZ 2 h after flower removal (Figs. 21, 22A). *TKN4* was one of the early down-regulated genes, whose expression was down-regulated 2 h after flower removal. Its expression was not affected by 1-MCP (Appendix 1, Fig. 11B), but it was increased in response to IAA treatment (Appendix 4, Fig. 3C). The results suggest that *TKN4* responds to IAA and not to ethylene. All these patterns of expression were very similar to those of *PHAN* (Fig. 20A; Appendix 2, Fig. 1C; Appendix 4, Fig. 3D). The tomato *KNOX* transcripts, which play a major role in generating cell identities (Sentoku et al., 1999) and in maintenance of SAM (Long et al., 1996), were expressed in leaves, inflorescences, floral meristems, and roots (Parnis et al., 1997; Janssen et al., 1998a,b; Koltai and Bird, 2000). We also showed that *TKN4* was expressed in leaves, shoots, and roots (Fig. 22B).

Our results suggest that *PHAN* and *KNOX*, which were specifically expressed in the FAZ, have regulatory roles in abscission, and they might be affected even at the earliest stage of AZ differentiation, as suggested by Van Nocker (2009). According to these findings, these genes might be good candidates for further study of abscission regulation.

6.5. Assessment of other regulatory genes as abscission regulators

A non-sense mutation in the single gene *OVATE* caused the transition of tomato fruits from round to pear shaped (Liu et al., 2002). *OVATE* was expressed in early flower and fruit development, and it is the major quantitative trait-controller (QTL) that controls pear-shaped fruit development in eggplant and tomato (Ku et al., 1999; Doganlar et al., 2002). *OVATE* was highly expressed in the FAZ at 0 h, but its expression was significantly reduced 2 h after flower removal, and was very low after 8 and 14 h (Fig. 28A). There was no expression of *OVATE* in the FNAZ, and it was not expressed in the LAZ, LNAZ, leaves, stems, and roots (Fig. 28B), suggesting that it was specific to the FAZ at 0 h. These results are consistent with those of Liu et al. (2002), who found that *OVATE* RNAs were undetectable in leaves, flowers, and fruits. However, they are contrary to those of Wang et al. (2007), who found that the *OVATE* ortholog

in Arabidopsis was expressed in roots, shoots, inflorescences, stems, and siliques. 1-MCP pretreatment before flower removal had little or no effect on *OVATE* expression in the FAZ (Appendix 2, Fig. 1D). Supplementation with auxin after flower removal had no effect on *OVATE* expression until 2 h after flower removal, but it was up-regulated gradually thereafter, reaching a peak after 14 h (Appendix 4, Fig. 3E). The sharp decline after 2 h of flower removal in *OVATE* expression was AZ-specific (Fig. 28A). Thus, *OVATE* might also be a good candidate gene, along with *PHAN* and *TKN4*, for further studies of abscission regulation.

Protein phosphatase-like gene was expressed in both the FAZ and the FNAZ, with a higher expression in the FAZ. The expression levels in both tissues increased gradually between 0 to 14 h (Fig. 27A), and it was more highly expressed in leaves than in shoots and roots (Fig. 27B). 1-MCP pretreatment before flower removal did not affect the expression patterns of *Protein phosphatase-like* in the FAZ and the FNAZ (Appendix 2, Fig. 1A), indicating that it is probably not an ethylene-responsive gene. Application of IAA treatment after flower removal strongly reduced the expression of the *Protein phosphatase-like* gene in the FAZ at all time points after flower removal (Appendix 4, Fig. 3A). Accordingly, the increases in *Protein phosphatase-like* expression in the FAZ and the FNAZ after flower removal can be explained as a result of auxin depletion. The expression levels of the *Protein phosphatase-like* gene were lower in the LAZ as compared to the LNAZ (Fig. 27B). There have been only a few studies of protein phosphatase. To the best of our knowledge, we are the first to demonstrate differential expression patterns of *Protein phosphatase-like* in flower and leaf AZs, shoots, and roots (Fig. 27B). Since the role of *Protein phosphtase-like* in abscission has been only little studied, we are interested in using silencing to study its functional role in abscission.

6.6. Selection of a *TAPG4* promoter and designing of a new vector

By using virus-induced gene silencing (VIGS), our collaborator team at UC-DAVIS, USA demonstrated that *TAPGs* are specifically associated with the tomato AZ and they act as key enzymes in the abscission process (Jiang et al., 2008). This conclusion was based on the observed retardation of petiole abscission in the *TAPG*-silenced plants, and on the increase in the force required for petiole separation. The abscission signal is first received in target cells localized in the vascular bundles, which initiates the signal for *TAPG4* gene expression in the

abscission program (Hong et al., 2000). This signal then spreads towards the cortex and pith cells, thereby demonstrating the lateral diffusion of the secondary signal (Thompson and Osborne, 1994). The vascular bundles act independently to transmit the signals across the separation layers. *TAPG* genes share 72% nucleotide sequence identity (Hong and Tucker, 1998), and a similarity of 85% (Jiang et al., 2008). *TAPG*s contain two domains: a partially conserved, 300-bp proximal domain, and an upstream divergent distal domain. *TAPG4:GUS* expression was observed in the AZs of leaves, petioles, flower and fruit pedicels, and fruit calyx and corolla (Hong and Tucker, 1998).

In our microarray (Appendix 1, Fig. 4C) and expression studies (Fig. 11A) we found that *TAPG4* was specifically expressed earlier and more highly in the FAZ compared to other *TAPG*s, and that it was not completely inhibited by 1-MCP pretreatment (Appendix 1, Fig. 4C). Therefore, we constructed the RNAi constructs that are driven by *TAPG4* as a promoter (Fig. 7), to induce tissue-specific silencing in the FAZ, rather than silencing of the entire plant system by using the constitutive CaMV 35S promoter. The constructs are already ready for two genes, *JERF3* (Fig. 30) and *TKN4* (Fig. 31), and they are at the phase V stage, with appearance of phenotypes expected in a few months. The constructs for *Proline-rich protein (TPRP-F1)* and *KD1* genes are at phase IV.

6.7. Selection of potential target genes for functional analysis

One of the main objectives of this study was to use the tomato microarray Gene Chip for identifying target genes for their further functional analysis by VIGS. Confirmed genes were used for further knockouts with RNAi vector and stable transformation by *Agrobacterium tumefaciens*. The genes were selected based on their change in expression pattern within a short time (2 h) after flower removal. As discussed in detail above, the selected genes, *JERF3, TKN4, ERF2, Protein Phosphatase-like, KD1*, and *TPRP-F1*, might be very good candidates for functional analysis in abscission regulation. We have already proceeded with several selected genes, such as *JERF3* (Fig. 30)*, TKN4* (Fig. 31)*, ERF2* (Fig. 32)*, Protein Phosphatase-like* (Fig. 33)*,* and cloned them into suitable vectors for their further stable transformation into plants. Other candidate genes will be similarly studied in the future.

6.8. Vectors and transformation

We primarily used the RNAi vector PGSA 1285 (Fig. 2) from ChromDB to serve as both RNAi and binary vectors. We faced many problems in cloning, transformation, chloramphenicol background resistance, and sequencing, because of the large size of the vector: sometimes the hairpin loop structure would detach itself from the vector. Therefore, we designed an alternative strategy to overcome this problem. We cloned a part of the PGSA 1285 vector (MCs including introns) into the pGEMT easy vector, which enabled us to clone sense and antisense in pGEMT, and to restrict the entire cassette and clone it back into the PGSA1285. In this way, we reached phase III for two genes, *ERF2* and *Protein phosphatase,* and two other genes, *TKN4* and *OVATE,* are in phase I. However, the error rates were high in this system of cloning, possibly because of the sequencing errors, and because of the large size of plasmids or competent cells used for transformation. It was already shown that the use of JM109 competent cells leads to increased variability in sequencing (Ref-hylabs sequencing procedure - http://www.hylabs.co.il/SiteFiles/1/59/137.asp). Therefore, we shifted to a new RNAi vector, pHANNIBAL, obtained from CSIRO, Australia, which has been widely used by us for constructing the hairpin RNAi in plants (Fig. 4). We used pHANNIBAL to silence the genes *JERF3, TKN4,* and *KD1*. In this case, we used DH5α strain for bacterial transformation, which yielded high transformation efficiency. This high efficiency was attributed not only to the competent host cells, but also to the small size of the primary plasmid.

7. SUMMARY AND FUTURE WORK

Expression studies by means of semi-quantitative PCR and quantitative real-time PCR validated the microarray results, and led us to identify the expression patterns of selected genes in other tissues in addition to the FAZ and the FNAZ. We selected a few genes for stable transformation into plants, which included genes that are specifically up- or down-regulated in the FAZ after flower removal. The selected genes were: *ERF2* (Fig. 14A)*, JERF3* (Fig. 16)*, TKN4* (Fig. 21), *Protein phosphatase-like* (Fig. 27A)*, TPRP-F1* (Fig. 29), and *KD1* (data not shown). The RNAi (hpRNA) vectors, PGSA 1285 and pHANNIBAL, driven by the CaMV 35S promoter were used to silence the selected genes, *ERF2, Protein phosphatase-like, JERF3,* and *TKN4*, which are currently in the stage of transforming into plants (Phase V). We successfully isolated the *TAPG4* promoter from the genomic DNA and cloned it into the pGEMT vector by modifying the restriction sites to suit our vectors. We assembled the RNAi constructs, driven by *TAPG4* as promoter (Fig. 7), to induce tissue-specific silencing in the FAZ, rather than silencing the entire plant system by using the constitutive CaMV 35S promoter. The constructs for two genes, *JERF3* and *TKN4,* are ready and they are currently at Phase V. Hence, we expect to see phenotypes in a few months. Constructs for *Proline-rich protein (TPRP-F1)* and *KD1* genes are in Phase III.

7.1. Future work

1. Study the phenotypic and functional roles of silenced genes in transformed plants.
2. Grouping of the functional characterization according to the promoters used (CaMV 35S/*TAPG4*).
3. Use of the antisense technique to silence the selected genes and to reveal the resulting phenotypes.
4. Identification and selection of other potential genes for further silencing studies.
5. If the transformed plant shows abscission phenotypes, i.e. with retarded or accelerated abscission, the transcriptome changes in its AZ will be studied using the microarray technique.

8. REFERENCES

Abebie B, Goren R, Huberman M, Meir S, Philosoph-Hadas S, Riov J (2005). Prevention of bud and floret abscission in Cestrum cut flowers is related to the mode of transport and metabolism of synthetic auxins. Acta Hort. 682: 789-794.

Abebie B, Lers A, Philosoph- Hadas S, Goren R, Riov J, Meir S (2007). Differential effects of NAA and 2,4- D in reducing floret abscission in cestrum *(Cestrum elegans* Schlecht) cut flowers are associated with their differential activation of *Aux/ IAA* homologous genes. Ann. Bot. 101: 249-259.

Abeles FB, Morgan PW, Saltveit ME (1992). Ethylene in Plant Biology, 2nd Edition. Academic Press, San Diego.

Addicott FT (1982). Abscission. University of California Press, Ltd. London.

Agusti J, Merelo P, Cercós M, Tadeo FR, Talón M (2008)**.** Ethylene-induced differential gene expression during abscission of citrus leaves. J. Exp. Bot. 59: 2717-2733.

Allen MD, Yamasaki K, Ohme-Takagi M, Tateno M, Suzuki M (1998). A novel mode of DNA recognition by a beta-sheet revealed by the solution structure of the GCC-box binding domain in complex with DNA. EMBO J 17: 5484–5496.

Andrew P. Gleave, (1992). A versatile binary vector system with a T-DNA organizational structure conducive to efficient integration of cloned DNA into the plant genome. Plant Mol. Biol. 20: 1203-1207.

Audran C, Chateigner-Boutin AL, Chaabouni S, Wang H, Mila I, Regad F, Bouzayen M (2006). Ethylene and auxin interplay throughout fruit development and ripening. The 7th International Symposium on The Plant Hormone Ethylene, Pisa, Italy. Abstract No 4-4, p. 80.

Bangerth F (1989). Dominance among fruit/sinks and the search for a correlative signal. Plant Physiol. 76: 608-614.

Baranowskij N, Frohberg C, Prat S, Willmitzer L (1994). A novel DNA binding protein with homology to *myb* containing only one repeat can function as a transcriptional activator. EMBO J. 13: 5383-5392.

Barg R, Sobolev I, Eilon T, et al. (2005). The tomato early fruit specific gene *Lefsm1* defines a novel class of plant-specific SANT/MYB domain proteins. Planta 221: 197-211.

Becker A, Theissen G (2003). The major clades of MADS-box genes and their role in the development and evolution of flowering plants. Mol. Phylo. Evol. 29: 464-489.

Beno-Moualem D, Gusev L, Dvir O, Pesis E, Meir S, Lichter A (2004). The effect of ethylene, methyl jasmonate and 1-MCP on abscission of cherry tomatoes from the bunch and expression of endo-1,4-β−glucanases. Plant Sci. 167: 499-507.

Bergey DR, Orozco-Cardenas M, de Moura DS, Ryan CA (1999). A wound- and system-inducible polygalacturonase in tomato leaves. Proc. Natl. Acad. Sci. USA 96: 1756–1760.

Bharathan G, Janssen B-J, Kellogg EA, Sinha N (1997). Did homeodomain proteins duplicate before the origin of angiosperms, fungi and metazoan. Proc. Natl. Acad. Sci. USA 94:13749–13753.

Bharathan G, Sinha NR (2001). The regulation of compound leaf development. Plant Physiol. 127: 1533-1538.

Bird DM, Wilson MA (1994). DNA sequence and expression analysis of root-knot nematode-elicited giant cell transcripts. Mol. Plant Microbe Inter. 7: 419-424.

Brown SM, Crouch ML (1990). Characterization of family abundantly expressed in *Oenothera organensis* pollen that shows sequence similarity to polygalacturonase. Plant cell 2: 263-274.

Brummell DA, Bird CR, Schuch W, Bennett AB (1997a). An endo-1,4-beta-glucanase expressed at high levels in rapidly expanding tissues. Plant Mol. Biol. 33: 87–95.

Brummell DA, Bradford DH, Bennett AB (1999). Antisense suppression of tomato endo-β-1,4-glucanase *Cel2* mRNA accumulation increases the force required to break fruit abscission zones but does not affect fruit softening. Plant Mol Biol 40: 615-122.

Brummell DA, Catala C, Lashbrook CC, Bennett AB (1997b). A membrane-anchored E-type endo-1,4-beta-glucanase is localized on Golgi and plasma membranes of higher plants. Proc. Natl. Acad. Sci. USA 94: 4794–4799.

Cai S, Lashbrook CC (2008). Stamen abscission zone transcriptome profiling reveals new candidates for abscission control: Enhanced retention of floral organs in transgenic plants overexpressing Arabidopsis *ZINC FINGER PROTEIN2*. Plant Physiol. 146: 1305-1321.

Campbell P, Braam J (1999). Xyloglucan endotransglycosylases: Diversity of genes, enzymes and potential wall-modifying functions. Trends Plant Sci 4: 361-366.

Carpita NC, Gibeaut DM (1993). Structural models of primary cell walls in flowering plants: Consistency of molecular structure with the physical properties of the walls during growth. Plant J. 3: 1–30.

Catala C, Bennett AB (1998). Cloning and sequence analysis of *tomcel8*; a new plant endo-beta-1,4-d-glucanase gene, encoding a protein with a putative carbohydrate binding domain (accession no. AF098292). Plant Physiol. 118L: 1535.

Catala C, Rose JKC, Bennett AB (1997). Auxin regulation and spatial localization of an endo-1,4-beta-d-glucanase and a xyloglucan endotransglycosylase in expanding tomato hypocotyls. Plant J. 12: 417–426.

Catala C, Rose JKC, Bennett AB (2000). Auxin-regulated genes encoding cell wall-modifying proteins are expressed during early tomato fruit growth. Plant Physiol. 122: 527–534.

Chang H, Jones ML, Banowetz GM, Clark DG (2003). Overproduction of cytokinins in petunia flowers transformed with *PSAG12-IPT* delays corolla senescence and decreases sensitivity to ethylene. Plant Physiol. 132: 2174–2183.

Chen JJ, Janssen BJ, Williams A, Sinha N (1997). A gene fusion at a homeobox locus: alternations in leaf shape and implications for morphological evolution. Plant Cell 9: 1289–1304.

Chen W, Provart NJ, Glazebrook J, Katagiri F, Changa H-S et al (2002). Expression profile matrix of Arabidopsis transcription factor gene suggests their putative functions in response to environmental stress. Plant Cell 14: 559–574.

Chuck G, Lincoln C, Hake S (1996). KNAT1 induces lobed leaves with ectopic meristems when overexpressed in Arabidopsis. Plant Cell, 8: 1277–1289.

Cote F, Hahn MG (1994). Oligosaccharins: structures and signal transduction. Plant Mol. Biol. 26: 1379–1411.

De Folter S, Shchennikova AV, Franken J, Busscher M, Baskar R, Grossniklaus U, Angenent GC, Immink RG (2006). A Bsister MADS-box gene involved in ovule and seed development in petunia and Arabidopsis. Plant J. 47: 934–946.

Del Campillo E, Bennett AB (1996). Pedicel breakstrength and cellulase gene expression during tomato flower abscission. Plant Physiol. 111: 813–820.

Djanaguiraman M, Devi DD, Shanker AK, Sheeba JA and Bangarusamy U (2004). The role of nitrophenol on delaying abscission of tomato flowers and fruits. Food Agric. Environ. 2: 183–186.

Doganlar S, Frary A, Daunay MC, Lester RN, Tanksley SD (2002). A comparative genetic linkage map of eggplant (*Solanum melongena*) and its implications for genome evolution in the Solanaceae. Genetics 161: 1697-1711.

Dower WJ, Miller JF, Ragsdale CW (1988). High efficiency transformation of *E. Coli* by high voltage electroporation. Nucl. Acids Res. 16: 6127-6145.

Ellis CM, Nagpal P, Young JC, Hagen G, Guilfoyle TJ, Reed JW (2005). *AUXIN RESPONSE FACTOR*1 and *AUXIN RESPONSE FACTOR*2 regulate senescence and floral organ abscission in *Arabidopsis thaliana*. Development 132: 4563-4574.

Emery JF, Floyd SK, Alvarez J, Eshed Y, Hawker NP, Izhaki A, Baum SF, and Bowman JL (2003). Radial patterning of Arabidopsis shoots by class III *HD-ZIP* and *KANADI* genes. Curr. Biol. 13: 1768–1774.

Fernandez DE, Heck GR, Perry SE, Patterson SE, Bleecker AB, Fang S-C (2000). The embryo MADS domain factor AGL15 acts postembryonically: Inhibits of perianth senescence and abscission via constitutive expression. Plant Cell 12: 183-197.

Fischer RL, Bennett AB (1991). Role of cell-wall hydrolases in fruit ripening. Annu. Rev. Plant Physiol. 42: 675–703.Frugis G, Giannino D, Mele G, Nicolodi C, Innocenti AM, Chiappetta A, Bitonti MB, Dewitte W, Van Onckelen H, Mariotti D (1999). Are homeobox Knotted-like genes and cytokinins the leaf architects? Plant Physiol. 119: 371–373.

Fujimoto SY, Ohta M, Usui A, Shinshi H, Ohme-Takagi M (2000). Arabidopsis ethylene-responsive element binding factors act as transcriptional activators or repressors of GCC box-mediated gene expression. Plant Cell 12: 393-404.

Gabrielsen OS, Sentenac A, Fromageot P (1991). Specific DNA binding by c-Myb: evidence for a double helix-turn-helix-related motif. Science 253: 1140-1143.

Gago CML, Monteiro JA, Rodrigues H (2001). Bougainvillea post-production: NAA and STS control of bract abscission is subject to exogenous ethylene. Acta Hort. 543: 47-53.

Golz JF, Roccaro M, Kuzoff R, Hudson A (2004). *GRAMINIFOLIA* promotes growth and polarity of *Antirrhinum* leaves. Development 131: 3661–3670.

Gomez-Cadenas A, Arbona V, Jacas J, Primo E, Talon M (2003). Abscisic acid reduces leaf abscission and increases salt tolerance in *Citrus* plants. J. Plant Growth Regul. 21: 234–240.

Gomez-Cadenas A, Tadeo FR, Talon M and Primo M E (1996). Leaf abscission induced by ethylene in water-stressed intact seedlings of Cleopatra Mandarin required previous abscisic acid accumulation in roots. Plant Physiol. 112: 401-408.

Greenberg JR, Goren J, Riov J (1975). Cellulase, PG and citrus fruit abscission . Physiol. Plant. 34: 1-7.

Gu Y-Q, Wildermuth MC, Chakravarthy S, Loh YT, Yang C, He X, Han Y, Martin GB (2002). Tomato transcription factors pti4, pti5, and pti6 activate defense responses when expressed in Arabidopsis. Plant Cell 14: 817–831.

Hackbusch J, Richter K, Muller J, Salamini F and Uhrig JF (2005). A central role of *Arabidopsis thaliana OVATE* family proteins in networking and subcellular localization of 3-aa loop extension homeodomain proteins. Proc. Natl Acad. Sci 102: 4908– 4912

Hareven D, Gutfinger T, Parnis A, Eshed Y, Lifschitz E (1996). The making of a compound leaf: genetic manipulation of leaf architecture in tomato. Cell 84: 735–744.

Hawes MC, Lin HJ (1990). Correlation of pectolytic enzyme activity with the programmed release of cells from root caps of pea (*Pisum sativum*). Plant Physiol. 94: 1855–1859.

Hay A, Kaur H, Phillips A, Hedden P, Hake S, Tsiantis M (2002). The gibberellin pathway mediates *KNOTTED1*-type homeobox function in plants with different body plans. Curr. Biol. 12: 1557–1565.

Hileman LC, Sundstrom JF, Litt A, Chen M, Shumba T, Irish VF (2006). Molecular and phylogenetic analyses of the MADS-box gene family in tomato. Mol. Biol. Evol. 23: 2245–2258.

Hong SB, Sexton R, Tucker ML (2000). Analysis of gene promoters for two tomato polygalacturonases expressed in abscission zone and the stigma. Plant Physiol. 123: 869–881.

Hong SB, Tucker ML (1998). Genomic organization of six tomato polygalacturonases and 59 upstream sequence identity with *tap1* and *win2* genes. Mol. Gen. 258: 479–487.

Hong SB, Tucker ML (2000). Molecular characterization of a tomato polygalacturonase gene abundantly expressed in the upper one-third of pistils from opened and unopened flowers. Plant Cell Rep. 19: 680-683.

Huberman M, Pressman E, Jaffe MJ (1993). Pith autolysis in plants: IV. The activity of polygalacturonase and cellulase during drought stress induced pith autolysis. Plant Cell Physiol. 34: 795–801.

Janssen BJ, Lund L, Sinha N (1998a). Overexpression of a homeobox gene, *Let6*, reveals indeterminate features in the tomato compound leaf. Plant Physiol. 117: 771–786.

Janssen BJ, Williams A, Chen JJ, Mathern J, Hake S, Sinha N (1998b). Isolation and characterization of two *knotted-like* homeobox genes from tomato. Plant Mol. Biol. 36: 417–425.

Jenkins E, Paul W, Coupe S, Bell S, Davies E, Roberts J. (1996). Characterization of an mRNA encoding a polygalacturonase expressed during pod development in oilseed rape (*Brassica napus* L.). J. Exp. Bot. 47: 1111–1115.

Jiang CZ, Gu J, Chopra S, Gu X, Peterson T (2004). Ordered origin of the typical two and three repeat *Myb* genes. Gene 326:13–22.

Jiang CZ, Lu F, Imsabai W, Meir S, Reid MS (2008). Silencing polygalacturonase expression inhibits tomato petiole abscission. J. Exp. Bot. 59: 973-979.

Jinn T-L, Stone JM, Walker JC (2000). *HAESA*, an Arabidopsis leucine-rich repeat receptor kinase, controls floral organ abscission. Genes Dev 14: 108-117.

Jiping L, Van Eck J, Cong B, Tanksley SD (2002). A new class of regulatory genes underlying the cause of pear-shaped tomato fruit. Proc. Natl. Acad. Sci. USA 99: 13302–13306.

Kalaitzis P, Hong SB, Solomos T, Tucker ML (1999). Molecular characterization of a tomato endo-beta-1,4-glucanase gene expressed in mature pistils, abscission zones and fruit. Plant Cell Physiol. 40: 905–908.

Kalaitzis P, Koehler SM, Tucker ML (1995). Cloning of a tomato polygalacturonase expressed in abscission. Plant Mol. Biol. 28: 647–656.

Kalaitzis P, Solomos T, Tucker ML (1997). Three different polygalacturonases are expressed in tomato leaf and flower abscission, each with a different temporal expression pattern. Plant Physiol. 113: 1303–1308.

Kerstetter RA, Laudencia D, Smith LG, Hake S (1997). Sequence analysis and expression pattern divide the maize knotted1-like homeobox genes into two classes. Development 124: 3045–3054.

Kim J, Harter K, Theologis A (1997). Protein-protein interactions among Aux/IAA proteins. Proc. Natl. Acad. Sci. USA 94: 11786-11791.

Kim M, McCormick S, Timmermans M, Sinha N (2003). The expression domain of *PHANTASTICA* determines leaflet placement in compound leaves. Nature 424: 438–443.

Klee HJ (2004). Ethylene signal transduction. Moving beyond Arabidopsis. Plant Physiol. 135: 660–667.

Klempnauer KH, Gonda TJ, Bishop JM (1982). Nucleotide sequence of the retroviral leukemia gene *v-myb* and its cellular progenitor *c-myb*: The architecture of a transduced oncogene. Cell 31: 453 463.

Kofuji R, Sumikawa N, Yamasaki M, Kondo K, Ueda K, Ito M, Hasebe M (2003). Evolution and divergence of the MADS-box gene family based on genome-wide expression analyses. Mol. Biol. Evol. 20: 1963–1977.

Koka CV, Cerny RE, Gardner RG, Noguchi T, Fujioka, S, Takatsuto S, Yoshida S, Clouse SD (2000). A putative role for the tomato genes *DUMPY* and *CURL-3* in brassinosteroid biosynthesis and response. Plant Physiol. 122: 85-98.

Koltai H, Bird DM (2000). Epistatic repression of *PHANTASTICA* and class1 *KNOTTED* genes is uncoupled in tomato. Plant J. 22: 455–459.

Ku HM, Doganlar S, Chen KY, Tanksley SD (1999). The genetic basis of pear-shaped tomato fruit. Theor. Appl. Genet. 9: 844–850.

Kutsumai SY, Lin AC, Pereival FW, Laties G, Christ-Offersen RE (1993). Ripening related polygalacturonase from avocado. Plant Physiol. 103: 289-290.

Lamm R (1949). Contributions to the genetics of the Gp-chromosome of *Pisum*. Hereditas 35: 203–214.

Lashbrook CC, Giovannoni JJ, Bradford DH, Fischer RL, Bennett AB (1998). Transgenic analysis of tomato *endo-β-1,4-glucanase* gene function. Role of *Cel1* in floral abscission. Plant J. 13: 303-310.

Lashbrook CC, Gonzalez-Bosch C, Bennet AB (1994). Two divergent *endo-β-1,4-glucanase* genes exhibit overlapping expression in ripening fruit and abcissing flowers. Plant Cell 6: 1485-1493.Leseberg CH, Li A, Kang H, Duvall M, Mao L (2006). Genomewide analysis of the MADS-box gene family in *Populus trichocarpa*. Gene 378: 84–94.

Lester RD, Speirs J, Orr G, Brady JC (1994). Peach (*Prunus persica*) endopolygalacturonase cDNA isolation and mRNA analysis in melting and non-melting peach cultivars. Plant Physiol. 105: 225- 231.

Lewis MW, Leslie ME, Liljegren SJ (2006). Plant separation: 50 ways to leave your mother. Curr. Opin. Plant Biol. 9: 59–65.

Li Y, Zhu B, Xu W, Zhu H, Chen A, Xie Y, Shao Y, Luo Y (2007)**.** *LeERF1* positively modulated ethylene triple response on etiolated seedlings, plant development and fruit ripening and softening in tomato. Plant Cell Rep. 26: 1999-2008.

Lipsick, JS (1996). One billion years of Myb. Oncogene 13: 223- 235.

Long JA, Moan EI, Medford JI, Barton MK (1996). A member of the KNOTTED class of homeodomain proteins encoded by the STM gene of Arabidopsis. Nature 379: 66–69.

Lorenzo O, Piqueras R, Sanchez-Serrano JJ, Solano R (2003). Ethylene Response Factor1 integrates signals from ethylene and jasmonate pathways in plant defense. Plant Cell 15: 165–178.

Mao L, Begum D, Chuang H, Budiman MA, Szymkowiak EJ, Irish EE, Wing RA (2000). *JOINTLESS* is a MADS-box gene controlling tomato flower abscission zone development. Nature 406: 910–913.

McConnell JR, Emery J, Eshed Y, Bao N, Bowman J, Barton MK (2001). Role of *PHABULOSA* and *PHAVOLUTA* in determining radial patterning in shoots. Nature 411: 709–713.

McKim SM, Stenvik GE, Butenko MA, Kristiansen W, Cho SK, Hepworth SR, Aalen RB, Haughn GW (2008). The *BLADE-ON-PETIOLE* genes are essential for abscission zone formation in Arabidopsis. Development 135: 1537–1546.

Meir S, Hunter DA, Chen JC, Halaly V, Reid MS (2006). Molecular changes occurring during acquisition of abscission competence following auxin depletion in *Mirabilis jalapa*. Plant Physiol. 141: 1604–1616.

Michaeli R, Philosoph-Hadas S, Riov J, Meir S (1999). Chilling-induced leaf abscission of *Ixora coccinea* plants. I. Induction by oxidative stress via increased sensitivity to ethylene. Physiol. Plant. 107: 166–173.

Nakano T, Nishiuchi T, Suzuki K, Fujimura T, Shinshi H (2006a). Studies on transcriptional regulation of endogenous genes by *ERF2* transcription factor in tobacco cells. Plant Cell Physiol. 47: 554–55.

Nakano T, Suzuki K, Fujimura T, Shinshi H (2006b). Genome-wide analysis of the *ERF* gene family in Arabidopsis and rice. Plant Physiol. 140: 411–432.

Nath P, Sane VA, Sane AP, Trivedi PK (2005). Plant gene expression, regulation of. In: Encyclopedia of Molecular and Cell Biology and Molecular Medicine. Meyer RA, ed., Vol. 10 (2nd Ed.); pp 307–358, Wiley-VCH Verlag Gmbh & Co, Weinheim, Germany.

Neil A. McHale R, Koning E (2004). *PHANTASTICA* regulates development of the adaxial mesophyll in *Nicotiana* leaves. Plant Cell 16: 1251–1262.

Niogret MF, Dubald M, Mandaron P, Mache R (1991). Characterization of pollen polygalacturonase encoded by several cDNA clones in maize. Plant Mol. Biol. 17: 1155-1164.

Ohta M, Matsui K, Hiratsu K, Shinshi H, Ohme M (2001). Repression domains of class II ERF transcriptional repressors share an essential motif for active repression. Plant Cell 13: 1959-1968.

Okushima Y, Mitina I, Quach HL, Theologis, A (2005a). Auxin response factor 2 (*ARF2*): A pleiotropic development regulator. Plant J 43: 29-46.

Okushima Y, Overvoorde PJ, Arima K, Alonso JM, Chan A, Chang C, Ecker JR, Hughes B, Lui A, Nguyen D, Onodera C, Quach H, Smith A, Yu G, Theologis A (2005b). Functional genomic analysis of the *AUXIN RESPONSE FACTOR* gene family members in *Arabidopsis thaliana:* Unique and overlapping function of *ARF7* and *ARF19*. Plant Cell 17: 444-463.

Onate-Sanchez L, Anderson JP, Young J, Singh KB (2007). *AtERF14*, a member of the ERF family of transcription factors, plays a non-redundant role in plant defense. Plant Physiol. 43: 400-409.

Osborne DJ (1989). Abscission. Critical Reviews in Plant Sciences 8: 103–129.

Osborne DJ (1990). Ethylene formation, cell types and differentiation. In: Polyamines and Ethylene: Biochemistry Physiology, and Interactions, Flores HE, Arteca RN, Shannon JC, Eds., pp. 203-215, Baltimore, MD: The American Society of Plant Physiologists.

Osborne DJ, Sargent JA. (1976). The positional differentiation of ethylene responsive cells in rachis abscission zone in leaves of *Sambucus nigra* and their growth and ultrastructural changes at senescence and separation. Planta 130: 203-210.

Overvoorde PJ, Okushima Y, Alonso JM, et al. (2005). Functional genomic analysis of the *AUXIN/INDOLE-3-ACETIC ACID* gene family members in *Arabidopsis thaliana*. Plant Cell 17: 3282–3300.

Parenicova L, De Folter S, Kieffer M, et al. (2003). Molecular and phylogenetic analyses of the complete MADS-box transcription factor family in Arabidopsis: New openings to the MADS world. Plant Cell 15: 1538-1551.

Parnis A, Cohen O, Gutfinger T, Hareven D, Zamir D, Lifschitz E (1997). The dominant developmental mutant of tomato, *mouse-ear* and *curl*, are associated with distinct modes of abnormal transcriptional regulation of a knotted gene. Plant Cell 9: 2143- 2158.

Patterson SE (2001). Cutting loose. Abscission and dehiscence in Arabidopsis. Plant Physiol. 126: 494-500.

Patterson, SE and Bleecker, AB. (2004). Ethylene-dependent and -independent processes associated with floral organ abscission in Arabidopsis. Plant Physiol. 134: 194–203.

Peretto R, Favaron F, Bettini V, Delorenzo G, Marini S, Alghisi P, Cervone F, Bonfante P (1992). Expression and localization of polygalacturonase during the outgrowth of lateral roots in *Allium porrum* L. Planta 188: 164–172.

Pien S, Wyrzykowska J and Fleming AJ (2001). Novel marker genes for early leaf development indicate spatial regulation of carbohydrate metabolism within the apical meristem. Plant J. 25: 663–674.

Pinyopich A, Ditta GS, Savidge B, Lilbergren SJ, Baumann E, Wlsman E, Yanofsky MF (2003). Assessing the redundancy of MADS-box genes during carpel and ovule development. Nature 424: 85-88.

Pirrello J, Miranda FJ, Ballesta MT, Tournier B, Ahmad QK, Regad F, Pech JC, Bouzayen M (2006). *Sl-ERF2*, a tomato ethylene response factor Involved in ethylene response and seed germination. Plant Cell Physiol. 47: 1195–1205.

Pnueli L, Abu M, Zamir D, Nacken W, Schwar Z, Lifschitz E (1991). The MADS-box gene family in tomato: Temporal expression during floral development conserved secondary structures and homology with homeotic genes from *Antirrhinum* and Arabidopsis. Plant J. 1: 255–266.

Pnueli L, Hareven D, Broday L, Hurwitz C, Lifschitz E (1994). The *TM5* MADS-box gene mediates organ differentiation in the three inner whorls of tomato flowers. Plant Cell 6: 175-186.

Quinet M, Dielen V, Batoko H, Boutry M, Havelange A, Kinet JM (2006). Genetic interactions in the control of flowering time and reproductive structure development in tomato (*Solanum lycopersicum*). New Phytol. 170: 701-710.

Rabinowicz PD, Braun EL, Wolfe AD, Bowen B, Grotewold E (1999). Maize *R2R3 Myb* genes: Sequence analysis reveals amplification in the higher plants. Genetics 153: 427-444.

Riechmann JL, Heard J, Martin G, Reuber L, Jiang CZ, et al., (2000). Arabidopsis transcription factors: Genome-wide comparative analysis among eukaryotes. Science 29: 2105-2110.

Roberts JA, Elliot KA, Gonzalez-Carranza ZH (2002). Abscission, dehiscence and other cell separation processes. Annu. Rev. Plant Biol. 53: 131–158.

Roberts JA, Gonzales-Carranza ZH (2009)**.** Pectinase function in abscission**.** Stewart Postharvest Review 1: 2

Roberts JA, Schindler CB, Tucker GA (1984). Ethylene-promoted tomato flower abscission and the possible involvement of an inhibitor. Planta 160: 159-163.

Roberts JA, Taylor JE, Laslett YV, Tucker GA (1989). Changes in gene expression during ethylene induced leaf abscission. In: Cell Separation in Plants, Osborne DJ, Jackson MB, Eds., NATO ASI series, Vol H 35, pp. 61-68.

Roberts JA, Whitelaw CA, Gonzalez-Carranza ZH, Mc-Manus, MT (2000). Cell separation processes in plants: models, mechanisms, and manipulation. Ann. Bot. 86: 223–235.

Rupp HM, Frank M, Werner T, Strnad M, Schmulling T (1999). Increased steady state mRNA levels of the *STM* and *KNAT1* homeobox genes in cytokinin overproducing *Arabidopsis thaliana* indicate a role for cytokinins in the shoot apical meristem. Plant J. 18: 557–563.

Sakamoto T, Kamiya N, Ueguchi-Tanaka M, Iwahori S, Matsuoka M (2001). KNOX homeodomain protein directly suppresses the expression of a gibberellin biosynthetic gene in the tobacco shoot apical meristem. Genes Dev. 15: 581–590.

Sawa S, Watanabe K, Goto K, Kanaya E, Morita EM, Okada K (1999). *FILAMENTOUS FLOWER*, a meristem and organ identity gene of Arabidopsis, encodes a protein with a zinc finger and HMG-related domains. Genes Dev. 13: 1079-1088.

Schaffer R, Ramsay N, Samach A, Corden S, Puterill J, Carre IA, Coupland G (1998). The late elongated hypocotyl mutation of Arabidopsis disrupts circadian rhythms and the photoperiodic control of flowering. Cell 93: 1219 1229.

Schellmann S, Schnittger A, Kirik V, Wada T, Okada K, Beermann A, Thumfahrt J, Jurgens G, Hulskamp M (2002). *TRIPTYCHON* and *CAPRICE* mediate lateral inhibition during trichome and root hair patterning in Arabidopsis. EMBO J. 21: 5036–5046.

Schneeberger R, Tsiantis M, Freeling M, Langdale JA (1998). The rough *sheath2* gene negatively regulates homeoboxgene expression during maize leaf development. Development 125: 2857–2865.

Sentoku N, Sato Y, Kurata N, Ito, Y., Kitano H and Matsuoka M (1999). Regional expression of the rice KN1-type homeobox gene family during embryo, shoot, and floral development. Plant Cell 11: 1651–1663

Sexton R (1995). Abscission. In M Pessarakli, ed, Handbook of Plant and Crop Physiology. Marcel Dekker, New York, pp 497–525

Sexton R (1997). The role of ethylene and auxin in abscission. Acta Hort. 463: 435-444.

Sexton R, Lewis LN, Trewavas AJ, Kelly P (1985). Ethylene and abscission. pp. 173-196. London, UK: Buttererworths.

Sexton R, Roberts JA (1982). Cell biology of abscission. Annu. Rev Plant Physiol. 33: 133-162.

Shani Z, Dekel M, Roiz L, Horowitz M, Kolosovski N, Lapidot S, Alkan S, Koltai H, Tsabary G, Goren R, Shoseyov O (2006). Expression of endo-1,4-β-glucanase (*Cel* 1) in *Arabidopsis thaliana* is associated with plant growth, xylem development and cell-wall thickening. Plant Cell Rep. 25: 1067–1074.

Siegfried KR, Eshed Y, Baum SF, Otsuga D, Drews GN, Bowman JL (1999). Members of the *YABBY* gene family specify abaxial cell fate in Arabidopsis. Development 126: 4117–4128.

Sinha N, Williams RE, Hake S (1993). Overexpression of the maize homeobox gene, *KNOTTED-1*, causes a switch from determinate to indeterminate cell fate. Genes Dev. 7: 787–795.

Solano R, Stepanova A, Chao Q, Ecker JR (1998). Nuclear events in ethylene signaling: a transcriptional cascade mediated by *ETHYLENE-INSENSITIVE3* and *ETHYLENE-RESPONSE-FACTOR1*. Genes Dev. 12: 3703–3714.

Song CP, Agarwal M, Ohta M, Guo Y, Halfter U, Wang P, Zhu JK (2005). Role of an Arabidopsis *AP2/EREBP*-type transcriptional repressor in abscisic acid and drought stress responses. Plant Cell 17: 2384-2396.

Sun Y, Zhou Q, Zhang W, Yanlei Fand Huang H (2002). *ASYMMETRIC LEAVES1*, an Arabidopsis gene that is involved in the control of cell differentiation in leaves. Planta 214: 694-702.

Taylor JE, Tucker JA, Lasslet Y, Smith CJS, Arnold CM, Waston CF, Shuch W, Grierson D, Roberts JA (1990). Polygalacturonase expression during leaf abscission of normal and transgenic tomato plants. Planta 183: 133-138.

Taylor JE, Webb STJ, Copue SA, Tucker JA, Lasslet Y, Roberts JA (1993). Changes in polygalacturonase activity and solubility of polyuronides during ethylene stimulated leaf abscission in *Sambacus nigra*. J. Exp. Bot. 44: 93-98.

Taylor JE, Whitelaw CA (2001). Signals in abscission. New Phytol. 151: 323–33.

Thompson DS, Osborne DJ (1994). A role for the stele in intertissue signaling in the initiation of abscission in bean leaves (*Phaseolus vulgaris* L.). Plant Physiol 105: 341–347.

Timmermans MCP, Hudson A, Becraft PW, Nelson T (1999). ROUGH SHEATH2: A Myb protein that represses *KNOX* homeobox genes in maize lateral organ primordia. Science 284: 151–153.

Tournier B, Sanchez-Ballesta MT, Jones B, Pesquet E, Regad F, Latche A, Pech JC, Bouzayen M (2003). New members of the tomato ERF family show specific expression pattern and diverse DNA-binding capacity to the GCC box element. FEBS Lett. 550: 149–154.

Tsiantis M, Brown MIN, Skibinski G, Langdale JA (1999). Disruption of auxin transport is associated with aberrant leaf development in maize. Plant Physiol. 121: 1163–1168.

Tucker ML, Burke A, Murphy CA, Thai VK, Ehrenfried ML (2007). Gene expression profiles for cell wall-modifying proteins associated with soybean cyst nematode infection, petiole abscission, root tips, flowers, apical buds, and leaves. J. of Exp. Bot 58: 3395-3406.

Tucker GA, Schindler B, Roberts JA (1984). Flower abscission in mutant tomato plants. Planta 160: 164–167.

Tucker ML, Whitelaw CA, Lyssenko NN, Nath P (2002). Functional analysis of regulatory elements in the gene promoter for an abscission-specific cellulase from bean and isolation, expression, and binding affinity of three TGA-type basic Leucine zipper transcription. Plant Physiol. 130: 1487-1496.

Ulmasov T, Hagen G, Guilfoyle TJ (1997). ARF1, a transcription factor that binds to auxin responsive elements. Science 276: 1865-1868.

Van Doorn WG, Woltering EJ (1991). Developments in the use of growth regulators for the maintenance of postharvest quality in cut flowers and potted plants. Acta Hort. 298: 195-204.

Van Nocker S (2009) Development of the abscission zone. Stewart Postharvest Review 1: 5

Wada T, Kurata T, Tominaga R, Koshino-Kimura Y, Tachibana T, Goto K, Marks MD, Shimura Y, Okada K (2002). Role of positive regulator of root hair development, CAPRICE, in Arabidopsis root epidermal cell differentiation. Development 129: 5409–5419.

Wada T, Tachibana T, Shimura Y, Okada K (1997). Epidermal cell differentiation in Arabidopsis determined by a Myb homolog, CPC. Science 277: 1113–1116.

Waites R, Hudson A (1995). *Phantastica*: A gene required for dorsoventrality of leaves in *Antirrhinum majus*. Development 121: 2143–2154.

Waites R, Selvandurai HRN, Oliver IR and Hudson A (1998). The *PHANTASTICA* gene encodes a MYB transcription factor involved in growth and dorsoventrality of lateral organs in *Antirrhinum*. Cell 93: 779-789.

Wang S, Chang Y, Guo J, Chen J-G (2007). Arabidopsis *OVATE* family protein 1 is a transcriptional repressor that suppresses cell elongation. Plant J. 50: 858–872.

Wang ZY, Kenigsbuch D, Sun L, Harel E, Ong MS, Tobin EM (1997). A Myb-related transcription factor is involved in the phytochrome regulation of an Arabidopsis *Lhcb* gene . Plant Cell 9: 491- 507.

Wang ZY, Seto H, Fujloka S, Yoshida S, Chory J (2001). BRI1 is a critical component of a plasma-membrane receptor for plant steroids. Nature 410: 380-383.

Webster BD (1968). Anatomical aspects of abscission. Plant Physiol. 43: 1512–1544.

Williams CE, Grotewold E (1997). Differences between plant and animal Myb domains are fundamental for DNA binding activity, and chimeric Myb domains have novel DNA binding specificities. J. Biol. Chem 272: 563 571.

Wu L, Chen X, Ren H, Zhang Z, Zhang H, Wang J, Wang XC, Huang R (2007). ERF protein JERF1 that transcriptionally modulates the expression of abscisic acid biosynthesis-related gene enhances the tolerance under salinity and cold in tobacco. Planta 226: 815–825.

Xu W, Purugganan MM, Polisensky DH, Antosiewicz DM, Fry SC, Braam J (1995). Arabidopsis *TCH4*, regulated by hormones and the environment, encodes a xyloglucan endotransglycosylase. Plant Cell 7: 1555-1567.

Xue GP, Loveridge CW (2004) *HvDRF1* is involved in abscisic acid-mediated gene regulation in barley and produces two forms of AP2 transcriptional activators, interacting preferably with a CT-rich element. Plant J. 37: 326–339.

Yang TF, Gonzalez-Carranza ZH, Martin JM and Roberts JA (2007). Ethylene and the regulation of senescence processes in transgenic *Nicotiana sylvestris* plants. Ann. Bot. 101: 301-310.

Yang Z, Tian L, Latoszek-Green M, Brown D, Wu K (2005). Arabidopsis *ERF4* is a transcriptional repressor capable of modulating ethylene and abscisic acid responses. Plant Mol. Biol. 58: 585–596.

Yuan R, Wu Z, Kostenyuk IA, Burns JK (2005). G-protein coupled a 2A-adrenoreceptor agonist differentially alter citrus leaf and fruit abscission by affecting expression of ACC synthase and ACC oxidase. J. Exp. Bot. 56: 1867–1875.

Zhang H, Huang Z, Xie B, Chen Q, Tian X, Zhang X, Zhang H, Lu X, Huang D, Huang R (2004). The ethylene, jasmonate, abscisic acid and NaCl-responsive tomato transcription factor *JERF1* modulates expression of GCC box-containing genes and salt tolerance in tobacco. Planta 220: 262–270.

Zhou J, Tang X, Martin GB (1997). The Pto kinase conferring resistance to tomato bacterial speck disease interacts with proteins that bind a *cis*-element of pathogenesis-related genes. EMBO J. 16: 3207–3218.

APPENDIX 1

Figures of a manuscript submitted to Plant Physiology

Microarray analysis of the abscission-related transcriptome in tomato flower abscission zone in response to auxin depletion

Shimon Meir[1], Sonia Philosoph-Hadas[1], Srivignesh Sundaresan[1], K.S. Vijay Selvaraj[1], Shaul Burd[1], Ron Ophir[2], Bettina Kochanek[1], Michael S. Reid[3], Cai-Zhong Jiang[4] and Amnon Lers[1]

[1]Department of Postharvest Science of Fresh Produce, ARO, The Volcani Center, Bet-Dagan 50250, Israel; [2]Plant Sciences, Fruit Tree Sciences, ARO, The Volcani Center, Bet-Dagan 50250, Israel; [3]Department of Plant Sciences, University of California, Davis, CA 95616, USA; [4]Crops Pathology and Genetic Research Unit, USDA-ARS, Davis, CA 95616, USA

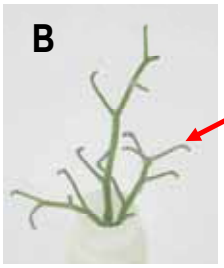

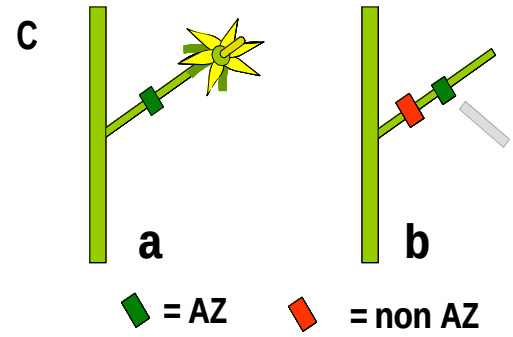

D

Treatments	Time after flower removal (h)				
	Flower AZ				
Flower removal	0	2	4	8	14
1-MCP pretreatment + flower removal	0	2	4	8	14
	non AZ (NAZ)				
Flower removal	0	2	4	ns	14
1-MCP pretreatment + flower removal	0	ns	4	ns	14

Figure 1: Experimental outline: Appearance of flower explants of cherry tomatoes (*Solanum lycopersicum* Mill, cv. 'Shiran' 1335) held in water, before (A) and after (B) flower removal; C, schematic presentation of the AZ and non-AZ (NAZ) tissue sampling for RNA extraction before (a) and after (b) flower removal (abscised pedicel is indicated by the gray bar); D, table of pretreatments and timing of tissue sampling for RNA extraction. Samples for zero time were excised without flower removal (C, scheme a). 1-MCP pretreatment was performed by exposing the flower explants to 0.4 nL L^{-1} 1-MCP for 12 h in the dark at 20°C, prior to flower removal. Vs, not sampled.

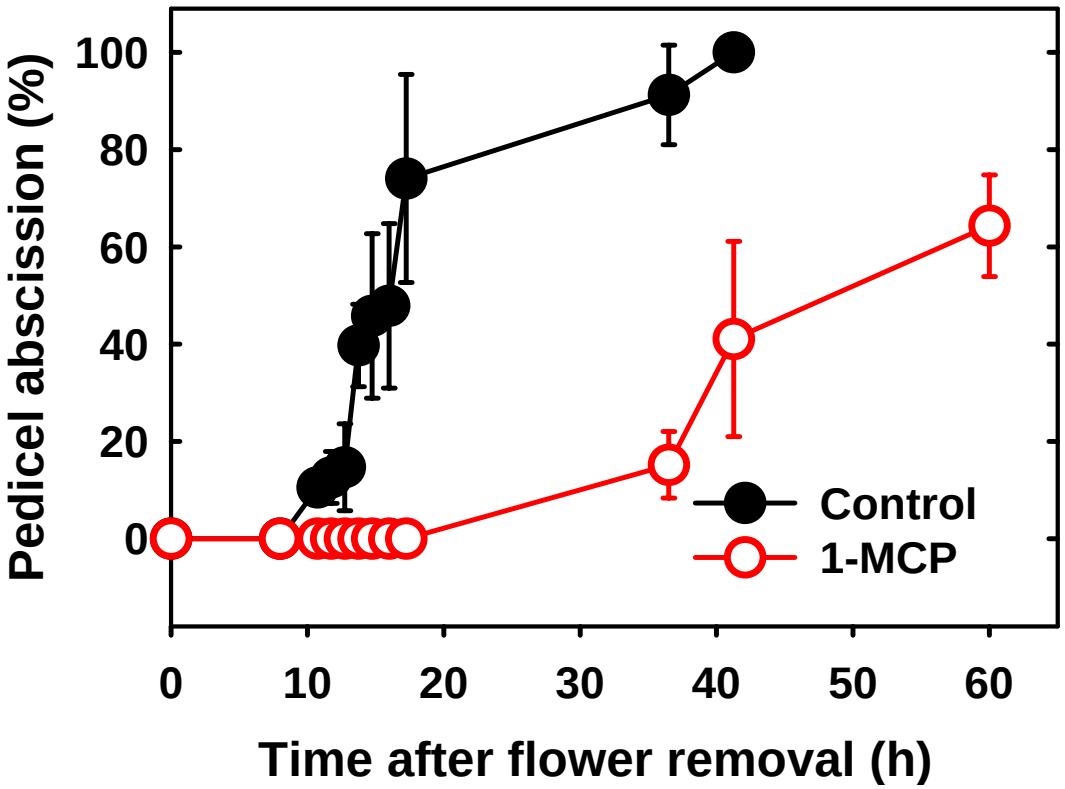

Figure 2: Effect of flower removal and 1-MCP pretreatment on the kinetics of pedicel abscission. Tomato flower explants held in water were exposed to 0.4 nL L^{-1} 1-MCP for 12 h in the dark at 20°C. Control flower explants were kept without 1-MCP under similar conditions for the same period. Then, flowers were removed, and the percentage of accumulated pedicel abscission was monitored at various time intervals following flower removal. The results are means of four replicates (30 flowers each) ± SE.

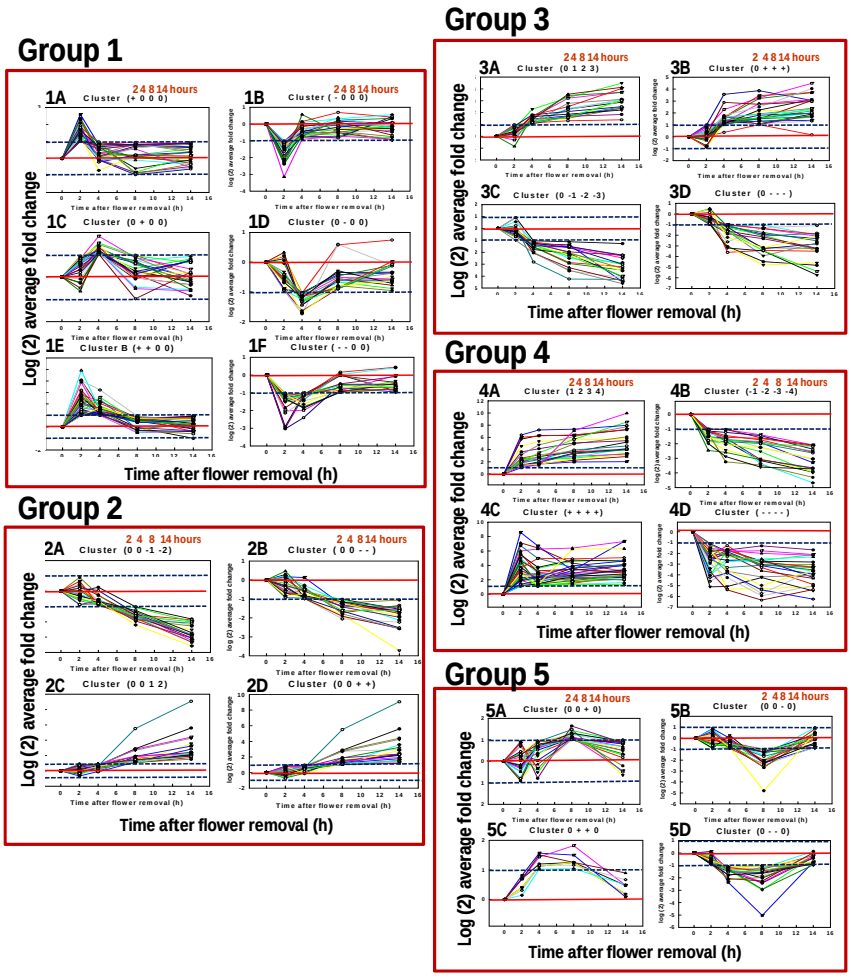

Figure 3: Gene expression profiles obtained by kinetics-based clustering of Groups 1-5: Group 1 - clusters of differentially expressed genes with early and transient changes of expression in the AZ following flower removal; Group 2 - clusters of genes with expression kinetics exhibiting late changes in the AZ following flower removal; Group 3 - clusters of genes modified in their expression in the AZ during 4-14 h following flower removal; Group 4 - clusters of genes modified in their expression in the AZ during 2-14 h following flower removal; and Group 5 - Clusters of genes with transient changes in their expression in the AZ following 4-8 h after flower removal. Numbers in red above each graph indicate the sampling time points (in h) after flower removal. The (+) and (-) signs below the time points represent up- or down-regulation of genes, respectively, while the (0) sign represents no change. The (1), (2), (3) or (4) and the (-1), (-2), (-3) or (-4) signs below the time points represent continuously up- or down-regulated genes, respectively. All of these changes were based on a two-fold change criterion (1 log ratio).

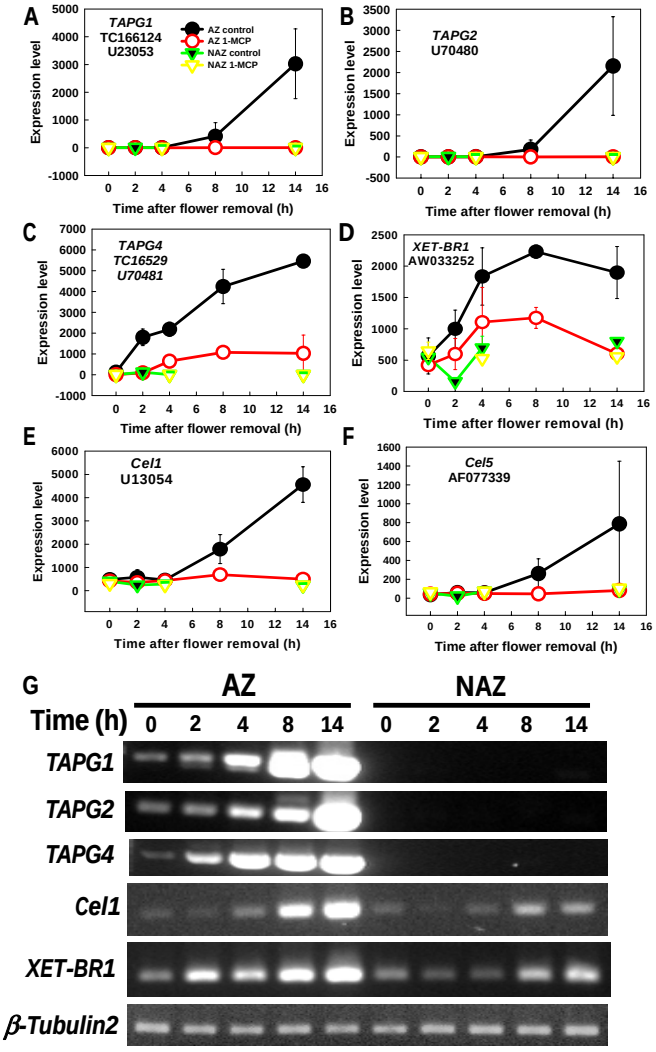

Figure 4: Effects of flower removal, 1-MCP pretreatment, and tissue type on kinetics of changes in array-measured (A-F) and semi-quantitative RT-PCR (SQ-RT-PCR)-validated (G) expression levels of genes encoding cell wall hydrolyzing enzymes. Expression levels were measured for tomato abscission polygalacturonases (*TAPG*s) (A, B, C), xyloglucan endohydrolase endotransglycosylase (*XET-BR1*) (D) and cellulases (*Cel*) (E, F). RNA samples were extracted from flower AZ or NAZ tissues taken from untreated (control) or 1-MCP-pretreated tomato flower explants, at the indicated time points after flower removal. The results are means of two or three biological replicates ± SD. Transcript identities are indicated in the graphs by their tentative consensus sequence (TC) number in The Institute for Genomic Research (TIGR) and/or accession numbers. The microarray and the SQ-RT-PCR analyses were performed with different samples taken from independent biological replicates of two separate experiments.

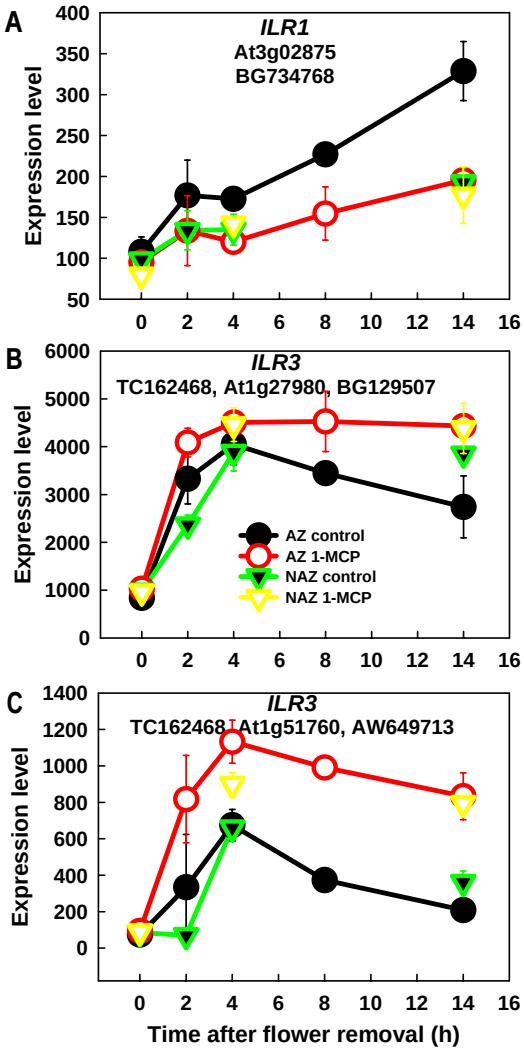

Figure 5: Effects of flower removal, 1-MCP pretreatment, and tissue type on kinetics of changes in array-measured expression levels of genes belonging to the IAA-amino acid hydrolyses (*ILR*) family (A-C). RNA samples were extracted from the flower AZ or NAZ tissues taken from untreated (control) or 1-MCP-pretreated tomato flower explants, at the indicated time points after flower removal. The results are means of two or three biological replicates ± SD. Transcript identities are indicated in the graphs by their *Arabidopsis thaliana* (At) gene number, TC number in TIGR, and/or accession number.

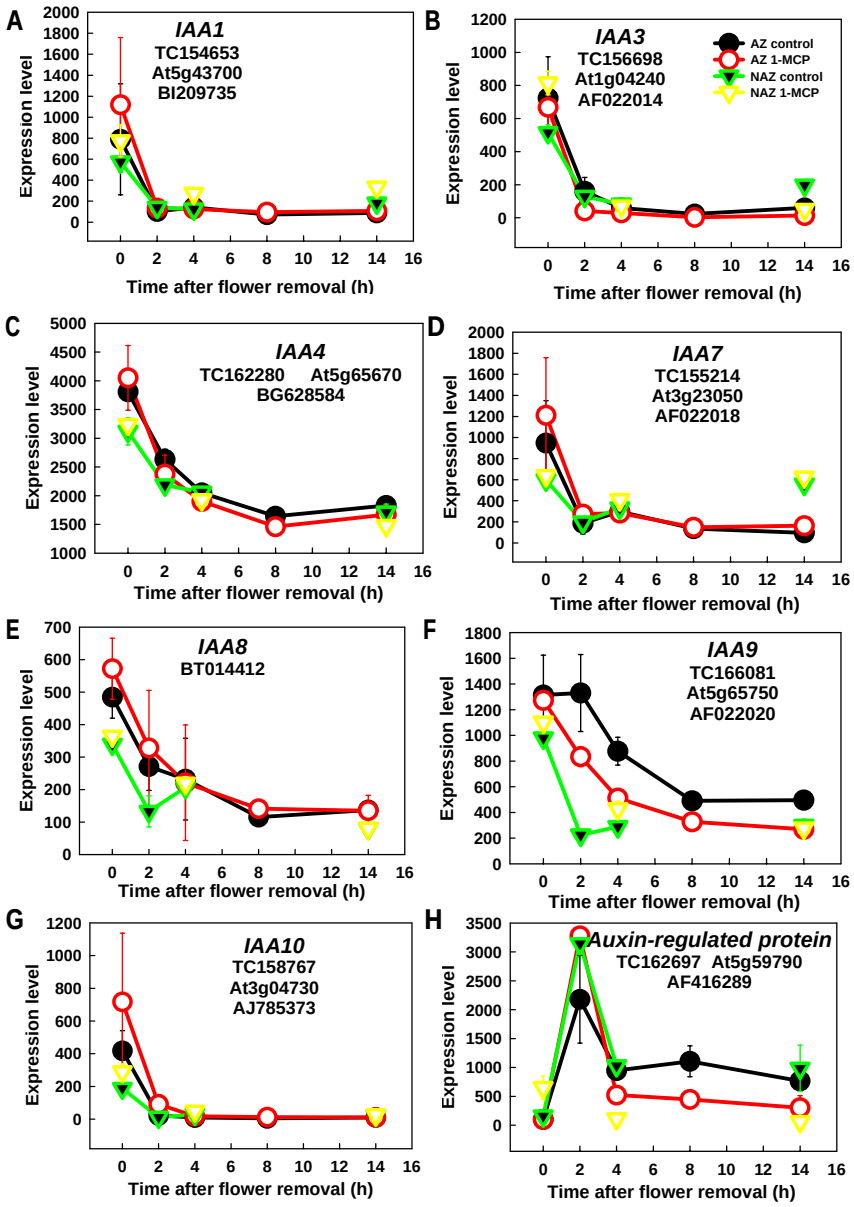

Figure 6: Effects of flower removal, 1-MCP pretreatment, and tissue type on kinetics of changes in array-measured expression levels of auxin-related genes including: *IAA1* (A), *IAA3* (B), *IAA4* (C), *IAA7* (D), *IAA*8 (E), *IAA9* (F), *IAA10* (G) and *Auxin-regulated protein* (H). The experiment was performed as detailed in Figure 5. The results are means of two or three biological replicates ± SD. Transcript identities are indicated in the graphs by their *Arabidopsis thaliana* (At) gene number, TC number in TIGR, and/or accession number.

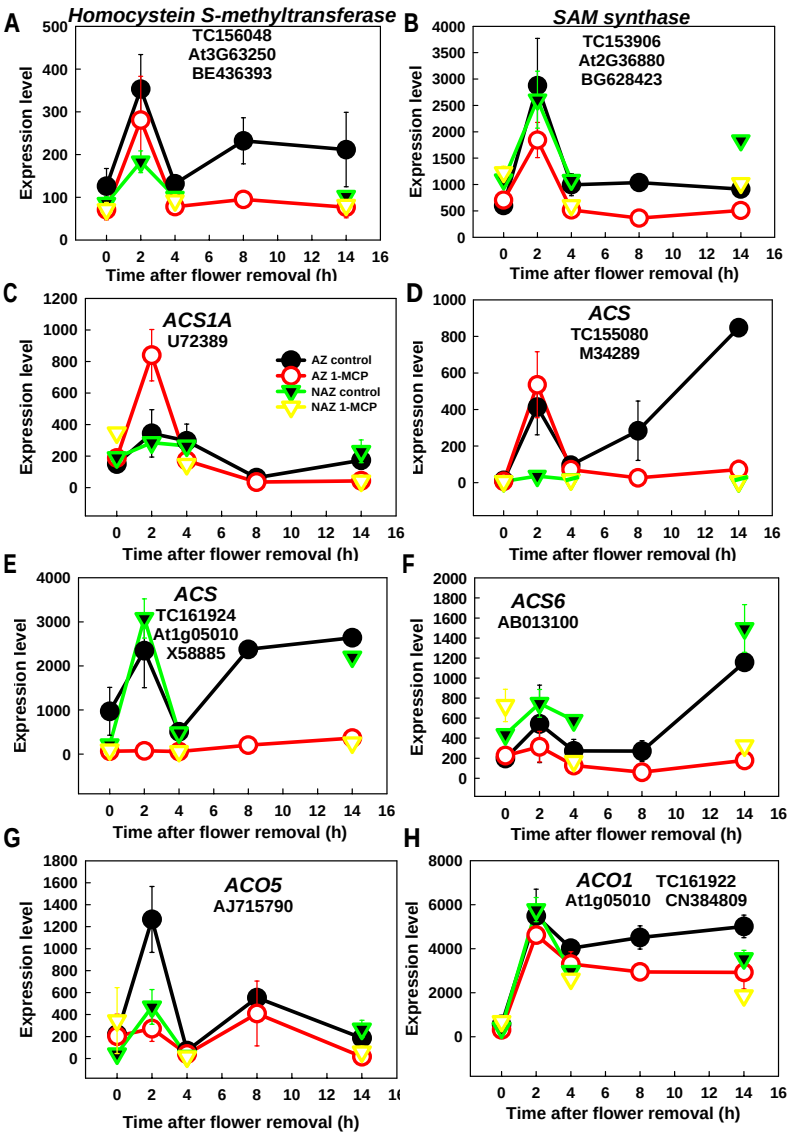

Figure 7: Effects of flower removal, 1-MCP pretreatment, and tissue type on kinetics of changes in array-measured expression levels of ethylene biosynthesis-related genes. The gene names are listed as follows: *Homocystein S-methyltransferase* (A), *S-adenosylmethionine (SAM) synthase* (B), *1-aminocyclopropane-1-carboxylic acid (ACC) synthase* (*ACS1A*) (C), *ACS* (D, E), *ACS6* (F), *ACC oxidase* (*ACO*5) (G) and *ACO*1 (H). The experiment was performed as detailed in Figure 5. The results are means of two or three biological replicates ± SD. Transcript identities are indicated in the graphs by their *Arabidopsis thaliana* (At) gene number, TC number in TIGR, and/or accession number.

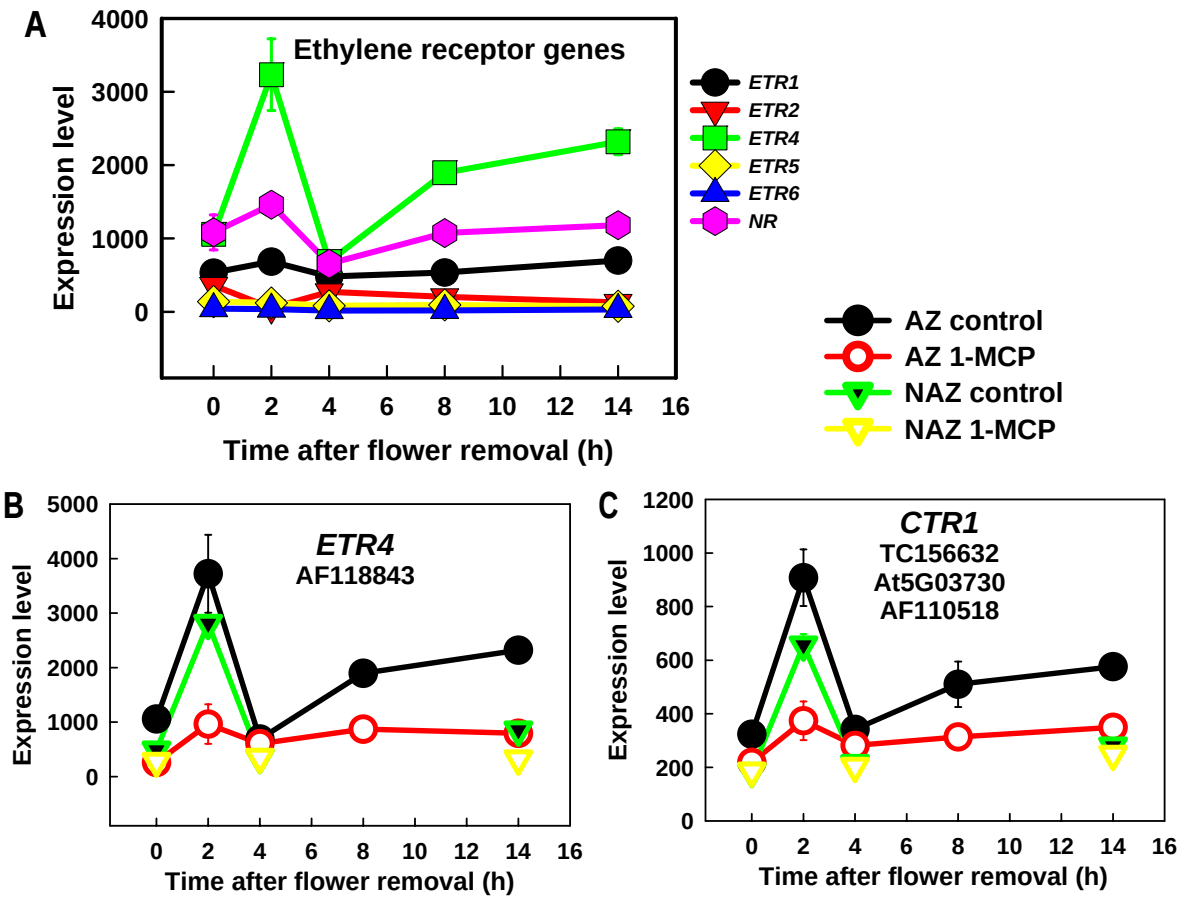

Figure 8: Changes in array-measured expression of ethylene receptor genes following flower removal (A), and effects of flower removal, 1-MCP pretreatment and tissue type on kinetics of changes in array-measured expression levels of the ethylene receptor homolog - ethylene resistant 4 (*ETR4*) (B) and constitutive triple response 1 (*CTR1*) (C). The experiment was performed as detailed in Figure 5. The results are means of two or three biological replicates ± SD. Transcript identities are indicated in the graphs by their *Arabidopsis thaliana* (At) gene number, TC number in TIGR, and/or accession number. *NR*, never ripe.

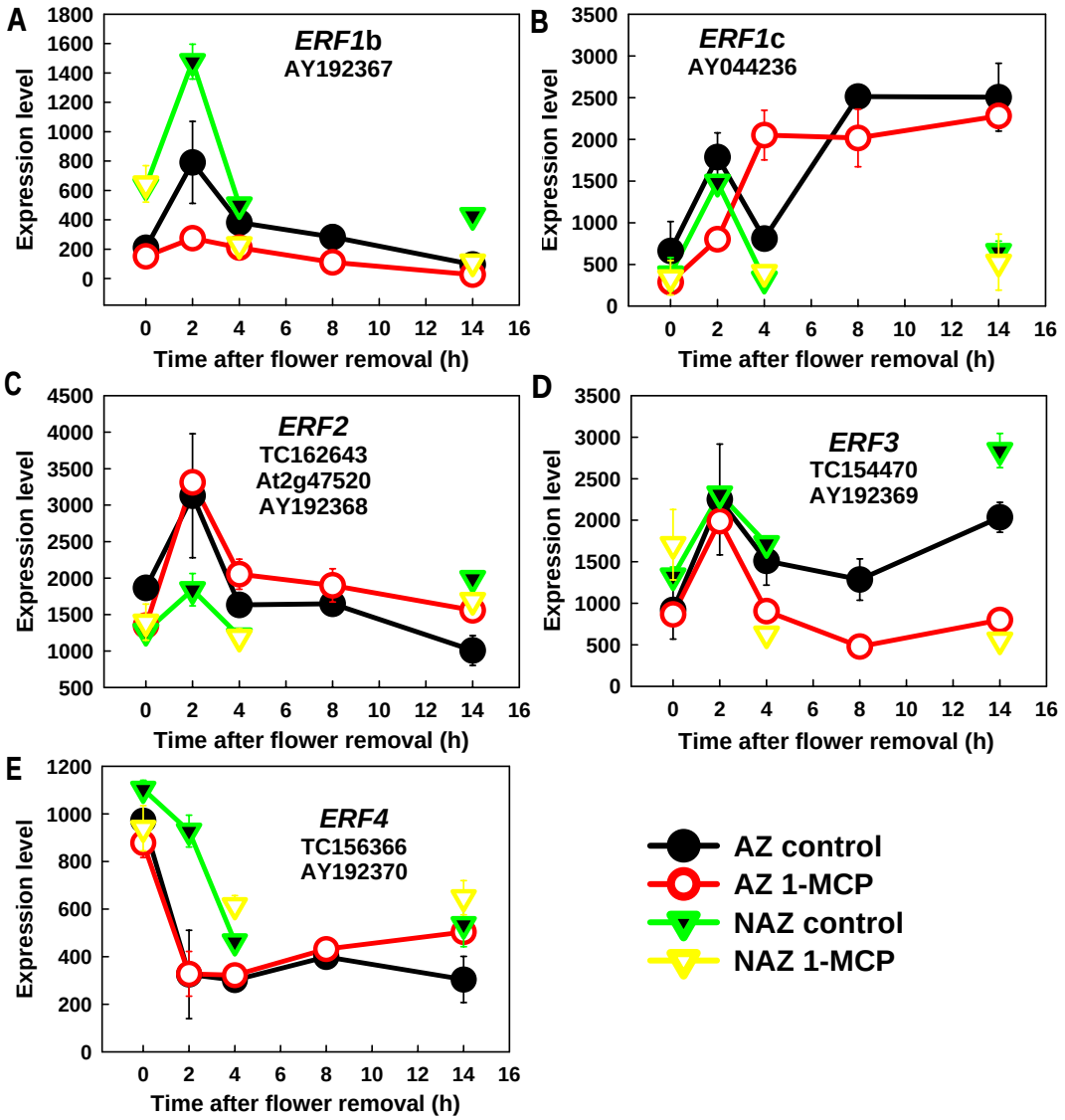

Figure 9: Effects of flower removal, 1-MCP pretreatment, and tissue type on kinetics of changes in array-measured expression levels of ethylene responsive factor (ERF) genes: *ERF1*b (A), *ERF*1c *(B), ERF*2 (C), *ERF*3 (D) and *ERF*4 (AP2 TF) (E). The experiment was performed as detailed in Figure 5. The results are means of two or three biological replicates ± SD. Transcript identities are indicated in the graphs by their *Arabidopsis thaliana* (At) gene number, TC number in TIGR and/or accession number.

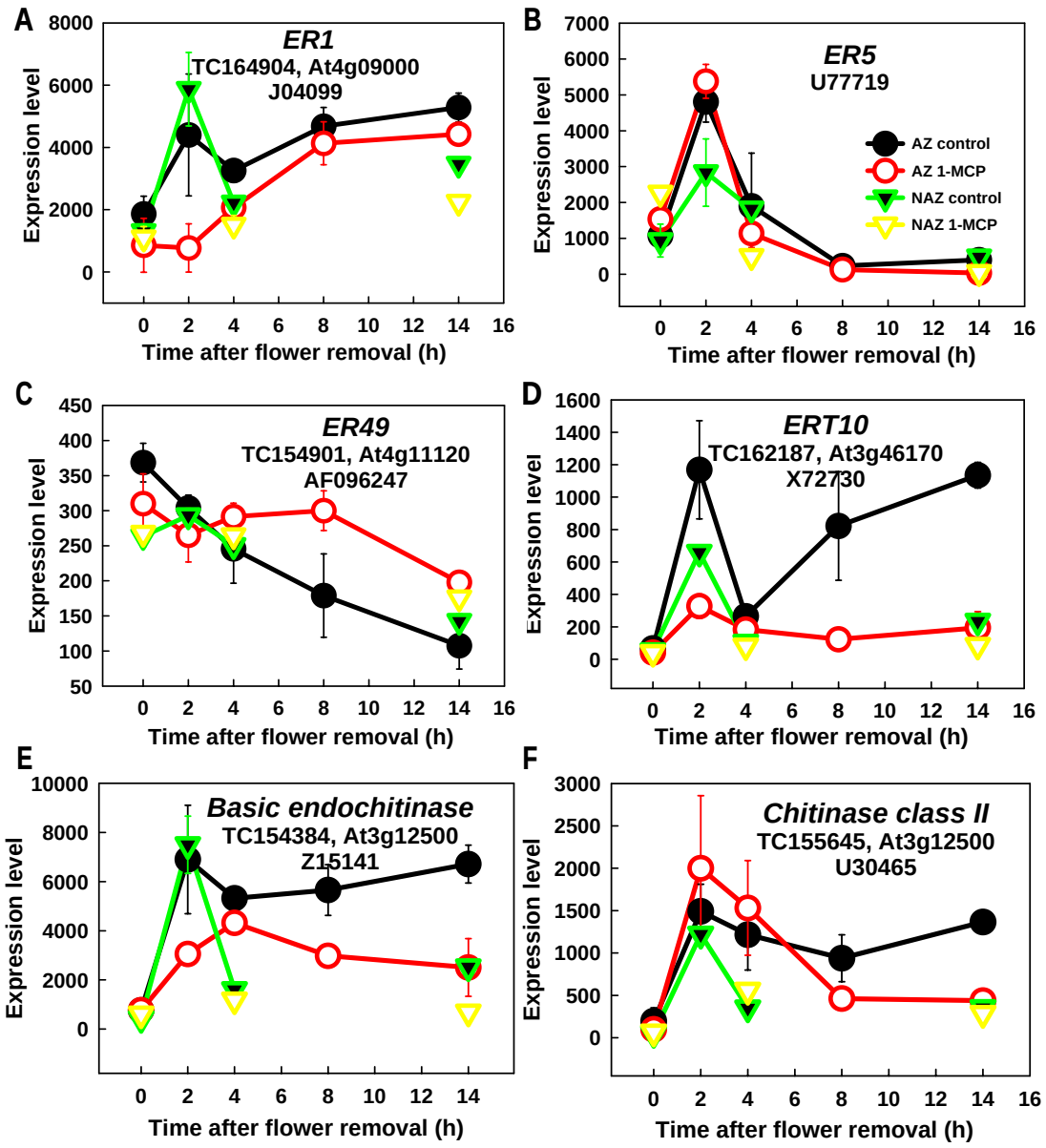

Figure 10: Effects of flower removal, 1-MCP pretreatment, and tissue type on kinetics of changes in array-measured expression levels of ethylene responsive (ER) genes. The gene names are listed as follows: *fruit ripening-related ER1 - Ser protease inhibitor 1* (*ER1*) (A), *ER*5 (B), *ER elongation factor* (*ER*49) (C), *ripening-related burst oxidase protein D* (*RbohD*) (D), *basic endochitinase* (E) and *chitinase class II* (F). The experiment was performed as detailed in Figure 5. The results are means of two or three biological replicates ± SD. Transcript identities are indicated in the graphs by their *Arabidopsis thaliana* (At) gene number, TC number in TIGR and/or accession number.

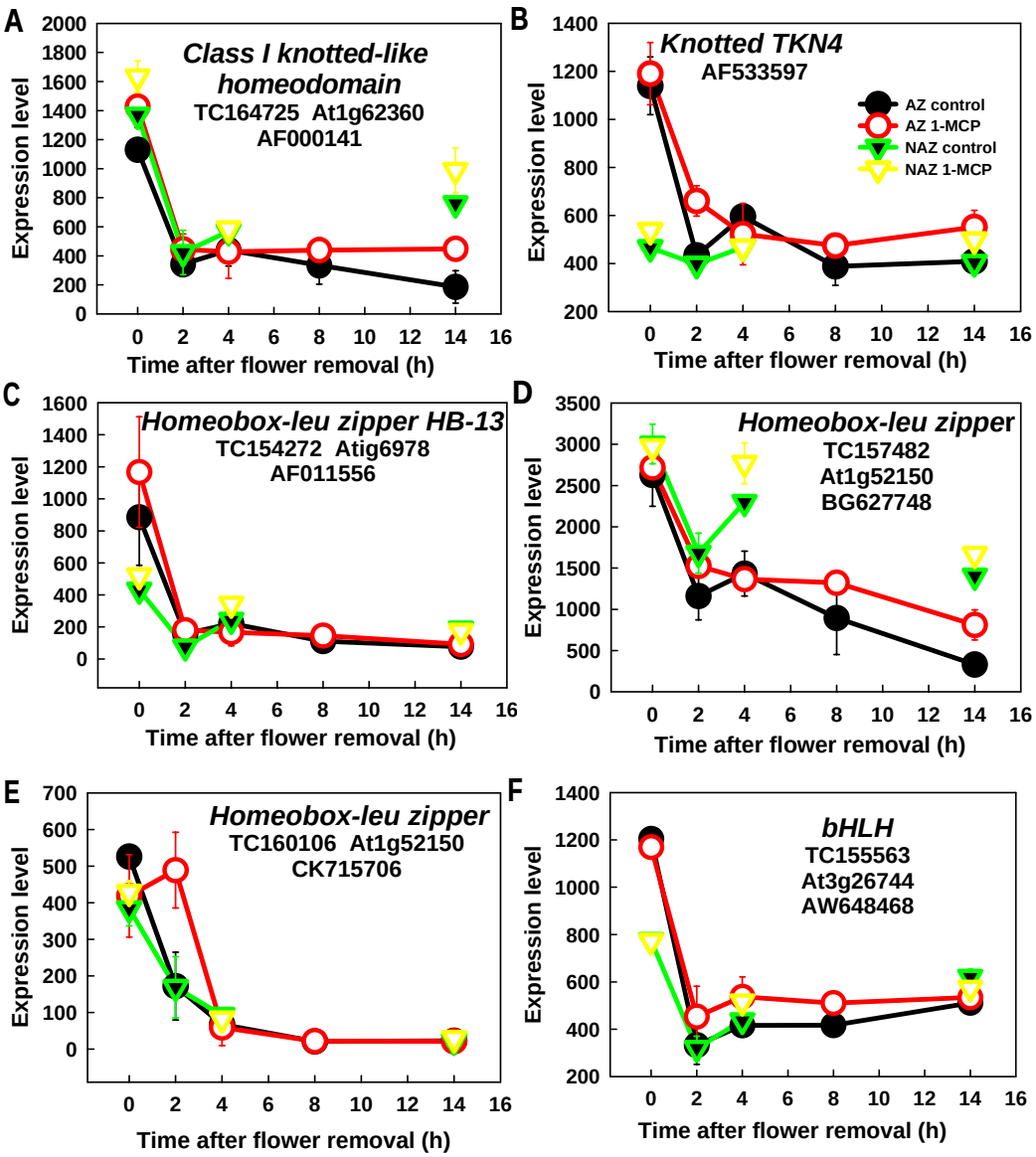

Figure 11: Effects of flower removal, 1-MCP pretreatment, and tissue type on kinetics of changes in array-measured expression levels of early down-regulated TF genes. The gene names are listed as follows: *Class I knotted-like homeodomain* (A), *Knotted TKN4* (B), *Homeobox-Leu zipper HB-13* (C), *Homeobox-Leu zipper* (D, E), and *Basix helix-loop-helix TF (bHLH*) (F). The experiment was performed as detailed in Figure 5. The results are means of two or three biological replicates ± SD. Transcript identities are indicated in the graphs by their *Arabidopsis thaliana* (At) gene number, TC number in TIGR, and/or accession number.

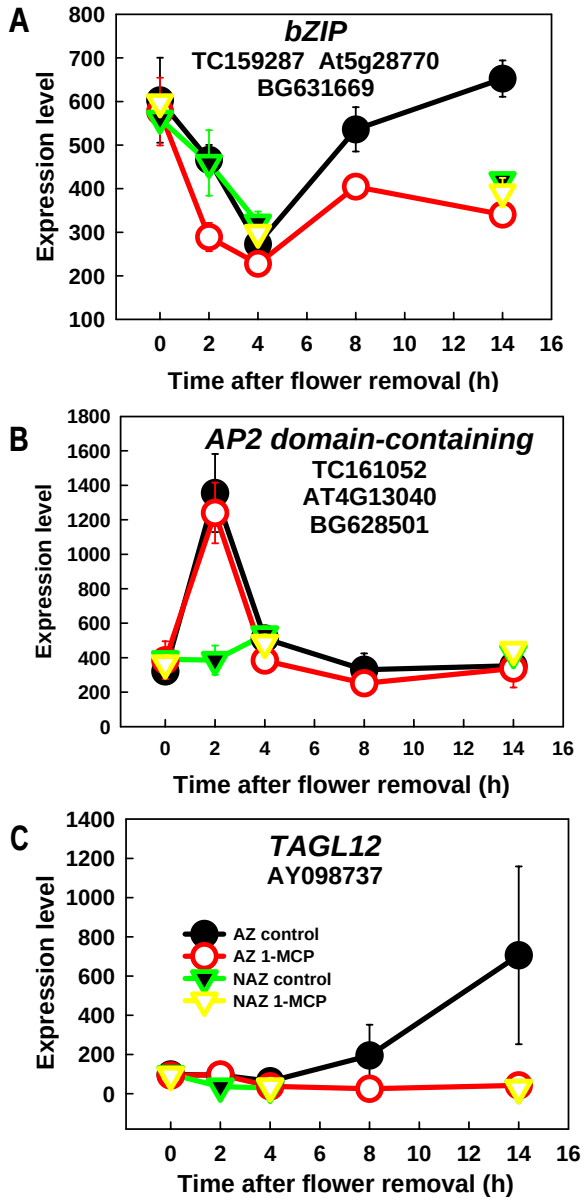

Figure 12: Effects of flower removal, 1-MCP pretreatment, and tissue type on kinetics of changes in array-measured expression levels of TF genes. The gene names are listed as follows: *bZIP TF* (A), *AP2 domain-containing TF* (B), and *TAGL12 MADS-box protein* (C). The experiment was performed as detailed in Figure 5. The results are means of two or three biological replicates ± SD. Transcript identities are indicated in the graphs by their *Arabidopsis thaliana* (At) gene number, TC number in TIGR, and/or accession number.

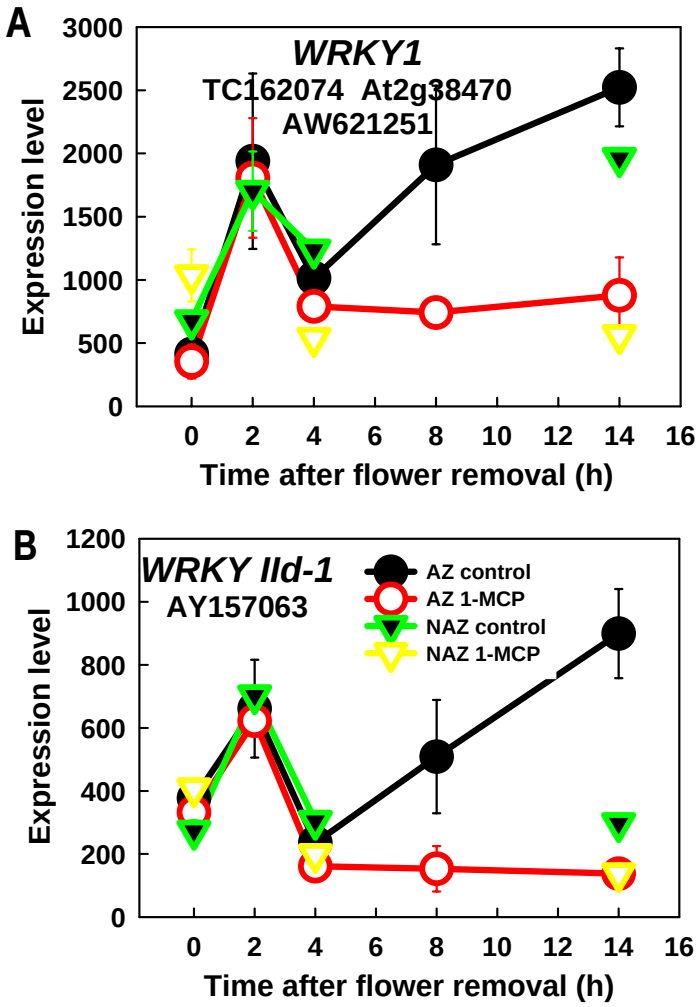

Figure 13: Effects of flower removal, 1-MCP pretreatment, and tissue type on kinetics of changes in array-measured expression levels of early- and late-regulated *WRKY TF* genes. The gene names are listed as follows: *WRKY*1 *TF* (A) and *WRKY lld*-1 (B). The experiment was performed as detailed in Figure 5. The results are means of two or three biological replicates ± SD. Transcript identities are indicated in the graphs by their *Arabidopsis thaliana* (At) gene number, TC number in TIGR, and/or accession number.

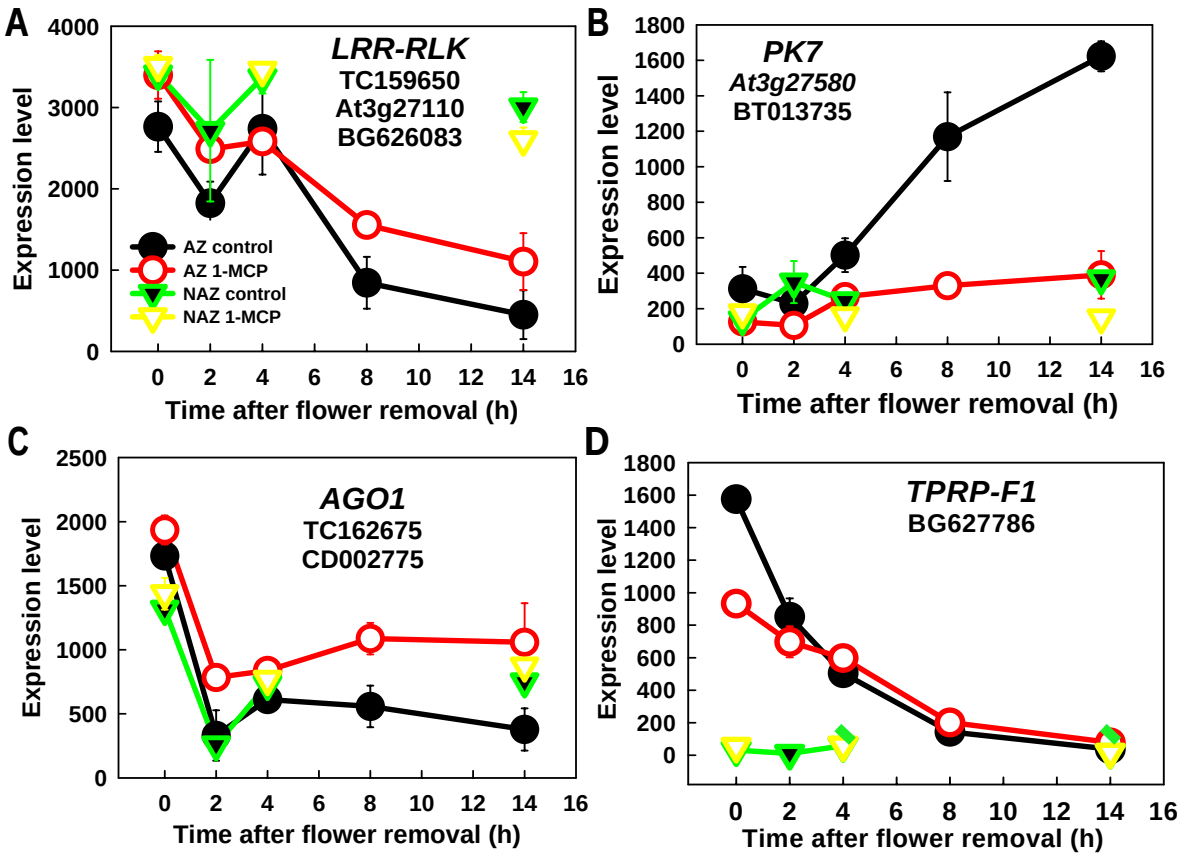

Figure 14: Effects of flower removal, 1-MCP pretreatment, and tissue type on kinetics of changes in array-measured expression levels of different regulatory genes including: *Leu-rich repeat trans-membrane receptor-like kinase* (*LRR-RLK*) (A), *Ser/Thr-protein kinase* 7 (*PK7*) (B), *argonaute-like protein* (*AGO1)* (C) and *Pro-rich protein* (*TPRP-F1*) (D). The experiment was performed as detailed in Figure 5. The results are means of 2 or 3 biological replicates ± SD. Transcript identities are indicated in the graphs by their *Arabidopsis thaliana* (At) gene number, TC number in TIGR, and/or accession number.

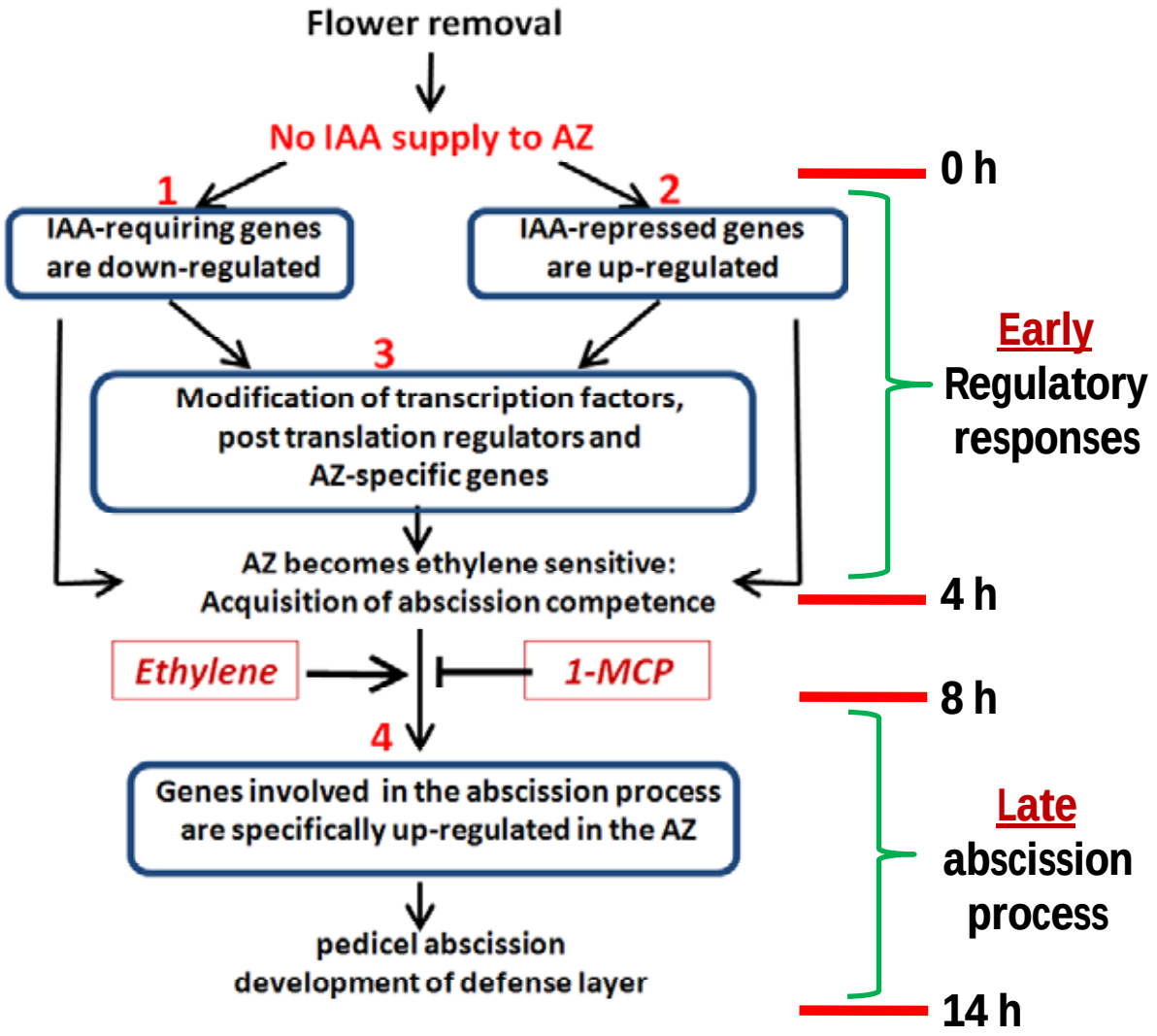

Figure 15: Summary of the postulated events leading to tomato pedicel abscission in response to auxin depletion following flower removal. The numbers in the scheme (1-4) denote different groups of genes as follows: group 1 – includes genes that are directly regulated by auxin and are therefore down-regulated early-on after IAA depletion; group 2 – includes genes that are directly IAA-repressed and which were observed to be up-regulated early-on after IAA depletion; group 3 – includes genes encoding TF and/or post transcription regulators; group 4 – includes TF genes or genes belonging to ethylene signal transduction or abscission regulators, genes encoding cell wall modifying proteins, and genes involved in the PR defense and development of the defense layer.

APPENDIX 2

Effect of flower removal, 1-MCP and tissue type on array-measured expression of additional six genes

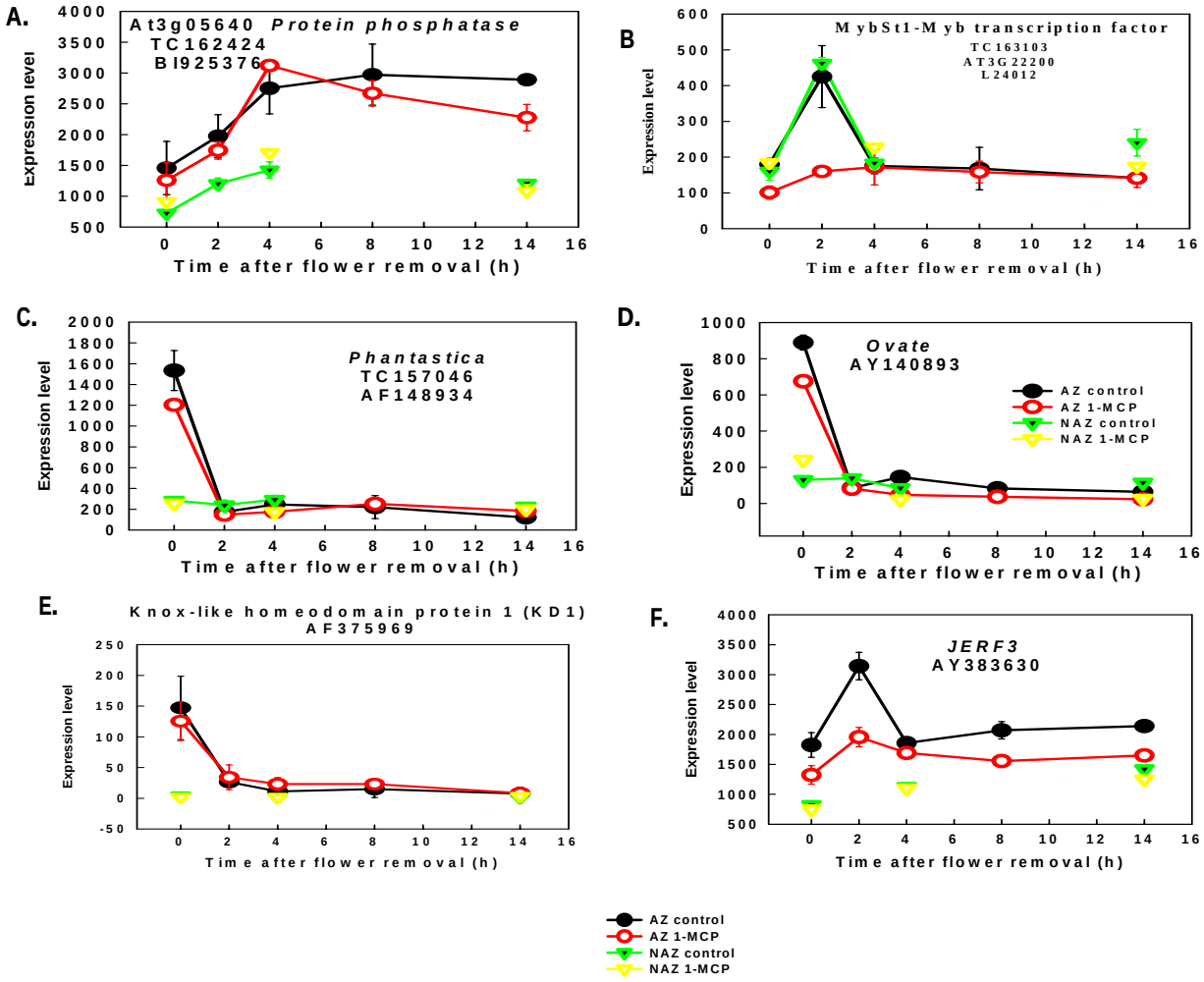

Figure 1: Effects of flower removal, 1-MCP pretreatment and tissue type on kinetics of changes in array-measured expression levels of TF and regulatory genes. The gene name and/or the protein encoded by each gene are listed as follows: *Protein phosphatase* (A), *MybSt1*-TF (B), *Phantastica* (C), *OVATE* (D), Knox like homeo domain protein (KD1) (E) and jasmonate ethylene-responsive factor gene (*JERF3*) (F). RNA samples were extracted from flower AZ or non-AZ (NAZ) tissues taken from untreated (control) or 1-MCP-pretreated tomato flower explants, at the indicated time points after flower removal. The results are means of 2 or 3 biological replicates ± SD. Transcript identities are indicated in the graphs by their *Arabidopsis thaliana* (At) gene number, TC number in TIGR, and/or accession number.

APPENDIX 3

Effect of flower or leaf removal, 1-MCP or IAA on organ abscission

Figure 1

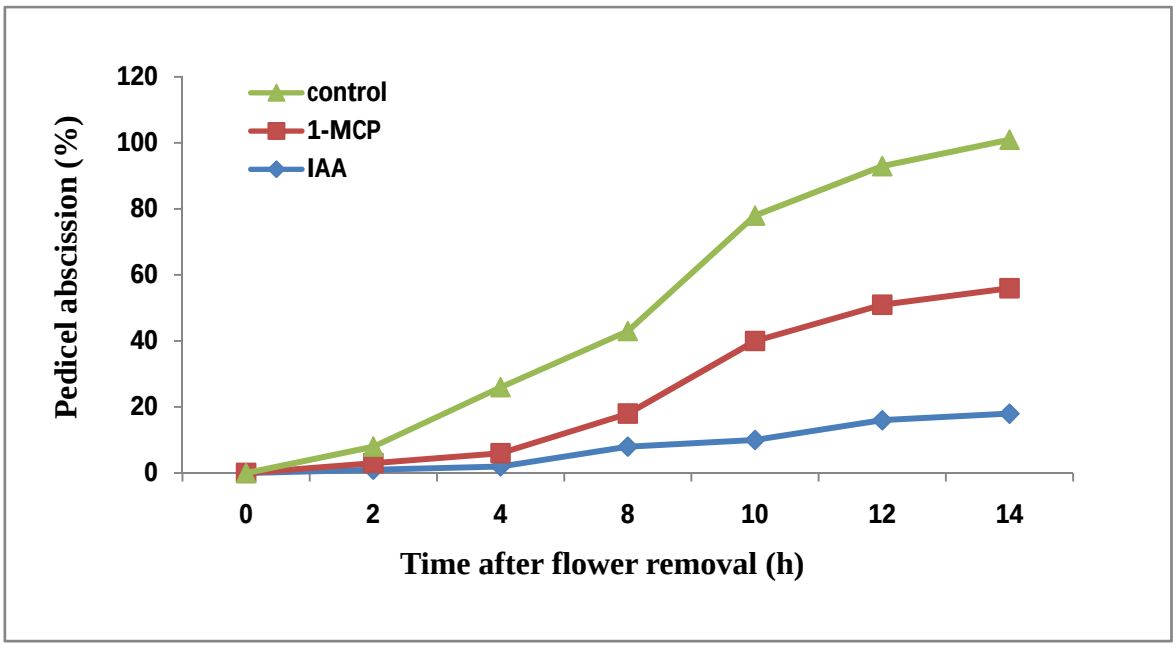

Figure 1. Effect of flower removal, 1- MCP pretreatment, or IAA application after flower removal on the kinetics of pedicel abscission. Tomato (cv. 'Shiran') flower explants held in water were exposed to 0.4 nL L^{-1} 1-MCP for 12 h in the dark at 20°C. Control flower explants were kept without 1-MCP under similar conditions for the same period. Then, flowers were removed, and IAA (1 mM aqueous solution) was applied to control explants, and the percentage of accumulated pedicel abscission was monitored at various time intervals following flower removal. The results are means of four replicates (30 flowers each) ± SE.

Figure 2

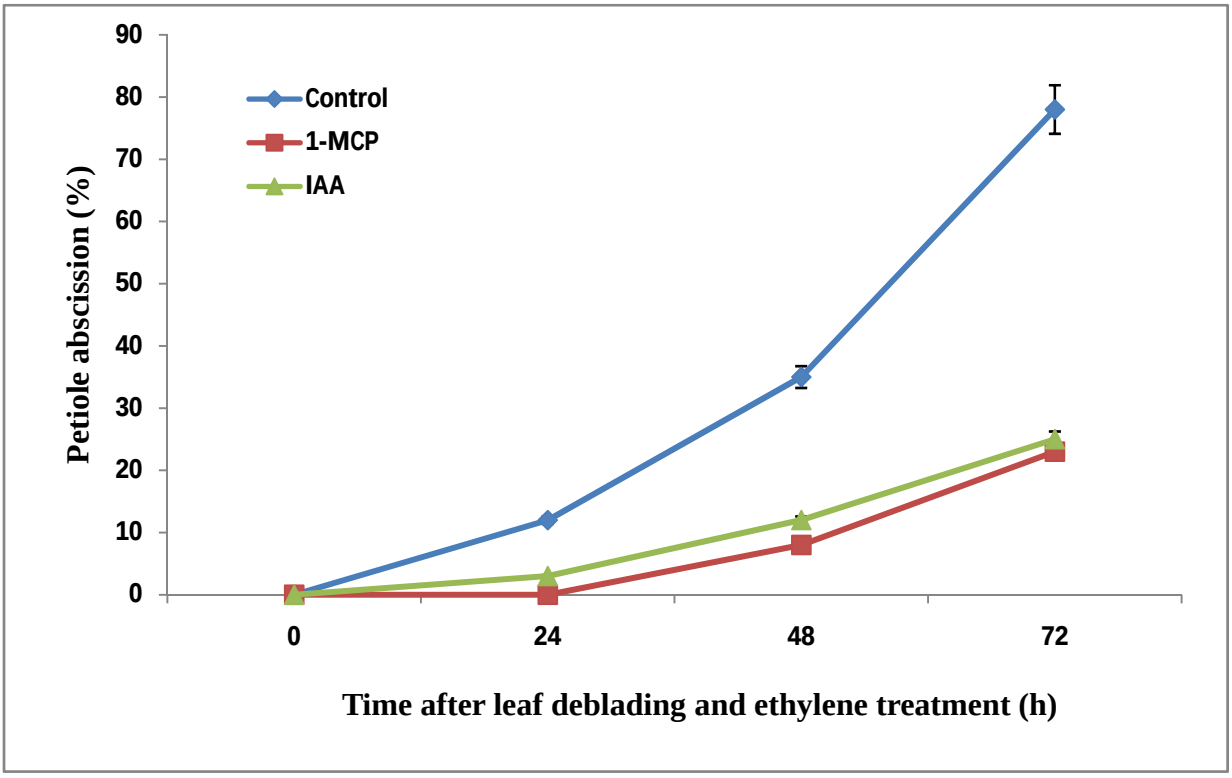

Figure 2: Effect of leaf deblading, 1- MCP pretreatment, or IAA application after deblading, on the kinetics of petiole abscission after ethylene treatment. Tomato explants (cv. 'VF-36') held in water were exposed to 0.4 nL L^{-1} 1-MCP for 12 h in the dark at 20°C. Control explants were kept without 1-MCP under similar conditions for the same period. Then, leaves were debladed, and IAA (5 mM aqueous solution) was applied to control explants. After 24 h, all explants were exposed to 5 µl/L ethylene for additional 24 h to enhance abscission, and the percentage of accumulated petiole abscission was monitored at various time intervals following leaf deblading and ethylene exposure. The results are means of four replicates (30 leaves each) ± SE.

APPENDIX 4

Effect of IAA application after flower removal

Figure 1

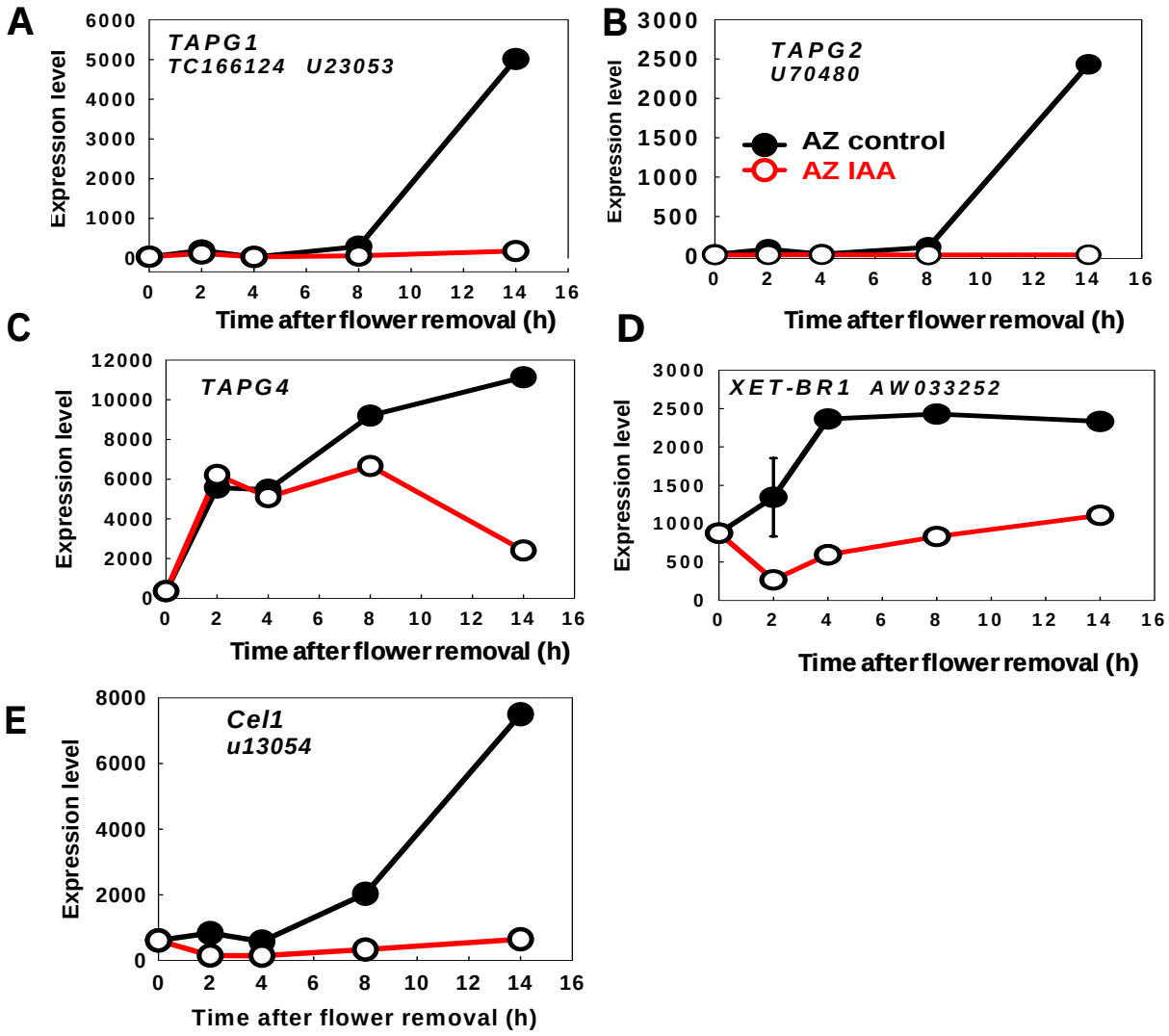

Figure 1: Effect of flower removal and IAA application after flower removal on the kinetics of changes in array-measured expression levels of cell wall hydrolyzing enzymes. Expression levels were measured for TAPGs (A, B, C), *XET-BR1* (D) and *Cel1* (E) genes. RNA samples were extracted from flower AZ tissues taken from untreated (control) or IAA-treated tomato flower explants, at the indicated time points after flower removal. The results are means of 2 or 3 biological replicates ± SD. Transcript identities are indicated in the graphs by their *Arabidopsis thaliana* (At) gene number, TC number in TIGR, and/or accession number.

Figure 2

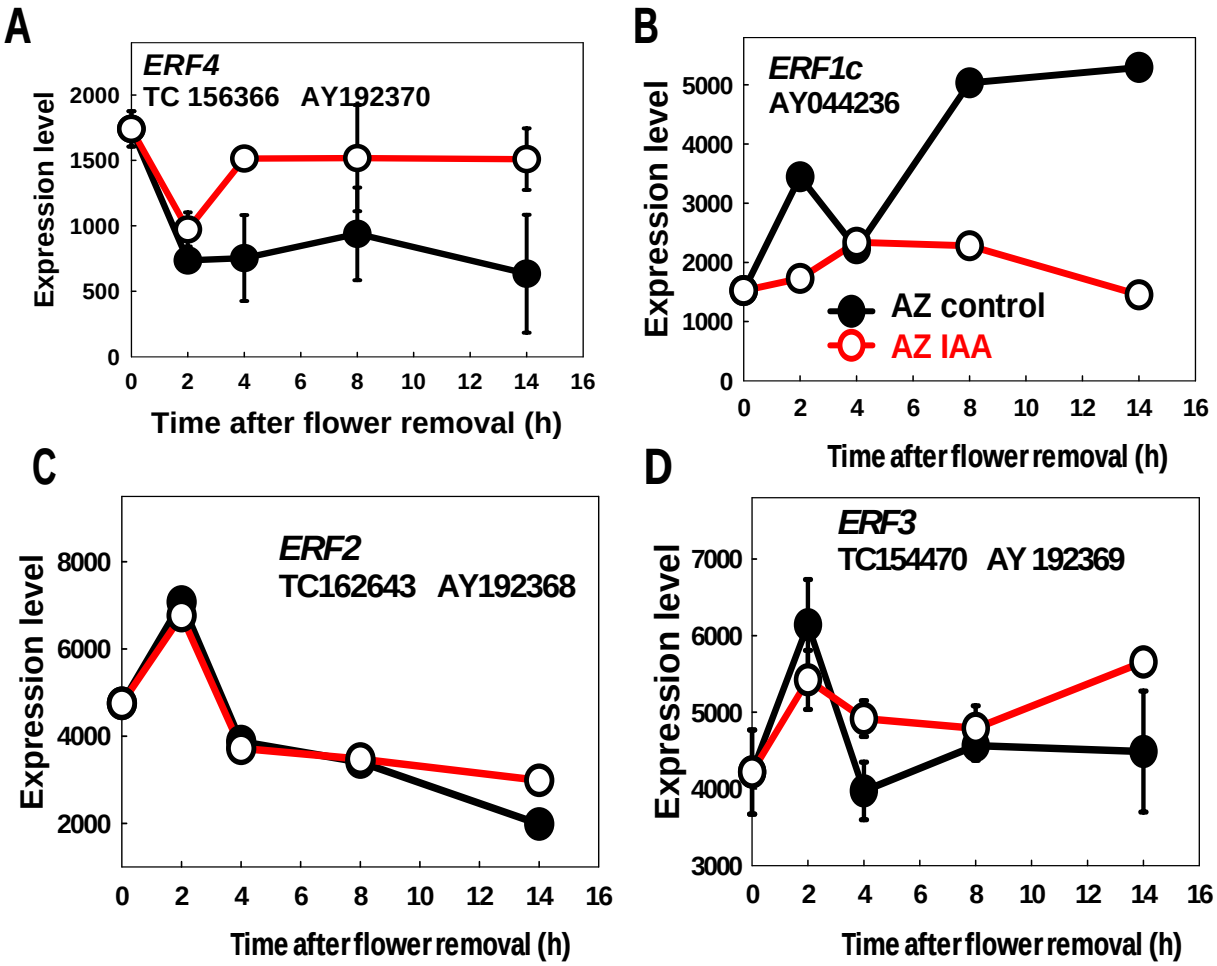

Figure 2: Effects of flower removal and IAA application after flower removal on the kinetics of changes in array-measured expression levels of *ERF* genes. Expression levels were measured for *ERF4* (A), *ERF1c (B), ERF2* (C) and *ERF3* (D) genes. RNA samples were extracted from flower AZ tissues taken from untreated (control) or IAA-treated tomato flower explants, at the indicated time points after flower removal. The results are means of 2 or 3 biological replicates ± SD. Transcript identities are indicated in the graphs by their *Arabidopsis thaliana* (At) gene number, TC number in TIGR, and/or accession number.

Figure 3

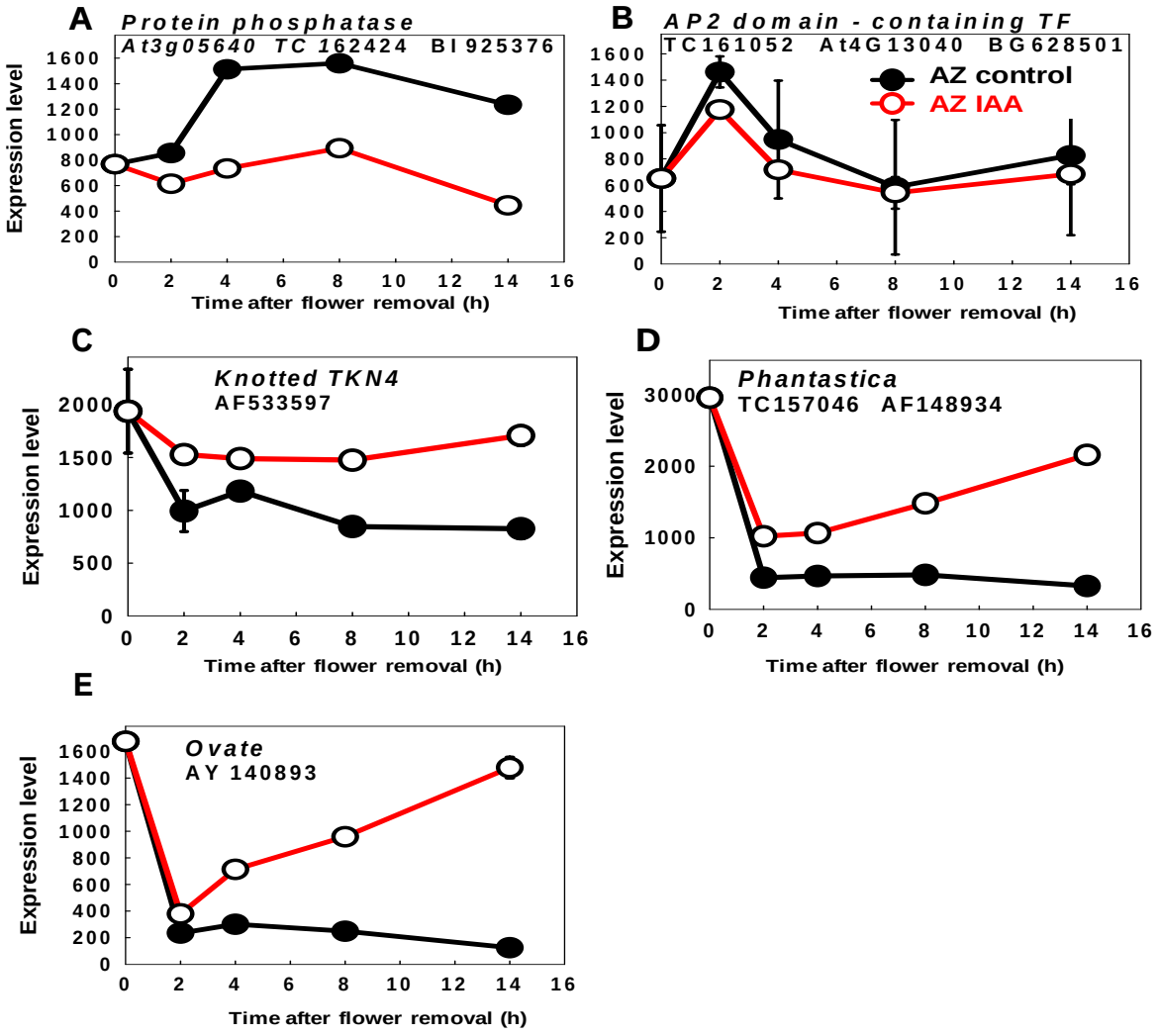

Figure 3: Effects of flower removal and IAA application after flower removal on the kinetics of changes in array-measured expression levels of TFs and regulatory genes. Expression levels were measured for *Protein phosphatase* (A), *MybSt1* - *AP2*-TF (B), *Knotted TKN4* (C), *Phantastica* (D) and *Ovate* (E) genes. RNA samples were extracted from flower AZ tissues taken from untreated (control) or IAA-treated tomato flower explants, at the indicated time points after flower removal. The results are means of 2 or 3 biological replicates ± SD. Transcript identities are indicated in the graphs by their *Arabidopsis thaliana* (At) gene number, TC number in TIGR, and/or accession number.

Figure 4

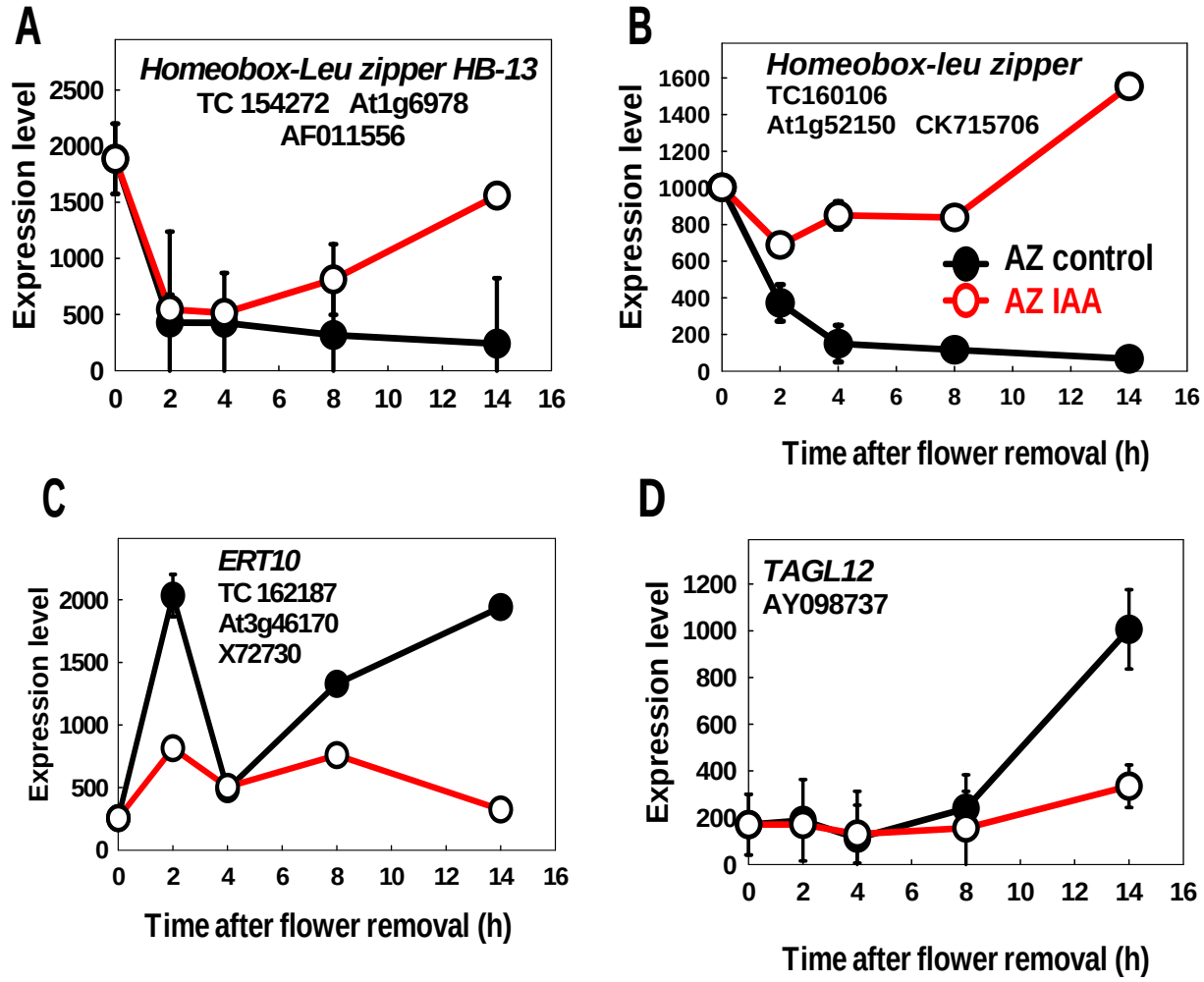

Figure 4: Effects of flower removal, and IAA application after flower removal on the kinetics of changes in array-measured expression levels of *Homeobox Leucine zipper HB-13* (A), *Homeobox Leucine zipper* (B), *ERT-10 Ripening-related burst oxidase protein D - RbohD* (C), and *TAGL12* MADS-box protein (D). RNA samples were extracted from flower AZ tissues taken from untreated (control) or IAA-treated tomato flower explants, at the indicated time points after flower removal. The results are means of 2 or 3 biological replicates ± SD. Transcript identities are indicated in the graphs by their *Arabidopsis thaliana* (At) gene number, TC number in TIGR, and/or accession number.

תקציר

תהליך הנשירה, המתבטא בניתוק איברים מצמח האם, גורם להפסדים גדולים לפני ואחרי הקטיף באיכות ובמשך חיי המדף של מוצרים שונים. כדי להתגבר על בעיה זו, מוצרים רבים מטופלים לאחר הקטיף בכימיקלים שונים כדי לעכב או למנוע את הנשירה. תהליך נשירת האיברים השונים בצמחים מתחיל עקב שינויים במפל ריכוזי האוקסין ברקמת הניתוק, מושרה בד"כ ע"י אתילן, ומואץ ע"י עקות לאחר הקטיף. התרחשות הנשירה תלויה במאזן ההורמונאלי האנדוגני של אתילן ואוקסין ברקמה. באופן כללי רגישות רקמת הניתוק לאתילן עולה כאשר ריכוז האוקסין ברקמה יורד.

למרות שדווח על שינויים בביטוי גנים שהופיעו במתאם חיובי עם התרחשות הנשירה המושרית ע"י אתילן, אין כמעט מידע על הבסיס המולקולארי והביוכימי של תהליך העלייה ברגישות רקמת הניתוק לאתילן. עד עתה טרם נעשה ניסיון להבין מהו המנגנון המולקולארי שבאמצעותו האוקסין משפיע על השינויים ברגישות הרקמה לאתילן, המתרחשים בשלב המקדים את העלייה בפעילות האנזימים ההידרוליטיים, והמקנים לרקמה את היכולת להגיב לאתילן בנשירת האיבר. נשירת איברים מלווה בשינויים בביטוי של מגוון גנים, הכוללים: גנים המושרים ע"י אתילן, גנים המגיבים לאוקסין, גנים הקשורים לפתוגנים (pathogen-related), וגנים המקודדים לאנזימים מפרקי דופן-תא. המטרה העיקרית של המחקר הנוכחי הייתה פיתוח כלים לביצוע אנליזה תפקודית של גנים חשובים המעורבים בבקרת תהליך הנשירה. השתמשנו במערכות מודל של אזורי ניתוק של עלים ופרחים מצמחי עגבנייה (*Solanum lycopersicum* Mill.) מהזנים 'Shiran 1335' ו- 'VF-36' כדי לבחון את תבניות הביטוי המרחביות והזמניות של הגנים המבקרים את המנגנונים המולקולאריים של תהליך הנשירה באזורי ניתוק אלה.

באמצעות השימוש בטכניקות של PCR חצי-כמותי וכמותי, נבחנו שינויים בטרנסקריפטום של אזורי הניתוק של פרחים ועלים במהלך הקניית הרגישות לאתילן לרקמה לאחר הסרת מקור האוקסין (הפרח או טרף העלה). במקביל, נבחנו קצב נשירת עוקץ הפרח וקצב נשירת פטוטרת העלה, המושרים ע"י הסרת הפרח או טרף העלה, בהתאמה. בוצע מעקב אחר שינויים בביטוי גנים באזורי הניתוק של פרחים ועלים בהשוואה לשנויי ביטוי באזורים מקבילים של רקמות אלה בהם לא מתרחש ניתוק, במועדים שונים לאחר הסרת הפרח (0, 2, 4, 8 ו- 14 שעות), או לאחר הסרת הטרף (0, 12, 24, 48 ו- 72 שעות). בנוסף, בוצע מעקב אחר הביטוי של הגנים שאותרו באזורי הניתוק גם ברקמות אחרות, כמו: גבעולים צעירים ובוגרים, עלים צעירים ובוגרים ושורשים. בהסתמך על לימוד מפורט זה של ביטוי הגנים, נבחרו מספר גנים לצורך ביצוע של התמרה יציבה בצמחי עגבנייה. לשם כך הגנים הנבחרים הושתקו כדי לבצע בעתיד אנליזה תפקודית שלהם בצמחי העגבנייה המותמרים. ההשתקה בוצעה באמצעות שני ווקטורים של RNAi, PGSA 1285 ו- pHANNIBAL, שחוברו לפרומוטר הקונסטיטוטיבי, CaMV 35S, או לפרומוטר הספציפי לאזור הניתוק, *TAPG4*, שבודד מרקמת עגבנייה.

המחקר בוצע על פי השלבים הבאים:

1) בוצע אימות, באמצעות השימוש בטכניקות של PCR חצי-כמותי וכמותי, של תוצאות המיקרואריי שהתקבלו במעבדה בשלב קודם לגבי ביטוי של גנים באזור הניתוק ובאזור-ללא-ניתוק של הפרח, לבחינת ההשפעות של טיפול הסרת הפרח במקטעי תפרחת של עגבניות, שהשרה את נשירת עוקץ הפרח. נבחנו תחילה גנים המקודדים לאנזימים מפרקי דופן-תא ברקמת הניתוק, כמו: *TAPG1, TAPG2, TAPG4, Cel1, XET-BR1*, כדי לאמת את מערכת הנשירה של עוקץ הפרח. בהמשך, נבחנו גנים שביטויים השתנה בצורה משמעותית זמן קצר (שעתיים) לאחר הסרת הפרח. גנים אלה כללו: גנים הפעילים במסלול העברת הסיגנל של

אתילן - *ERF2*, *ERF1c*, *ERT10, JERF3*; גנים של בקרה - *Protein phosphatase-like*; גנים של גורמי שעתוק - *MybSt1*; וגנים חדשים שנמצאו ייחודיים לרקמת הניתוק - *PHANTASTICA*, *TAGL12* (MADS-box), *TKN4, OVATE*, *KD1, TPRP-F1*. התוצאות שהתקבלו בטכניקות ה-PCR החצי-כמותי וכמותי היו בהתאמה מלאה לתוצאות שהתקבלו בשיטת המיקרואריי, פרט לגן *MybSt1*. ממצאים אלה מראים, שהתוצאות שהתקבלו בשיטת המיקרואריי אכן משקפים בצורה נאמנה את התהליכים המתרחשים באזור הניתוק של הפרח.

2) הגנים המפורטים לעיל הראו תבניות ביטוי שונות גם באזור הניתוק ובאזור-ללא-ניתוק של העלים במועדים שונים לאחר הסרת הטרף, וכן ברקמות אחרות של הצמח כגון: עלים צעירים ובוגרים, גבעולים ושורשים.

3) נלמדה הקינטיקה של נשירת פטוטרת העלה בתגובה להסרת הטרף (הסרת מקור האוקסין) ולחשיפה לאתילן חיצוני. התוצאות של ניסויים אלה מראות שאתילן היה יעיל בהשראת הנשירה של הפטוטרת רק לאחר הסרת הטרף, עקב הגברת הרגישות של אזור ניתוק זה לאתילן.

4) על סמך התוצאות של ביטוי הגנים, איתרנו מספר גנים פוטנציאליים העשויים לבקר את תהליך הנשירה של פרחים ועלים. גנים אלה נבחרו כמועמדים להשתקה בשיטת RNAi לצורך ביצוע התמרה יציבה שלהם בצמחי עגבנייה, כדי לעקוב בעתיד אחר תפקודם. בחירת הגנים המתאימים להיות מעורבים בתהליך הבקרה התבססה על גנים שביטויים עלה או ירד באופן משמעותי וספציפי באזור הניתוק של הפרח שעתיים לאחר הסרת הפרח, או באזור הניתוק של העלה 24 שעות לאחר הסרת הטרף.

5) לצורך ההשתקה, נבנו הקונסטרקטים המתאימים עם ווקטורים של RNAi תחת הבקרה של הפרומוטר הקונסטיטוטיבי, CaMV 35S, לששת הגנים הנבחרים הבאים: *ERF2, JERF3, TKN4, Protein phosphatase-like, Proline-rich protein - TPRP-F1, KD1*. ששת הגנים הנ"ל נמצאים כעת בפאזה V של תהליך ההתמרה, כך שבקרוב יהיו בידינו צמחי עגבנייה מותמרים, שבהם תיבחן השפעת השתקתם של גנים אלה על מופע הנשירה לצורך האנליזה התפקודית.

6) בודד הפרומוטר הספציפי לאזור הניתוק, *TAPG4*, מספריית DNA גנומית, ושובט לווקטור pGEMT באמצעות שינוי אתרי הרסטריקציה שלו כדי שיתאימו לווקטורים בהם השתמשנו. הקונסטרקטים של RNAi של ששת הגנים הנבחרים שפורטו לעיל חוברו לפרומוטר *TAPG4*, וע"י שימוש בפרומוטר זה הושגה השתקה ספציפית באזור הניתוק של הפרח, במקום השתקה של כל מערכת הצמח המתקבלת ע"י שימוש בפרומוטר הקונסטיטוטיבי CaMV 35S. הקונסטרקטים עם הפרומוטר *TAPG4* של שני גנים, *JERF3* ו- *TKN4*, נמצאים כעת בפאזה V של תהליך ההתמרה, וקונסטרקטים דומים לשני גנים נוספים, *Proline-rich protein - TPRPF1* ו-*KD1*, נמצאים בשלב IV של תהליך ההתמרה. כך שתוך מספר חודשים יהיו בידינו צמחי עגבנייה מותמרים גם עם הפרומוטר *TAPG4*, להמשך האנליזה התפקודית של גנים אלה.

במחקר הנוכחי אותרו גנים חשובים המעורבים בבקרת תהליך הנשירה, ופותחו כלים מולקולאריים לביצוע אנליזה תפקודית שלהם. הממצאים של המחקר הנוכחי תורמים ומקדמים את הבנת המנגנונים המולקולאריים האחראיים להקניית היכולת ליצור רקמת ניתוק. הבנה זו תתרום בעתיד לפיתוח גישות חדשות לבקרת תהליך הנשירה, וליישומן במערכות חקלאיות לצורך שיפור איכות המוצרים.

לימוד הבקרה של גנים המעורבים בנשירת פרחים ועלים בצמחי עגבנייה (*Lycopersicon esculentum* Mill.)

עבודת גמר

מוגשת לפקולטה לחקלאות, מזון וסביבה ע"ש רוברט ה. סמית

של האוניברסיטה העברית בירושלים

לשם קבלת תואר "מוסמך במדעי החקלאות"

מאת

סריוויגנש סנדרסאן

אייר תש"ע רחובות אפריל 2010

עבודה זו נעשתה בהדרכתם של:

ד"ר שמעון מאיר
המחלקה לחקר תוצרת חקלאית לאחר הקטיף
מינהל המחקר החקלאי, מרכז וולקני

ופרופ' יוסף ריוב
המכון למדעי הצמח וגנטיקה בחקלאות ע"ש רוברט ה. סמית,
הפקולטה לחקלאות, מזון וסביבה ע"ש רוברט ה. סמית
האוניברסיטה העברית בירושלים